VOLTAGE BALANCE IMPROVEMENT IN URBAN LOW VOLTAGE DISTRIBUTION NETWORKS

Houman Pezeshki

BEng, MSc in Electrical Engineering

A Thesis Submitted in fulfilment of the requirements for the degree of

Doctor of Philosophy

Science and Engineering Faculty

School of Electrical Engineering and Computer Science

Queensland University of Technology

Queensland, Australia

2015

Keywords

dSTATCOM

Low voltage distribution networks

Optimisation

Particle swarm optimisation (PSO)

Rooftop PVs

Voltage profile

Voltage unbalance

Abstract

Voltage unbalance (VU) along with voltage drop and rise at network peak and off–peak period are considered as growing concerns in modern multiphase distribution networks. These systems are gradually forced to operate closer to their limits due to many factors such as increasing load level, lack of reactive power sources, and high installation of single-phase distributed generators. System operators must be able to quickly identify trouble spots and take corrective steps to avoid critical voltage balance and magnitude violations.

To achieve this, suitable methods and techniques must be defined to assess system and take corrective actions. In this regard, a phase identification tool for single-phase and three-phase residential customers has been developed in this thesis that could enable the utilities to automatically identify the phase of each customer by correlating voltage information from the utility's transformer system with voltage information from individual smart meters.

Phase identification is the first step towards solving the larger problem of voltage and load balancing and this issue is further investigated, taking into account various costs associated with voltage and current unbalance. The distribution network under study for this thesis has a significant degree of current unbalance and also has close to 35% penetration of rooftop solar panels; this has enabled the study of the impact of both unbalance loading and PV generation on transformer insulation life and ageing. A thermal model was developed to assess the transformer temperatures over a 12-month cycle allowing a cumulative measure of loss of life (LOL) to be determined for various scenarios.

Different cost-effective methods to mitigate voltage unbalance in a number of urban residential feeders are studied. In the first approach the phase connection of a limited number of customers is altered. The decision to change a customer's phase connection is based on varying levels of information. This method was compared with other established technical methods for mitigation of VU such as distribution static compensator dSTATCOMs.

The introduced method of voltage unbalance mitigation in LV systems through customer phase swaps and/or dSTATCOM is further investigated to explore the impact the voltage unbalance improvement in one LV feeder could bring to its neighbouring LV systems. This investigation lays the groundwork for the rollout of smaller and more economical dSTATCOMs that could bring voltage improvements both in terms of magnitude and in terms of balance locally where they are most needed, in comparison with larger STATCOMs that could be placed in medium voltage (MV) systems.

Table of Contents

Keywords iii
Abstract iv
List of Figures ix
List of Tables xii
List of Principal Symbols and Abbreviations xiv
Publications Arising From the Thesis xv
Statement of Original Authorship xvi
Acknowledgements xvii
Chapter 1 Introduction 1
1.1 Background 1
1.2 Aims and Objectives of the Thesis 2
1.3 Significance of Research 3
1.4 Key Contributions of this Research 3
1.5 Thesis Outline 5
Chapter 2 Literature Review 7
2.1 Meaning of Unbalance 7
2.2 Voltage Unbalance Limits 10
2.3 Voltage Unbalance Effect 11
2.3.1 Induction Machines 12
2.3.2 Transmission and Distribution Lines 12
2.4 Effects of Current Unbalance 13
2.4.1 Transformers 13
2.5 Rooftop PV 14
2.6 Mitigation of Voltage Unbalance 15
2.7 dSTATCOM 16
2.7.1 Location of dSTATCOM 18
2.8 Radial Load Flow 19
2.8.1 Forward Backward Power Flow 19
2.8.2 Component Models 20
2.8.3 Conductor Model 21
2.8.4 Transformer Model 22
2.8.5 Load Model 23
2.8.6 Slack Bus 24
2.9 Optimisation Methods for Power System Problems 25
2.9.1 Particle Swarm Optimisation (PSO) 27
2.10 Summary 30
Chapter 3 Phase Identification in a Three Phase LV Distribution Network 31
3.1 Introduction 31
3.2 Phase Identification Approach 33
3.3 The Perth Solar City Project 36

3.4 Experimental Results....38
3.4.1 Phase Allocation Based on Transformer Data....39
3.4.2 Phase Allocation Based on Three-Phase Meter Data....42
3.5 Measurement Set-up and Errors....47
3.6 Summary....50
Chapter 4 Impact of Load Unbalance and Rooftop PV on Transformer Life 53
4.1 Introduction....54
4.2 Impact of Rooftop PV on Transformer Loading....55
4.3 Unbalanced vs. Balanced Transformer Loading....55
4.4 Distribution Transformer Thermal Model....56
4.5 Transformer Thermal Diagram....57
4.6 IEC Thermal Model....58
4.6.1 HST for Unbalanced Loading:....60
4.7 Loss of Life of Distribution Transformer....61
4.8 Thermal Model Inputs....63
4.8.1 Ambient Temperature and Rooftop PV Generation....63
4.8.2 Household Load Profiles....64
4.8.3 Distribution Transformer Thermal Parameters....65
4.9 Results and Discussion....65
4.9.1 Unbalanced Operating Conditions (With Solar Input)....66
4.9.2 Unbalanced Operating Conditions (No Solar Input)....71
4.9.3 Balanced Operating Conditions (With Solar Input)....76
4.9.4 Balanced Operating Conditions (No Solar Input)....77
4.10 Summary....80
Chapter 5 Voltage Balance Improvement in Urban Residential Feeders....83
5.1 Introduction....83
5.2 Structural Modifications of Single-phase Loads....85
5.3 Case Study Networks....86
5.3.1 Australian LV Distribution Network....87
5.3.2 UK LV Network....88
5.4 Voltage Unbalance in the Australian LV Network....89
5.5 Phase Swapping Scheme....94
5.5.1 Case 1-Billing....95
5.5.2 Case 2-Billing and PV....100
5.5.3 Case 3-Particle Swarm Based Optimisation Phase Swap....106
5.6 Impact of Phase Swap on VUF in UK Network....108
5.7 Summary....110
Chapter 6 Distribution System Wide Voltage Balancing Methods....113
6.1 Introduction....113
6.2 dSTATCOM....113
6.3 Optimal Sizing and Location of dSTATCOM....114
6.3.1 Problem Formulation....114
6.3.2 Candidate Location of dSTATCOMs....115
6.3.3 Applying Modified PSO to Problem....115

6.4 Implementation of Proposed Work 120
6.4.1 Scenario 1: dSTATCOM with Battery Storage 120
6.4.2 Scenario 2: dSTATCOM without Battery Storage 123
6.4.3 Scenario 3: Phase Swap and dSTATCOM 124
6.5 Impact on Neighbouring LV Feeders 125
6.6 Simulation Results 126
6.6.1 Identical Loading 126
6.6.2 Random Loading 129
6.7 Summary 132
Chapter 7 Conclusions and Recommendations 133
7.1 Conclusions 133
7.2 Recommendations for Future Research 135
7.2.1 Studying More LV Networks 135
7.2.2 Statistical Analysis of Test Cases 135
7.2.3 Single-phase dSTATCOM 136
7.2.4 Single/Three Phase Inverters 136
References 137
Appendix A Transformer Characteristic 145
A1. 200 kVA Transformer Characteristics 145
Appendix B Case Study Networks 146
B1. Australian LV Network-Overhead 146
B2. UK LV Network-Underground 147
Appendix C Annual Consumption data 148
Appendix D Particle Swarm Optimization Extended Results 149

List of Figures

Figure 2-1. Circulating zero sequence current in delta winding 14
Figure 2-2. Schematic diagram of dSTATCOM [42]..... 17
Figure 2-3. Two-bus and single-line representation of distribution networks for the solution of BFS algorithm [45] 20
Figure 2-4. Model of the three-phase, four-wire multi-grounded distribution line, based on the model proposed in [46]..... 22
Figure 2-5. D-yg1 transformer bank connection and its positive-sequence current [46]..... 23
Figure 2-6. A typical daily load profile of each of 75 customers on Pavetta. (vertical axis: Current (A) horizontal axis: Time (Hours)) 24
Figure 2-7. Classification of optimization techniques [58]..... 26
Figure 2-8. Flow chart of the proposed MPSO method..... 29
Figure 3-1. Simplified diagram of network under study..... 35
Figure 3-2. Perth solar city high penetration feeder site, image courtesy Western Power..... 37
Figure 3-3. Pole-mounted transformer and data logger under study (Pavetta TX1)..... 37
Figure 3-4. Pavetta feeder diagram..... 38
Figure 3-5. Auto-correlation & cross-correlation of transformer phase voltages 1st-7th September 2011..... 39
Figure 3-6. Flow chart of phase identification based on cross correlation 41
Figure 3-7. Cross-correlation of three-phase and single-phase house with transformer 42
Figure 3-8. Comparison of aggregation of correlated meters with transformer reading, power and current (21-27 January 2012)..... 45
Figure 3-9. Comparison of aggregation of correlated meters with transformer reading, power and current (25 January 2012) 46
Figure 3-10. Replaced wooden power pole..... 47
Figure 3-11. Comparison between the RMSE value of all four cases..... 50
Figure 4-1. Pavetta transformer power output, 21-27 January 2012 56
Figure 4-2. Thermal diagram of oil-immersed transformers..... 57
Figure 4-3. Block diagram representation of the differential equations 60
Figure 4-4. Flow chart of transformer life assessment using the thermal model..... 63
Figure 4-5. Ambient temperature from June 2011 - July 2012 64
Figure 4-6. Pavetta transformer power output, 21-27 January 2012 65

Figure 4-7. Comparison of the daily evolution of the hotspot, top oil and ambient temperature peak day (a) low load day (b) 69
Figure 4-8. (a) Daily evolution of the loss of life on each phase of transformer, peak day (b) daily evolution of the loss of life on each phase of transformer lightly load day 70
Figure 4-9. Effect of possible load growth on TOT and HST 71
Figure 4-10. Improvement in top oil temperature and HST in presence of PV at different loading conditions 72
Figure 4-11. Temperature difference in hot spot and oil of transformer and reduction in LOL as a result of PV generation 73
Figure 4-12. Balanced vs unbalanced loading, HST, TOT and LOL 77
Figure 5-1 Australian LV aerial network 88
Figure 5-2. Existing public UK LV underground network 89
Figure 5-3. Individual phase loading on 23-bus LV network 90
Figure 5-4. Voltage unbalance in base case 91
Figure 5-5. Australian LV feeder VUF histogram 91
Figure 5-6. Vectorial distribution of VU (magnitude and angle)-each phase loading is varied while the other phases loadings are maintained constant. 92
Figure 5-7. Vectorial distribution of VU (magnitude and angle) base case 94
Figure 5-8 Improvement in VUF- phase swap based on billing 95
Figure 5-9. Maximum VU in the feeder before and after phase swaps 96
Figure 5-10. Minimum phase voltage at 23 buses, base case vs phase swap (across the year) 97
Figure 5-11. Maximum phase voltage at 23 buses, base case vs phase swap (across the year) 97
Figure 5-12. Complex voltage unbalance-base case 98
Figure 5-13. Complex voltage unbalance-phase swap-billing 99
Figure 5-14. Complex voltage unbalance-phase swap-billing & PV 101
Figure 5-15.Load profile-phase swap cases 1 and 2 102
Figure 5-16. Maximum voltage with increase in PV penetration 103
Figure 5-17. Voltage unbalance factor with increase in PV penetration 104
Figure 5-18. Maximum VUF in UK LV feeder-31-buses, base case 109
Figure 5-19. Maximum VUF at UK LV feeder-31-buses, base case vs billing vs billing and PV 110
Figure 6-1. Structure of a particle 116
Figure 6-2. VUF mitigation after dSTATCOM placement 122
Figure 6-3. MV/LV distribution network 126

Figure 6-4. Maximum VUF of all 5 LV feeders 127
Figure 6-5. Improvement in VUF of all feeders.....128
Figure 6-6. VUF mitigation after dSTATCOM in LV3 & LV5.....129
Figure 6-7. Max VUF of all 5 LV feeders with random loading 130
Figure 6-8. VUF mitigation after dSTATCOM in LV4 & LV5.....131
Figure D-1 Simulation results produced by the PSO at different iterations for sample case study.....149
Figure D-2 Location of dSTATCOM at each iteration.....150
Figure D-3 Size of dSTATCOM at each iteration.....150

List of Tables

Table 2-1. Voltage unbalance limit 11
Table 3-1. Allocation of the single-phase houses 43
Table 3-2. Allocation of the three phase-houses 44
Table 3-3. Solar PV system connections on LV network (Pavetta) 44
Table 3-4. Comparison between RMSE values of the four cases 49
Table 3-5. Comparison between RMSE values of the four cases (percentage) 50
Table 4-1. Top oil and HST comparison under different loading conditions 74
Table 4-2. Seasonal variation in LOL of transformer 75
Table 4-3. Loss of life improvement with PV growth 76
Table 4-4. Loss of Life under different scenarios 79
Table 4-5. LOL under different loading scenarios (balanced vs. unbalanced) 79
Table 5-1. Comparison of VUF occurrences in different cases (1 year) 100
Table 5-2. Voltage unbalance duration 100
Table 5-3. Voltage unbalance mitigation by billing only phase swap in presence of more PV 105
Table 5-4. Voltage unbalance mitigation by billing and PV phase swap in presence of more PV 106
Table 5-5. Comparison of all cases 107
Table 5-6. Impact on voltage boundaries in one year: (base 230 V, +10%, -6%) 108
Table 5-7. Comparison of three main cases for UK network 110
Table 6-1. Results of dSTATCOM-battery 123
Table 6-2. Results of dSTATCOM-no battery 124
Table 6-3. Results of phase swap-dSTATCOM-no battery 125
Table 6-4 Rating and placement of dSTATCOMs in LV 5 128
Table 6-5. VUF improvement in all feeders 128
Table 6-6 Rating and placement of dSTATCOMs in LV 3 & LV5 129
Table 6-7. VUF improvement in all feeders with random loading 131
Table 6-8. Rating and placement of dSTATCOMs in LV4 & LV5 131
Table A-1. Electric characteristics of transformer under study 145
Table A-2. Geometric characteristics of transformer under study 145
Table A-3. Parameters for the thermal model of the 200 kVA transformer 145
Table B-1. Australian overhead cable parameters 146

Table B-2. Australian overhead system connectivity 146
Table B-3. UK underground cable parameters.....147
Table B-4. UK underground system connectivity 147
Table C-1. Annual consumption data of customers connect to Australian LV feeder.....148

List of Principal Symbols and Abbreviations

dSTATCOM	distribution static compensator
HST	hot-spot temperature
IEC	international electrotechnical commission
IEEE	institute of electrical and electronics engineers
LOL	loss of life
LV	low voltage
MPSO	modified particle swarm optimisation
MV	medium voltage
PCC	point of common coupling
PV	photovoltaic cells
VU	voltage unbalance
VUF	voltage unbalance factor

Publications Arising From the Thesis

Journal papers

1. **Pezeshki, H**.; Wolfs, P.J.; Ledwich, G., "Impact of high pv penetration on distribution transformer insulation life," *Power Delivery, IEEE Transactions on* , vol. 29, no. 3, pp.1212-1220, June 2014.

Conference papers

2. **Pezeshki, H**.; Wolfs, P.; Johnson, M., "Multi-agent systems for modelling high penetration photovoltaic system impacts in distribution networks," Innovative Smart Grid Technologies Asia (ISGT), 2011 IEEE PES , pp.1-8, 13-16 Nov. 2011
3. **Pezeshki, H**.; Wolfs, P., "Correlation based method for phase identification in a three phase LV distribution network," *Universities Power Engineering Conference (AUPEC), 2012 22nd Australasian* , 26-29 Sept. 2012
4. **Pezeshki, H**.; Wolfs, P.J., "Consumer phase identification in a three phase unbalanced LV distribution network," *Innovative Smart Grid Technologies (ISGT Europe), 2012 3rd IEEE PES International Conference and Exhibition on* ,14-17 Oct. 2012
5. **Pezeshki, H**.; Wolfs, P., "Impact of high PV penetration on distribution transformer life time," *Power and Energy Society General Meeting (PES), 2013 IEEE* , 21-25 July 2013

Statement of Original Authorship

The work contained in this thesis has not been previously submitted to meet requirements for an award at this or any other higher education institution. To the best of my knowledge and belief, the thesis contains no material previously published or written by another person except where due reference is made.

QUT Verified Signature

28/04/2015

28 April 2015

Acknowledgements

First of all, I would like to express my deepest gratitude to my principle supervisor, Professor Gerard Ledwich, for his support and guidance throughout my research. In addition to being my academic supervisor, he was my sympathetic and kind friend.

I also wish to extend my sincere appreciation to my associate supervisors, Professor Peter Wolfs and Associate Professor Geoffrey Walker, for their invaluable support and advice during my PhD.

Special thanks to all of my colleagues at Power Engineering Group for providing a warm and supportive environment.

Finally yet importantly, I would like to express my heartiest appreciation to my beloved wife, Samar for her endless encouragement and support during this period. I also need to thank my parents and my brother for their patience and unconditional love that have supported me through the PhD study.

Chapter 1 Introduction

This chapter examines the context of this research and its relevance to the challenges and opportunities facing future electrical distribution networks, in particular in the Low Voltage (LV) sections. It shows that there is considerable potential to improve the voltage balance and, as a result, voltage limits through cost-effective methods in Australian LV distribution networks. The first section of this chapter outlines the background and context of the research, and its purposes. The next section describes the significance and scope of the research and provides definitions of terms used. Finally, the last section includes an outline of the remaining chapters of the thesis.

1.1 **Background**

It is desirable that the utilities ensure that their customers are supplied with a high power quality. Among the power quality parameters, voltage profile and voltage unbalance are the major concerns in low voltage distribution networks [1, 2]. Voltage drop can be experienced in network peak hours while voltage rise can be experienced in network off-peak hours with high generation and penetration of distributed generation (DG) units [3]. The utilities are responsible for keeping the voltage in their network within the standard limits to prevent malfunction of customer devices.

Voltage unbalance is more common in individual customer loads due to phase load unbalance, especially where large single–phase power loads are used [4]. Single-phase loads in LV distribution networks are continually connected to, and disconnected from, the distribution system and are not evenly distributed between the three phases. Additionally, the level of unbalance present in distribution networks also depends on phase-conductor configurations, such as unsymmetrical spacing

between phase conductors [5]. Voltage unbalance until now has generally not been of great concern, because the distribution of single-phase customer loads has been centrally planned by utilities who attempt to allocate them equally across the three phases. The single-phase nature of DG units, however, along with the fact that their growth is consumer-driven and not centrally planned may result in additional unbalanced currents and voltages. In addition to generation unbalance, load behaviour is also likely to change significantly in the future adding further complexity to the inherent symmetry of distribution systems [6].

An increase in the voltage unbalance can result in overheating and derating of all three phase induction motor loads such as squirrel cage induction motors, swimming pool pumps and air-conditioning compressors [4]. It also should be note that this could be intensified by the fact that a small unbalance in the phase voltages can cause a disproportionately large unbalance in the phase currents [5].Voltage unbalance can also cause network problems such as incorrect operation of protection relays and voltage regulation equipment, and generation of harmonics from power electronic loads [5].

1.2 **Aims and Objectives of the Thesis**

The following research aims are integrated to deliver the main goal of this research:

1. development of a technique to identify the phase connection of customers in distribution networks
2. development of a tool to analyse the impact of load unbalance and rooftop photovoltaic (PV) on transformer insulation life and ageing
3. development of cost-effective compensation techniques used to mitigate the negative sequence current and voltage that is generated in the power system

4. development of distribution system wide voltage balancing routine through cost-effective methods

1.3 **Significance of Research**

The economic benefits for energy providers and users are strongly dependent on the supply reliability, security and efficiency of the power system and consequently, on the supply quality and the loading quality. For instance, negative sequence current increases energy loss at delivery. The negative sequence voltage causes temperature increase of three phase induction motors. In addition, there are other negative effects of the voltage and current asymmetries. The presences of excessive levels of voltage unbalance (VU) stands as a problem of power quality that has significant consequences for both customers and electric utilities. Thus, the development of well-researched engineering practices is required to maintain acceptable voltage unbalance levels while utilising the total voltage unbalance absorption capacity of the power system. Since the voltage and current unbalance causes various negative effects in power systems, these effects and methods to mitigate their impacts and magnitude are the subject of concern and investigation in this research.

1.4 **Key Contributions of this Research**

The main objective of this thesis is to analyse and propose new strategies for improving the voltage profile and reducing voltage unbalance problems in the low voltage distribution networks. To achieve this goal, the aims of the research project are identified as:

1. Phase identification of customers in distribution networks

The main aim of this study is to investigate the techniques and methods to mitigate the impact of voltage unbalance on low voltage distribution systems. One of

the main contributors to voltage unbalance is improper customer phase allocation and loading. A method based on cross correlation is introduced in this work that enables the utilities to automatically identify the phase of each customer by correlating voltage information from the utility's transformer system or three-phase customers with voltage information from individual smart meters.

This work demonstrates that the voltage profile of any residential consumer is well correlated with the voltage profile on the same phase of the transformer and establishes a new method to determine the phase connection of consumer loads on a LV distribution network. Phase identification is the first step towards solving the larger problem of phase balancing and this issue is further investigated, taking into account various costs associated with phase rebalancing (claim 3 and 4).

2. Analysis of the impact of solar rooftop and load unbalance on transformer insulation life

In the current literature the impact of unbalance loading on transformer has not been fully investigated; this thesis examines the improvement in transformer ageing and loss of life that is brought about by balancing the loading on each phase leg of the transformer.

The distribution network under study for this thesis has a significant number of installed rooftop solar panels; this has enabled the study of the impact of PV generation on transformer ageing. Rooftop solar PV generation does reduce the temperature rise of oil-immersed distribution transformers even when peak demand occurs well after sunset. The time lag due to thermal inertia and ambient temperature decline allow overloading of the transformer beyond its normal rating without significant loss of life. A thermal model was developed to assess the transformer temperatures over a 12-month cycle, allowing a cumulative measure of loss of life to

be determined for various scenarios. The presented results correspond to a pole-top transformer feeding a residential LV system. It is expected as the coincidence of PV with commercial load is higher and even better loss of life trends can be observed in the case of the commercial and office building transformers.

3. Cost effective voltage balance improvement in urban residential feeders

Voltage unbalance mitigation is analysed in a number of different LV systems including an actual suburban low voltage network; two different methods were investigated. In the first approach the phase connection of a limited number of customers is altered. The decision to change customer phase connection is based on varying levels of information. This method was compared with other established technical methods for mitigation of voltage unbalance such as dSTATCOMs. The placement and sizing of the dSTATCOMs in the LV system is performed through a Modified Particle Swarm Optimisation (MPSO).

4. Distribution system wide voltage balancing through cost effective methods.

The introduced method of voltage unbalance mitigation in LV systems through customer phase swaps and/or dSTATCOM is further investigated to explore the impact that voltage unbalance improvement in one LV feeder could bring to its neighbouring LV feeders. This investigation lays the groundwork for the roll-out of smaller and more economical dSTATCOMs that could bring voltage improvements in terms of both magnitude and balance locally, where they are most needed, in comparison with larger STATCOMs that are usually placed in MV systems.

1.5 **Thesis Outline**

This thesis is organised in seven chapters. An overview of the research along with the features and aims are outlined in **Chapter 1**. The key contributions are also

named in this chapter. A literature review is carried out in **Chapter 2**. In this chapter, the justification for doing this research is presented. It is shown that a comprehensive voltage unbalance mitigation technique is required to cover almost all aspects of a MV/LV distribution network. A practical technique is proposed in **Chapter 3**, which can be a reliable method for identifying the phase connection of the residential customers in distribution networks. This technique could be used to improve the voltage and current balance profile in the low voltage systems.

Chapter 4 is concerned with the technical impacts associated with the distribution transformer loss of life because of unbalance loading on each leg of the transformer. This chapter also explores the benefit that installation of rooftop PV could bring to transformer ageing by reducing the internal temperature of the transformer. In **Chapter 5**, the application of manual phase swaps and dSTATCOM is proposed and studied for voltage balance improvement in low voltage distribution networks. **Chapter 6** discusses the voltage unbalance reduction across multiple LV feeders through limited manual phase swaps and/or correct placement and sizing of dSTATCOMs. Conclusions drawn from this research as well as recommendations for future work are given in **Chapter 7**. The list of references and a list of publications resulting from this thesis are presented after this chapter. The parameters of the 200-kVA distribution transformer and the parameters of two LV feeders used in the simulations are presented in appendices A and B.

Chapter 2 Literature Review

2.1 **Meaning of Unbalance**

Voltage unbalance (VU) is described as a state in electric power systems in which the fundamental phase voltages are not equal [7]. Strictly speaking, “asymmetrical voltages” qualifies the physical significance better as both the difference in amplitude and phase displacement are of concern. The level of VU can be specified using a number of definitions [8, 9]. The widely used concept for voltage unbalance originates from the theory of symmetrical components, which mathematically decomposes a three-phase unbalanced system into three balanced sub-systems known as positive, negative and zero sequence systems. Accordingly, VU can exist in two forms in a three-phase power system: zero sequence and negative sequence unbalance. Negative sequence unbalance is relatively significant and is of more concern compared to zero sequence unbalance, as negative sequence current can flow through all power system components in a similar way to positive sequence currents. The zero sequence unbalance is a concern only when the coupling transformer allows zero sequence currents to flow from higher voltage to lower voltage systems [10]. It is generally noted that the zero sequence unbalance can be controlled through system design and maintenance [7]. Thus, the common practice is to pay more attention to negative sequence unbalance in power systems.

Since unbalance is inherent in the power system, standards were developed for evaluation of acceptable levels of current and voltage asymmetry for generation, transmission and distribution equipment and also for customer’s loads. Therefore, it is imperative that the level of current and voltage asymmetry be calculated in an efficient and effective manner. The level of unbalance that is used in this thesis is

specified as the ratio of the RMS value of the negative sequence component to the RMS value of the positive sequence component. This is not in line with a variety of different approaches and standards. Some of these different approaches are due to the measurement technology that existed at the time the measure was proposed and some measures are application oriented as discussed below.

Several papers, such as [5] and [9], compared some definitions based on whether they use the phase angle or not in their calculation of the VUF. For example, NEMA, IEEE, IEC and CIGRE all provide different ways to calculate the VUF. The concern regarding their respective definition of the level of asymmetric current and voltage is whether the calculation without the use of the phase angle produces an accurate expression of the asymmetric current and voltage level. NEMA uses line to line voltage while IEEE uses phase voltage in its calculation and as a result both exclude phase angle asymmetry from their calculations [5], [9]. However, IEC uses both phase angle and RMS magnitudes in its calculation. In the context of this work the true definition of voltage unbalance is used based on IEC Std. 61000-3-13:2008 [11]. It is defined as the ratio of the fundamental negative sequence voltage component (V2) to the positive sequence voltage component (V1) [11]. The percentage voltage unbalance factor (% VUF), or the true definition is given by:

$$VUF = \left|\frac{V_2}{V_1}\right| \times 100\% \qquad (2.1)$$

where $V_1 = \frac{V_{ab} + a \times V_{bc} + a^2 \times V_{ca}}{3}$ $V_2 = \frac{V_{ab} + a^2 \times V_{bc} + a \times V_{ca}}{3}$

where a =1∠120°

Although the common practice is to use the absolute value of the ratio V2/V1 to represent the degree of VU, the VUF actually represents a complex number, which

carries phase angle information. Sometimes it does not suffice to use only the value of voltage unbalance for the performance analysis of a system under unbalanced supply conditions. This is due to the large number of combinations of the terminal voltages that could be assumed for the same degree of unbalance. Introduction of the complex voltage unbalance factor (CVUF) reduces the size of the subset of the terminal voltages that can result in a given value of the VUF. This is due to the phase angle θ of the unbalance being taken into account in this definition, in addition to the unbalance magnitude. According to this, the complex voltage unbalance factor (CVUF) can be expressed as follows:

$$CVUF = VUF\angle\theta = (V_2 / V_1)\angle\theta \tag{2.2}$$

There exists a collection of recent research based on the complex VU factor to investigate various effects of VU [12, 13]. A convenient equivalent formulation which utilises only the magnitudes of the fundamental RMS line-line voltages to evaluate VUF as given in 61000-3-13:2008 [11] is:

$$VUF = \sqrt{\frac{1-\sqrt{3-6\beta}}{1+\sqrt{3-6\beta}}} \tag{2.3}$$

where $\beta = \dfrac{|V_{ab}|^4 + |V_{bc}|^4 + |V_{ca}|^4}{(|V_{ab}|^2 + |V_{bc}|^2 + |V_{ca}|^2)^2}$ and V_{ab}, V_{bc} and V_{ca} are the fundamental line-line, RMS voltages.

The definition for VU given by National Electrical Manufacturers Association (NEMA) [14] is shown in (2.4).

$$\text{Voltage unbalance} = \frac{\text{Maximum voltage deviation from the average line - line voltage}}{\text{Average line - line voltage}} \tag{2.4}$$

It is important to note that the IEC definition is mathematically rigorous compared to the NEMA definition and the two definitions can sometimes lead to different outcomes when calculating the VU factors for the same scenarios.

According to [9], IEC is the most accurate, because it uses the ratio of negative sequence to positive sequence voltage. Different voltage asymmetric conditions such as under-voltage unbalance, over-voltage unbalance were undertaken to illustrate this finding. The under-voltage case produces a higher value of the voltage unbalance factor (VUF) when compared to the over-voltage case due to the increase in the negative sequence voltage, while the positive sequence voltage decreases [9, 15]. In addition, because the change of the phase angle does not affect the magnitude of the phases but affect the sequence components, it is evident that IEC would give a more accurate result. If the line-to-neutral voltages are used in the formulas, the inclusion of the zero sequence components can give erroneous results. Zero sequence current does not flow in a three-wire system. Therefore, the calculation of a zero sequence voltage unbalance factor is irrelevant however, for a four-wire system it would be relevant. This would be the ratio of the zero sequence voltage to the positive sequence voltage but this is not being discussed in detail here.

2.2 **Voltage Unbalance Limits**

According to [16], the allowable limit for VUF is 2.0% in LV networks. The UK Engineering Recommendation P29 not only limits the VU of the whole network to 2%, but also limits the VU to 1.3% at the load point [17]. The ANSI standard for "Electric Power Systems and Equipment Voltage Ratings (60 Hertz)" recommends that electrical supply systems should be designed to limit the maximum VU to 3% when measured at the electric utility end points at no-load conditions [18]. Utilities aim to maintain the level of voltage unbalance in their networks between certain

limits. EN 50160 [19] stipulates the average 10-minute VUF must not exceed 2% for more than 5% over any 1-week measurement period. The National Electricity Code Australia (NECA) [20] specifies various voltage unbalance limits as given in Table 2-1:

Table 2-1. Voltage unbalance limit

Nominal Supply Voltage	Negative Sequence Voltage (% of Nominal Voltage)			
	No contingency event	Credible contingency event	General	Once per hour
	30-minute average	30-minute average	10-minute average	1-minute average
>100 kV	0.5%	0.7%	1.0%	2.0%
10 kV to 100 kV	1.3%	1.3%	2.0%	2.5%
<10 kV	2. 0%	2. 0%	2. 5%	3. 0%

2.3 **Voltage Unbalance Effect**

Three phase power systems, can become unbalanced at the distribution level mainly due to unbalanced loads and system inherent asymmetries, even though they are quite well balanced at the upstream generator [5]. Uneven distribution of single-phase and two-phase loads and asymmetrical three-phase loads can cause unbalanced currents, which can lead to voltage unbalance, even if the line impedances are symmetrical. The presence of unequal mutual impedances resulting from the asymmetrical electromagnetic coupling between the conductors of untransposed/partially transposed overhead lines, can lead to unbalanced voltages at the load terminals, this could occrue even with a perfectly balanced three-phase voltage source supplying a perfectly symmetrical load through [21, 22]. In addition, unbalanced transformer impedances and their connections such as open-wye open-delta transformers can also contribute to unbalanced voltages [5]. ; In some transformer connections the voltage unbalance of the primary system can convert

primary side zero sequence voltage into negative sequence voltage on the secondary side [23].

2.3.1 Induction Machines

When an unbalanced voltage is supplied to a three-phase induction (asynchronous) motor, its performance can deteriorate and the life expectancy be reduced [24-26]. This voltage unbalance causes current asymmetry. For example, according to NEMA MG-1, 1% voltage unbalance in an induction motor can contribute to a 6% to 10% increase in current unbalance. The current unbalance causes increased losses, by extension increased temperature, which leads to reduced life expectation, and reduced efficiency of the induction motor. Furthermore, it causes torque pulsations, increased vibration and mechanical stresses.

2.3.2 Transmission and Distribution Lines

The primary function of the transmission/distribution lines is to efficiently transmit energy to various destinations to be used by customers. The negative sequence voltage component contributes, along with other reasons, to the asymmetry of the line currents, meaning a negative sequence component occurs in the current. In practice, this current does not convey substantial energy, because it is orthogonal to the positive sequence voltage. However, it contributes to energy loss in the line resistance and this increases the temperature of conductors. Therefore, the negative sequence current reduces the capacity of the transmission/distribution line [27, 28]. Three-phase synchronous generators exhibit a phenomenon similar to that of three-phase induction motors, where the negative sequence current results in excess machine losses and heating in addition to possible hazards to structural components [29].

2.4 **Effects of Current Unbalance**

Current unbalance reduces efficiency at generation, transmission and distribution of electric energy. This is because the negative sequence component does not contribute to useful energy transmission, but to the transmission of energy which is dissipated in power system equipment in the form of heat. As a consequence, the ampacity of cables, transmission and distribution lines has to be selected based on the anticipated level of negative sequence current it will be subjected to during operations. In addition, the capacity of transformers and the efficiency of motors are reduced. In other words the negative sequence current increases losses in the cables, transmission and distribution lines, transformers and equipment on the power system [12]. Furthermore, the negative sequence current causes voltage unbalance. For instance, the current unbalance caused by very large single-phase loads such as traction systems and AC arc furnaces contribute to different voltage drops on the three phases of the supply system and consequently, it produces voltage unbalance. Some of the major impacts of current asymmetry are compiled and discussed in more detail below.

2.4.1 Transformers

Transformers are affected based on the vector group configuration, with regard to the connection or existence of a neutral wire on the primary and or secondary. For example, if the connection is delta-wye-grounded, then the zero sequence current is converted into a circulating current in the delta side. This circulating current causes energy loss and the windings heat as a result. The magnetic fluxes produced by this current are in phase with each other and as a result, they do not cancel each other. This magnetic flux passes through the parts of the transformer causing eddy currents

and energy losses. The positive and negative sequence components behave in the same way in the transformer, regardless of the configuration [12].

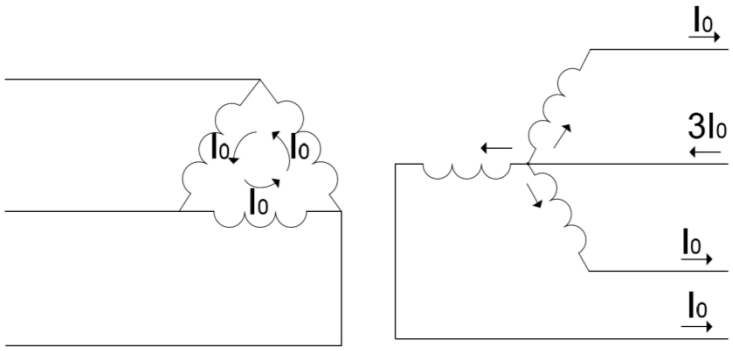

Figure 2-1. Circulating zero sequence current in delta winding

2.5 **Rooftop PV**

Recent years have seen a consistent growth of distributed PV sources. Distributed PV, like other DG sources, can be located at or near load points and provide benefits which traditional generation may lack. However, distribution systems were not designed to accommodate such power generation sources as these sources can lead to operational as well as power quality issues [30-32]. A high penetration of distributed PV resources may lead to bi-directional power flow resulting in voltage swells, increased losses and overloading of conductors. Voltage unbalance is a concern in distribution systems and the effect of single-phase residential PV systems on voltage unbalance needs to be explored.

The utilities try to minimise the unbalance index in their network by distributing single-phase loads equally across all three phases. Probabilistic studies have shown that it is very rare for the residential and small business loads to result in higher values of the voltage unbalance in the network. However, this can only be achieved if sound engineering judgements have been applied for selecting the appropriate size of the conductors and cables and transformer ratings. With load changes over time, it may be necessary to reallocate loads among the three phases following later observations and

measurements. If the appropriate designs have not been correctly done or there is an excessive voltage drop in the network, it is highly probable that the network also suffers from higher voltage unbalance.

Rooftop PVs that are currently being installed in Australia mainly depend on the outlook and financial condition of householders. Therefore, it can be expected that these installations are randomly placed along distribution feeders. For example, it is possible that 80% of customers on a phase have installed PVs, while the other two phases have only 50% and 10% installed. Under such a condition, even if the voltage unbalance of the network was within the standard limits without any PVs, it is not guaranteed to remain so. Therefore, the possible PV installation numbers or ratings of such systems must be investigated in such a way that the voltage unbalance is still kept within the standard limits.

2.6 **Mitigation of Voltage Unbalance**

Distributing single phase loads equally across all three phases can be a key voltage unbalance mitigation technique [33]. Balancing of electrical distribution systems can be performed by altering the system configuration through manual and/or automatic feeder switching operations to transfer loads among phases/feeders [34, 35]. The complete transposition of overhead lines can theoretically, cancel the unsymmetrical electromagnetic coupling effects and limit the voltage unbalance which arise due to line asymmetries [36]. However, these ideal conditions can rarely be achieved in practice due to economic constraints and practical difficulties. The implementation of more appropriate design options in terms of phase swapping and reconfiguration at transposition points of multi-circuit lines are therefore recommended [37].

In situation where high levels of voltage unbalance are unavoidable, special balancing equipment can be installed at the utility and/or plant level [38, 39]. Devices such as unified power quality conditioners (UPQC) [40], which are capable of compensating various power quality disturbances simultaneously, can be employed to mitigate voltage and current unbalance. Among custom power devices, the distribution static compensator (dSTATCOM) is the most popular and can inject reactive power to balance the supply side currents and to improve power factor.

2.7 **dSTATCOM**

dSTATCOM is a static VAR generator whose output can be varied so as to maintain or control certain specific parameters of the electric power system [41]. The dSTATCOM is a power electronic component that can be applied to the dynamic control of the reactive power and the grid voltage. The reactive output power of the compensator is varied to control the voltage at given transmission network terminals, thus maintaining the desired power flows during possible system disturbances and contingencies.

dSTATCOMs have the ability to address transient events at a faster rate and with better performance at lower voltages than a Static Voltage Compensator (SVC). The maximum compensation current in a dSTATCOM is independent of the system voltage. The dSTATCOM ratings are based on many parameters that are mostly governed by the intended duty. A STATCOM stabilising a wind farm will be designed to provide the amount of reactive power the system needs to recover and ride through typical faults on the power system and to reduce the interaction of other system equipment to prevent the wind turbines falling out of synchronism with the grid. Although the final rating of the dSTATCOM is determined by system economics, the capacity chosen will need to be at least adequate for the system to

stabilise after temporary system disturbances. The type of faults that the system is expected to recover from also determines the size of the dSTATCOM. For example, a three- phase impedance fault of low impedance requires a very high rating dSTATCOM while a high impedance short circuit fault needs a lower rating device to support the system during the fault and help recover after the fault.

Figure 2-2 shows the schematic diagram of a dSTATCOM connected to a three phase AC mains feeding three phase loads. Three phase loads may be a lagging power factor load or an unbalanced load or non-linear loads or mixed of these loads. For reducing ripple in compensating currents, interfacing inductors (L_f) are used at AC side of the voltage source converter (VSC). A small series connected capacitor (C_f) and resistor (R_f) represent the ripple filter installed at PCC in parallel with the loads and the compensator to filter the high frequency switching noise of the voltage at PCC.

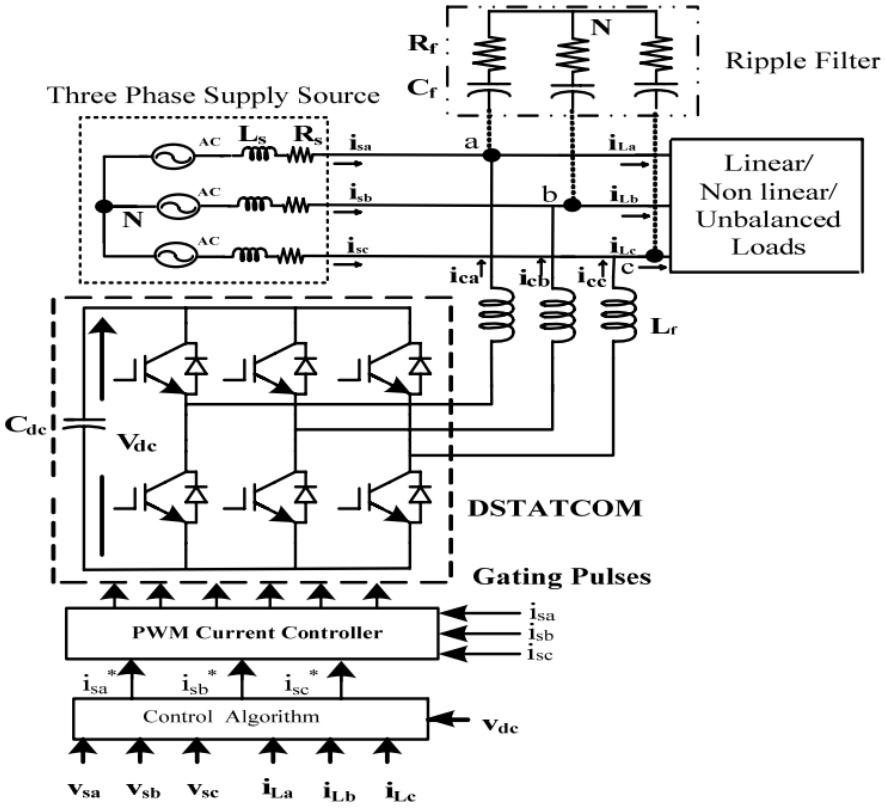

Figure 2-2. Schematic diagram of dSTATCOM [42]

In this thesis, dSTATCOMs are studied with respect to balance correction and the rating determined by the minimum values of negative sequence current that can be injected to bring the power system voltages to just within the statutory limits. The converter current ratings and the size of the DC bus capacitors of the dSTATCOM also decide the capability of the dSTATCOM. Although Figure 2-2, show a three phase-three wire system, the dSTATCOM envisioned in this work assumed a three phase-four wire connection which can compensate the negative and positive sequence voltages and currents. The negative sequence currents are detected in a reverse rotating synchronous dq frame and the components are forced to zero using PI control loops. Zero sequence compensation is performed using a sine cosine transformation that reduces the zero sequence currents to DC terms [43].

2.7.1 Location of dSTATCOM

Often a dSTATCOM is placed as close as possible to a significant load bus for various reasons. The first reason is that the location of the negative sequence and/or reactive power support should be as close as possible to the point at which the support is needed. Secondly, in the studied test system the location of the dSTATCOM at the load bus is more appropriate because the effect of voltage change is the highest at this point. In a distribution network, there are generally a number of load buses and some study is determined to find which buses are the most significant. The location of the dSTATCOM is based on quantitative benefits evaluation. The main benefits of using a dSTATCOM in a system are improved balance, reduced losses and increased maximum transfer capability. The location of the dSTATCOM is generally chosen to be the location in the system which needs negative sequence or reactive power. To place a dSTATCOM at any load bus can reduce the reactive

power and negative sequence flow through the lines, thus, reducing line current and also the I^2R losses.

2.8 **Radial Load Flow**

One of the most important tools for the power engineer is the *power flow,* or *load flow,* study. The power flow study is the basic calculation used to determine the state of a given power system operating at steady state under the specified conditions of power input, power demand, and network configuration. Minimum requirements of a load flow solution will vary, depending on whether the power system under study is a transmission or distribution network. Exemplifying this, power flow in transmission networks is usually balanced and the network structures likely to contain meshed or looped lines. Therefore, it is sufficient to represent transmission systems as single-phase components. On the other hand, distribution networks typically accommodate single/dual/three-phase loads and four-wire cables/lines so that load flow solutions shall handle unbalanced power flow with three-phase modelling of network components. Since distribution networks mostly operate in radial structure, more straightforward and convergence guaranteed load flow solutions can be employed by taking advantage of this structure.

2.8.1 Forward Backward Power Flow

A three-phase power flow method, suitable for radial and unbalanced distribution systems, is implemented in MATLAB for this work, based on the development of two basic matrices, which relate the bus injections to branch currents and the branch currents to bus voltages [44]. The Backward Forward Sweep (BFS) method is the most suitable solver due to its simplicity and better convergence performance compared to Gauss-like and Newton-Raphson based methods under the assumption of radial network structures. The main advantage of the BFS algorithm is

the straightforward implementation of Kirchoff's current and voltage laws on the feeders. In this way, branch currents and bus voltages are updated by traversing between the root (source or slack) bus and end buses in an iterative way (Figure 2-3). Specifying initial bus voltages and nominal ratings of shunt components (loads, capacitor banks, and generators), backward sweep updates branch currents by summation of child branches and shunt currents from end nodes towards the root node. Similarly, starting from the specified root bus voltage and knowing the branch currents from the previous backward sweep, bus voltages are updated from the root node towards end nodes by means of voltage drops along the branches. Consecutive backward-forward sweeps are terminated when the difference between resulting bus voltage magnitudes based on the previous iteration are less than the predetermined tolerance value.

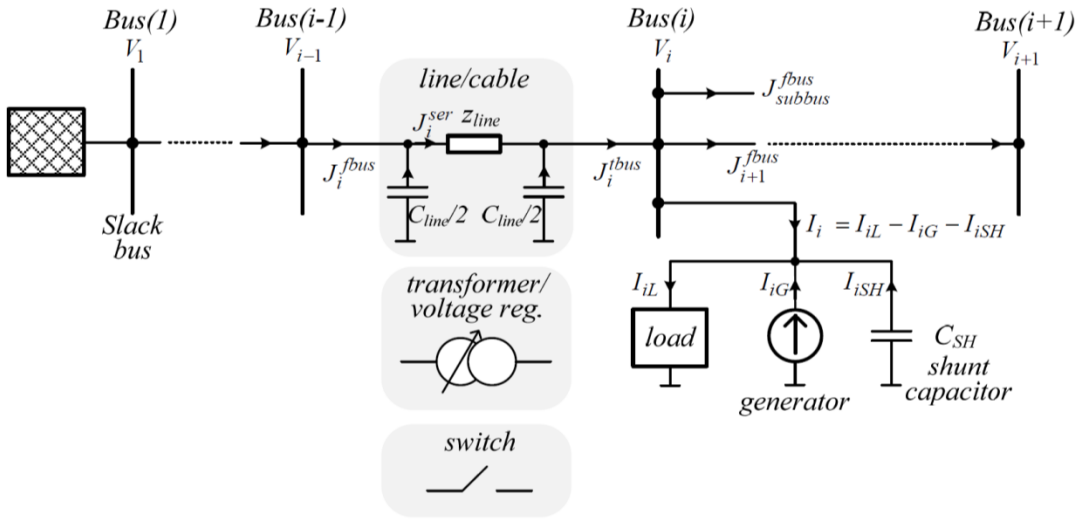

Figure 2-3. Two-bus and single-line representation of distribution networks for the solution of BFS algorithm [45]

2.8.2 Component Models

Realistic mathematical representations for each of the system components are needed in order to achieve accurate and meaningful results from the power flow study. Detailed models for distribution system components such as line sections,

transformers, and loads can be found in [46]. A brief summary of some of these typical three-phase models is given below.

2.8.3 Conductor Model

Low voltage distribution feeders are typically constructed with four-wire line segments where the fourth wire is the neutral wire. Unsymmetrical spacing between phase conductors without transposition is a very common property of distribution lines. It is likely to produce unequal voltage drops among the phases, even though power flow is balanced along a distribution line. For this reason, unbalanced three-phase load flow solution will require accurate modelling of distribution lines for the steady-state voltage analysis.

Carson's line equations have been used to generate a series impedance matrix for the given line/cable configuration in this work. Figure 2-4 depicts typical three-phase four-wire overhead line and its equivalent circuit. The LV line admittance matrix of the test system is given below using a 4X4 matrix model, which in turn is reduced to a 3X3 matrix using the Kron reduction method [47]:

$$\left[Z_{ij}^{abcn}\right]=\begin{bmatrix} z_{ij}^{aa} & z_{ij}^{ab} & z_{ij}^{ac} & z_{ij}^{an} \\ z_{ij}^{ba} & z_{ij}^{bb} & z_{ij}^{bc} & z_{ij}^{bn} \\ z_{ij}^{ca} & z_{ij}^{cb} & z_{ij}^{cc} & z_{ij}^{cn} \\ z_{ij}^{na} & z_{ij}^{nb} & z_{ij}^{nc} & z_{ij}^{nn} \end{bmatrix}$$

$$\left[Z_{ij}^{abc}\right]=\begin{bmatrix} z_{ij}^{aa-n} & z_{ij}^{ab-n} & z_{ij}^{ac-n} \\ z_{ij}^{ba-n} & z_{ij}^{bb-n} & z_{ij}^{bc-n} \\ z_{ij}^{ca-n} & z_{ij}^{cb-n} & z_{ij}^{cc-n} \end{bmatrix}$$

where $\hat{Z}_{ii} = R_i + j0.12134.f.\left(\ln\frac{2h_i}{GMR_i}\right)$ $\hat{Z}_{ij} = j0.12134.f.\left(\ln\frac{\sqrt{d_{ij}^2+(h_i+h_j)^2}}{d_{ij}^2+(h_i-h_j)^2}\right)$

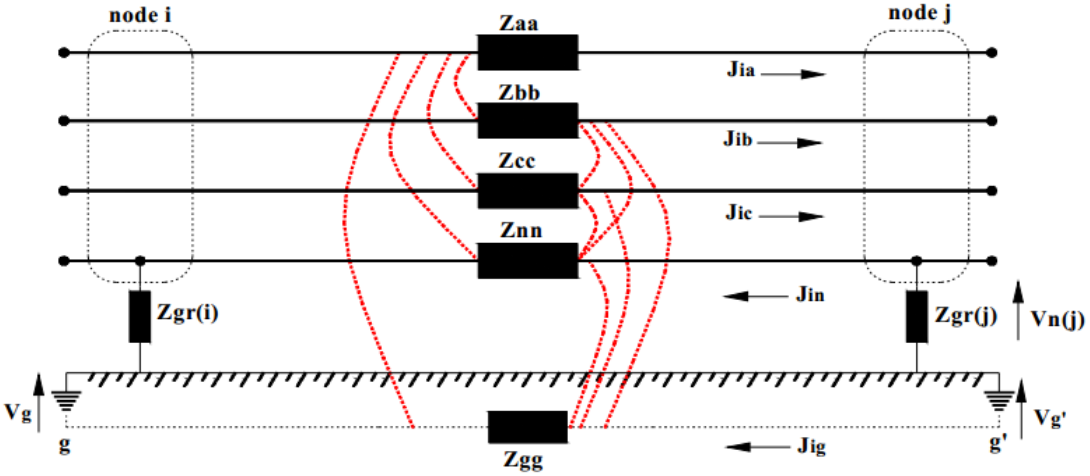

Figure 2-4. Model of the three-phase, four-wire multi-grounded distribution line, based on the model proposed in [46]

2.8.4 Transformer Model

It is important to have a realistic three-phase representation of the transformers found in distribution systems in order to analyse their effects on system loss. Each of the MV/LV transformers feeding the LV networks studied in this thesis has a rating of 200-500 kVA. The transformer has an impedance of 5%, an X/R ratio of 15, and is equipped with off-load taps in the HV winding. Transformer taps were assumed to move the voltage on the secondary side of the transformer as close as possible to the voltage set point. The transformer's connection type is D-yg, (i.e. a delta-connected HV primary and a wye-connected LV secondary winding). All transformers were assumed to be solidly grounded on the LV side of the transformer. The three-phase admittance matrix for the transformer was formed by taking into account the positive, negative, and zero-sequence admittances of the transformer, and described in detail in [46].

In this work, nodal admittance matrix-based transformer modelling tailored for BFS load flow algorithm has been developed. It will be assumed that the secondary

side line-to-line voltages are lagging the primary side line-to-line voltages by 30º which represents the prevalent class of transformers (D-yg1) in Australia (Figure 2-5). In this respect, secondary side terminal currents will be also lagging the primary side terminal currents by 30º. As another assumption, the magnetising impedance of the transformer is sufficiently high to be neglected as compared to leakage impedance. Furthermore, each primary-secondary phase winding is assumed to be formed by separate and identical single-phase transformers.

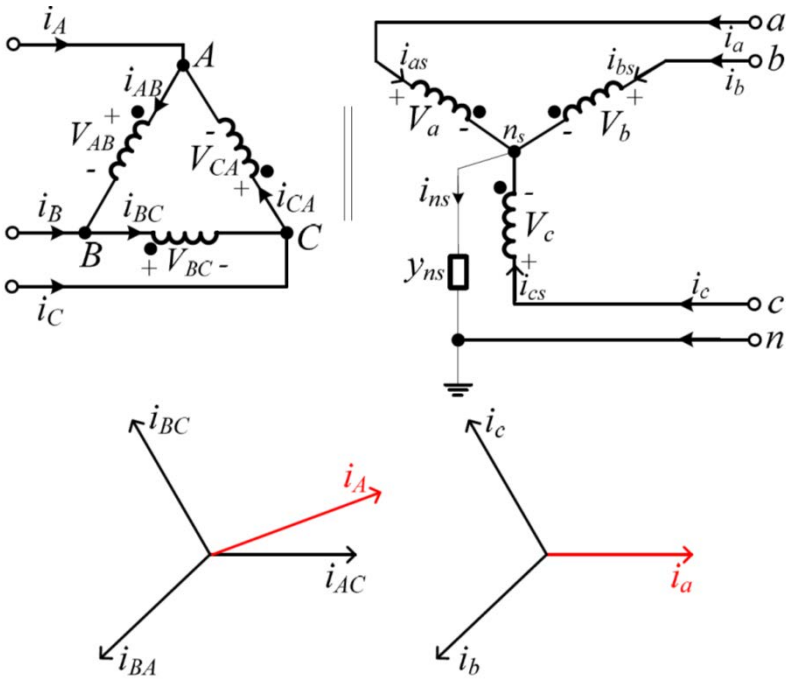

Figure 2-5. D-yg1 transformer bank connection and its positive-sequence current [46]

2.8.5 Load Model

For the purpose of analysing the steady-state behaviour of a distribution system the customer loads are assumed to be constant complex power elements. In other words, load buses are modelled as PQ specified buses. In this work, 15-minute intervals are used, so a daily load curve is made up of 96 pairs of time and demand values. In order to guarantee a representative set of field data, a total of 365 days of measurements were collected from operating smart meters from the high PV

penetration trial in Perth. A snapshot of all customers load profiles (current) is shown in Figure 2-6.

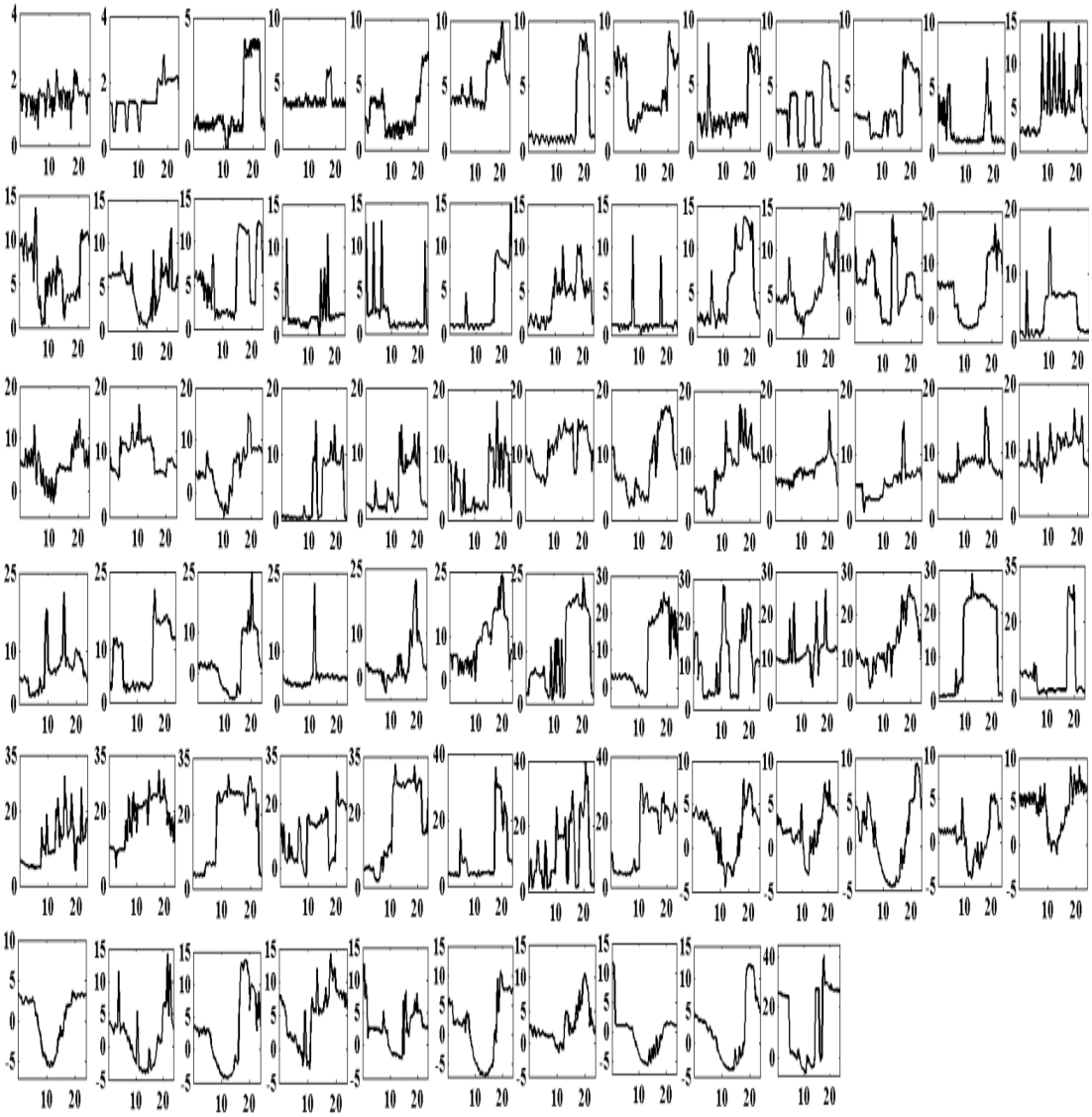

Figure 2-6. A typical daily load profile of each of 75 customers on Pavetta. (vertical axis: Current (A) horizontal axis: Time (Hours))

2.8.6 Slack Bus

The slack bus was assumed to be represented by an asymmetrical source, its three-phase magnitude was based on the actual measurement from the field transformer 15-minute data logger.

2.9 **Optimisation Methods for Power System Problems**

A variety of optimisation methods exist in the literature for solving power system problems. These optimisation methods can be divided into two main groups: analytical-based methods and heuristic-based methods. The simplest analytical method is linear programming which is employed when the objective function and constraints are linear. This method has been applied to various problems such as, power system planning and operation and optimal power flow [48, 49]. Since some or all variables are discrete, the integer and mixed-integer programming techniques were introduced into power system analysis. These techniques have been used for planning and expansion of distribution and transmission networks [50, 51]. The objective function associated with most of the power system problems contains nonlinearity. The analytical techniques for power system optimization are highly sensitive to initial values and frequently get trapped in local minima particularly for the complex problems which have nonlinearity and discreteness [52]. This has led to the need for developing another class of optimisation methods, called heuristic methods. GA is a search technique for finding the approximate solutions to the optimisation problems. This technique is inspired by evolutionary biology, such as mutation and crossover [53]. PSO is a population-based and self-adaptive technique introduced originally by Kennedy and Eberhart [54]. This algorithm handles a population of individuals in parallel to search capable areas of a multidimensional space where the solution is searched. The individuals are called particles and the population is called a swarm. Particles as the variables are updated during the optimisation procedure.This method is not highly sensitive to the size and nonlinearity of the problem and can converge to a reasonable solution where analytical methods fail [55]. That is why a number of papers have been published in

the past few years based on this optimisation method, such as in the allocation of DG in distribution networks, planning of dSTATCOMs and loss minimisation [55-57].

Figure 2-7 shows a summary of optimization techniques that were discussed so far. Evolutionary optimization algorithm is very sensitive to the initial feasible values may be termed as initial population selected to start the search procedure. A heuristic search method can be proposed for the selection of initial values to start the search which should not be a cumbersome procedure[58]. The methods are also sensitive to the parameter tuning. The search techniques easily work even if the objective function is non-convex, discontinuous and non-differential at some points. Other population based optimization techniques such as particle swarm optimization, and evolutionary Programming sometimes struck to local minimum solution [58]. This issue can be resolve through the use of modified particle swarm optimization and it can combines both local and global population to achieve the best result for the give constraint and objectives.

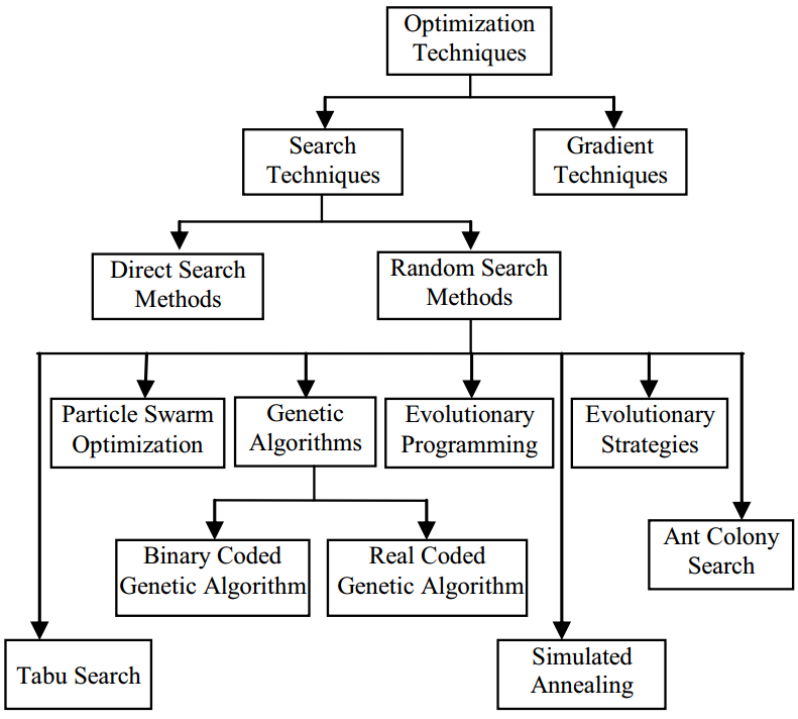

Figure 2-7. Classification of optimization techniques [58]

The main aim of distribution networks planning is to minimise an objective function composed of the line loss cost, reliability cost, and the investment cost. Since the line loss and system reliability values have a nonlinear relation with the element sizes and given that the size of elements is discrete, the planning problem is highly nonlinear and discrete. Additionally, a large number of variables should be optimized during the planning procedure. All these characteristics ensure that the planning problem is a complex problem. Given that, PSO is a reliable optimisation method in the literature, and the core of this research is dealing with a multi objective problem (reducing the voltage unbalance and improving voltage magnitude while performing the least number of phase swaps or installing smallest size dSTATCOM). The particle swarm optimisation method is employed in this work for solving the distribution system-planning problem. In chapters 5 and 6, a modification is applied to the PSO method to increase the diversity of the optimising variables.

2.9.1 Particle Swarm Optimisation (PSO)

PSO is a population-based and self-adaptive technique. This algorithm handles a population of individuals in parallel, to search feasable areas of a multidimensional space where the solution is searched [54]. The individuals are called “particles” and the population is called a “swarm”, which is randomly generated. Each particle in the swarm denotes a possible solution of the optimisation problem. With a random velocity, each particle moves through an M-dimensional search space [56]. Particles describe the solution variables and are updated during the optimisation procedure. In the discrete version of PSO, the solution can be reached by rounding off the actual particle value to the nearest integer during the iterations. In [55], it is mentioned that the performance of the PSO is not influenced by this rounding-off process.

The balance between the global and local search throughout the run makes PSO a successful optimisation algorithm. In past several years, PSO has been successfully applied in many research and applications areas [108]. It is demonstrated that PSO gets better results faster when compared with other methods. Also in order to minimise the computational burden, this work has been solved using PSO instead of the classic method mentioned in [109]. The Modified Particle Swarm optimisation (MPSO) will be discussed in further detail in the next section.

2.9.1.1 Modified Particle Swarm Optimisation (MPSO)

The distribution system allocation and sizing problem has a discrete nature with several local minima. This highlights the importance of selecting a proper optimisation method. Modified discrete particle swarm optimisation as a heuristic method is introduced in this research to solve this complex problem. In normal PSO, a particle searches in the region of its neighbours in order to discover the one with the finest result so far, and uses information from that source to change its search in a promising direction. However, there is no assumption that the best neighbour at a given time has actually found a better region than the second or third best neighbours. Important information about the search space may be neglected through overemphasis on the single best neighbour [110]. The main features of the proposed MPSO algorithm are the usage of a primary PSO loop, a secondary PSO loop, and applying the mutation function. It will be observed that the results obtained by conventional PSO are improved when the crossover and mutation operators are included in PSO procedure. Furthermore, the robustness of the optimisation method is improved by this modification. This is mainly because these operators increase the diversity of variables. Figure 2-8 shows the flow chart of the proposed method. The description and comments of the steps are presented in the following section.

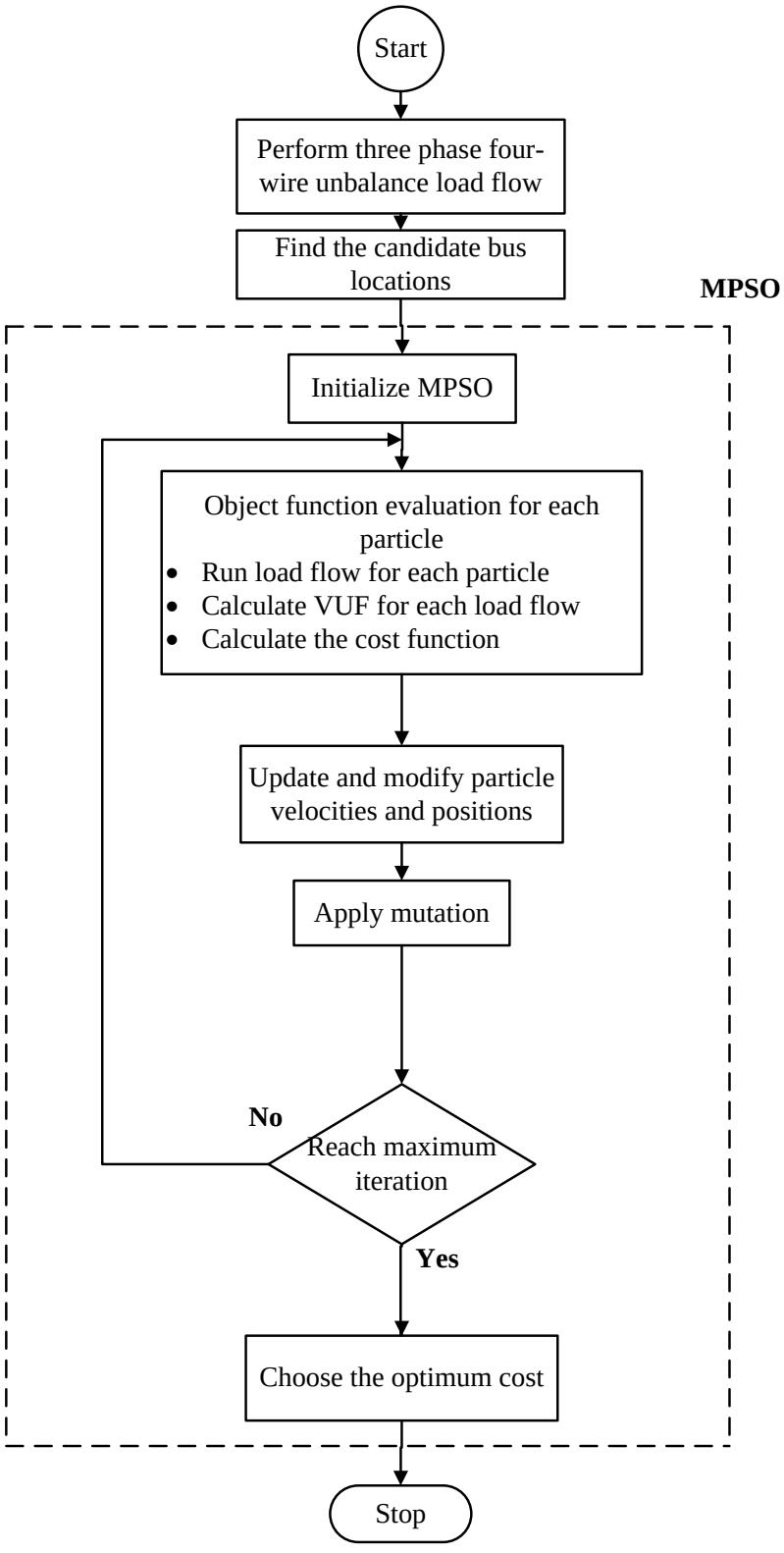

Figure 2-8. Flow chart of the proposed MPSO method

2.10 **Summary**

In this chapter, a brief review is presented based on the previous research work on voltage unbalance effects. It also provides general information in relation to voltage unbalance, which includes definitions, sources and mitigation techniques.

The chapter has discusses the IEC and IEEE definitions of voltage unbalance factor and the importance of including the phasor angle of voltage unbalance in the form of CVUF. Methods for the development of radial load flow that is capable of analysing an unbalanced, three-phase four-wire LV feeder, are described, establishing the background information relevant to the remaining chapters. Further, established approaches on the VU mitigation techniques are summarised to identify extended research scope for the development of comprehensive methodologies for cost effective techniques to improve voltage profile in MV/LV residential feeders, which is strongly linked to the main objective of this thesis.

Chapter 3 Phase Identification in a Three Phase LV Distribution Network

A new method for automatically identifying the phase of each customer by correlating voltage information from the utility's transformer system with voltage information from customer smart meters is introduced in this chapter. The technique was tested on an existing residential low voltage distribution system in Western Australia.

3.1 **Introduction**

While utilities usually have knowledge of the grid topology, accurate information regarding the connectivity at the LV consumer side of the network is variable. In some cases the phase may be recorded when connecting a new house however this is not always possible due to the remoteness of the distribution transformer or a lack of phase identification in cables or bundled conductor systems. Furthermore the information typically deteriorates over time due to maintenance and repair. There is considerable motivation to ensure an accurate record of phase per household. These motivations are based on improving the efficiency of the electrical network, extending the lifetime of assets and facilitating the infusion of renewable energy within the grid.

The operator may compute the load carried by a transformer as a collective three-phase load. Unfortunately this does not highlight that one phase may be experiencing a significantly higher load in comparison to the other phases. Depending on customer demands, and how they are assigned to different phases, loads on the three phases of a transformer can remain continually unbalanced. By

identifying their phase, households may be reassigned to a different phase so that load is more evenly balanced between the phases, thus reducing power loss and improving the operational efficiency of the network.

In order to improve the reliability and efficiency of the electric power grid, utility distribution systems are being made increasingly intelligent. Advanced monitoring and management technologies are being deployed. More recently energy distributors have commenced upgrades of manually-read analogue household meters with automated smart meters that communicate meter readings with greater frequency back to the distributors [59-61]. Collectively these initiatives form a key component of many smart grid transformations that energy distributors are undertaking.

With smart grid driving the uptake of artificial intelligence, telecommunication and power electronics equipment in power systems, it is becoming easier to envisage automation of the phase and load balancing problem [59]. The automation implementation will be technically advantageous as well as economical for the utilities and the customers, in terms of the reduction in cost and better service quality, respectively [60].

Unbalanced feeders not only increase power losses but also affect power quality. Imbalances also lead to overheating and consequently, shorten the lifespan of the grid assets such as transformers [62-65]. Another outcome for phase identification is to facilitate the introduction of distributed energy generation at the households [65]. The excess energy generated at the households can be injected back into the network over one of the three phases. Hence, the need to determine phase is important to ensure a balanced infusion of power into the grid. The reasoning for

balancing this is similar to the distribution of energy in the other direction from the grid to the households.

Accurate knowledge of the phase connection at the household level allows operational improvements such as rebalancing three phase distribution transformers and feeders to reduce both system losses and voltage unbalance factors. Selective rebalancing will allow higher levels of rooftop PV generation to be accepted into residential networks. Automatic phase identification is the precursor to intelligent automated systems that will detect unbalance issues and recommend optimal reconfiguration solutions.

3.2 **Phase Identification Approach**

Several potential methods for customer phase identification were considered before voltage correlation was selected for further study. The present approach was selected for initial study because it did not necessarily require any additional field equipment or functionality that could not possibly be supported by existing smart systems.

This study is constructed on the hypothesis that the voltage profile of a consumer is well correlated with the voltage profile on the same phase of the transformer. The correlation between two signals (cross correlation) is a standard approach to feature and signal detection [66-68] as well as a component of more sophisticated techniques [69]. In this work we consider the short time variation in the voltage signal, if the transformer voltage profile is x(t) and y(t) is the consumer main voltage profile it could be described by:

$$x_i(t) = X_i + \tilde{x}_i(t) \tag{3.1}$$

where $X_i = 1/T \int_0^T x(t)dt$ and T is our observation period.

$$y_i(t) = Y_i + \tilde{y}_i(t) \tag{3.2}$$

where $Y_i = 1/T \int_0^T y(t)dt$ and T is our observation period.

Similarity between two signals can be calculated using cross-correlation:

$$R_{\tilde{x}_i \tilde{y}_i}(t) = \tilde{x}_i(t) * \tilde{y}_i(t) \tag{3.3}$$

$$R_{\tilde{x}_i \tilde{y}_i}(t) = \frac{1}{T} \int_0^t \tilde{x}_i(t-\tau)\tilde{y}_i(t) \tag{3.4}$$

where T is the observation time and it could be normalized as follows

$$-1 \le \frac{R_{\tilde{x}\tilde{y}}(\tau)}{[R_{\tilde{x}\tilde{x}}(0) R_{\tilde{y}\tilde{y}}(0)]^{1/2}} \le 1 \tag{3.5}$$

where $R_{\tilde{y}\tilde{y}}(0)$ and $R_{\tilde{x}\tilde{x}}(0)$ are the mean square values of the signals ỹ and x̃, respectively.

Correlation is the optimal technique for detecting a known waveform in random noise. That is, the peak is higher above the noise using correlation than can be produced by any other linear system. (To be perfectly correct, it is only optimal for random white noise). The cross correlation function measures the dependence of the values of one signal on another signal. The voltage measurements contain a wanted component and a disturbance component. Concerning the noise the resulting cross-correlation is:

$$\tilde{x}(t) = x_\omega(t) + z(t) \tag{3.6}$$

$$\tilde{y}(t) = y_\omega(t) + z'(t) \tag{3.7}$$

where $x_{\omega}(t)$ and $y_{\omega}(t)$ are the desired signals and $z(t)$ $z'(t)$ are the Gaussian noise.

$$R_{\tilde{x}\tilde{y}}(t)=R_{x_{\omega}y_{\omega}}+R_{x_{\omega}z'}+R_{y_{\omega}z}+R_{zz'} \tag{3.8}$$

Impedance based voltage drops contribute significantly to disturbances z(t) and ź(t) but a possibly Gaussian component occurs in any physical measurement. The above formula does converge to $R_{X_{\omega}Y_{\omega}}$ for increasing integration time, because the other terms have an expected value of zero when the signal and the noise sources are uncorrelated. It can be shown that the effective noise power added by the system decreases by 1.5 dB for every doubling of measurement time and can be reduced by as much as 50 dB [70, 71].

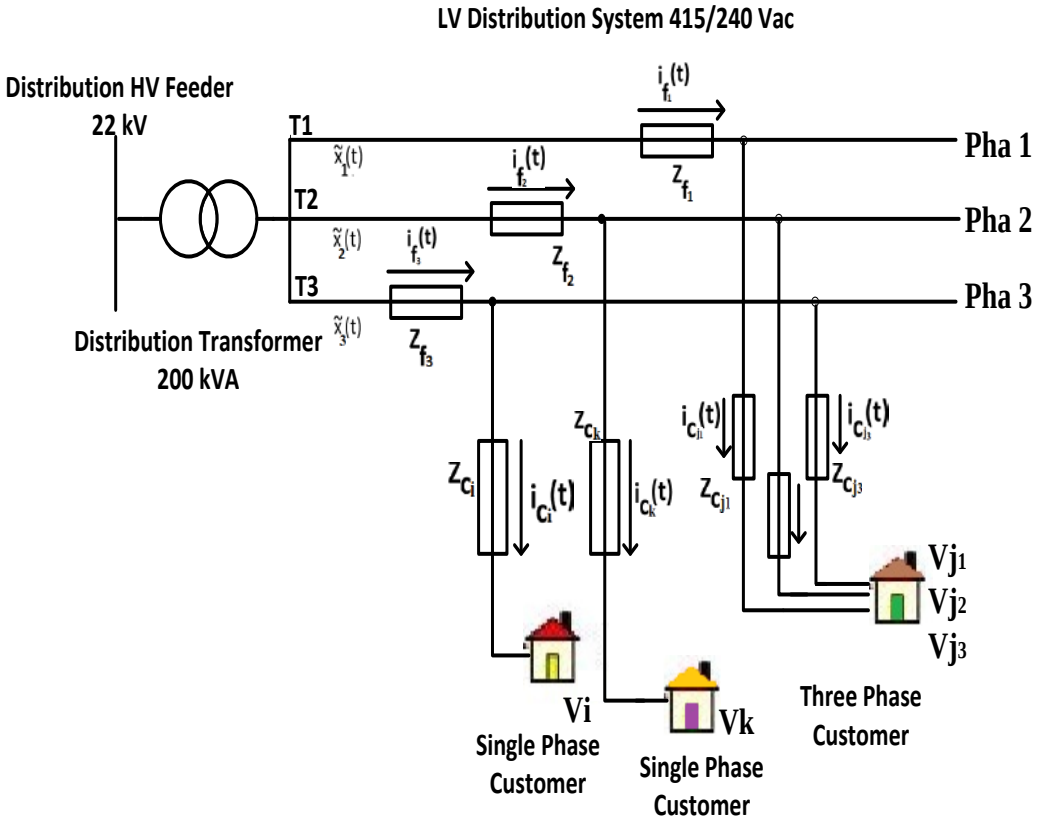

Figure 3-1. Simplified diagram of network under study

3.3 **The Perth Solar City Project**

Perth Solar City is a research program funded by the Australian Government Department of Climate Change and Energy Efficiency. As part of the Perth Solar City program, Western Power, the regional transmission and distribution network services provider, undertook a technical trial to understand the impact of large numbers of solar photovoltaic systems on the electricity distribution network. A low voltage feeder, “Pavetta 1”, in the suburb of Forrestfield, was selected by Western Power after desktop audits and site visits for the high penetration trial. The 400/230V feeder site, shown in Figure 3-2, is supplied from a 200 kVA 22 kV/400 V distribution transformer (Figure 3-3) and includes 77 consumers. Of these, 34 consumers have rooftop PV systems that have average ratings of 1.88 kW. Total rated PV installation capacity is 63.92 kW representing a penetration on the branch of 32%.

In the context of this thesis, the PV penetration level is defined as “capacity penetration”. Capacity penetration is the ratio of the nameplate rating of the transformer capacity to the peak PV rating.

Figure 3-2. Perth solar city high penetration feeder site, image courtesy Western Power

Figure 3-3. Pole-mounted transformer and data logger under study (Pavetta TX1)

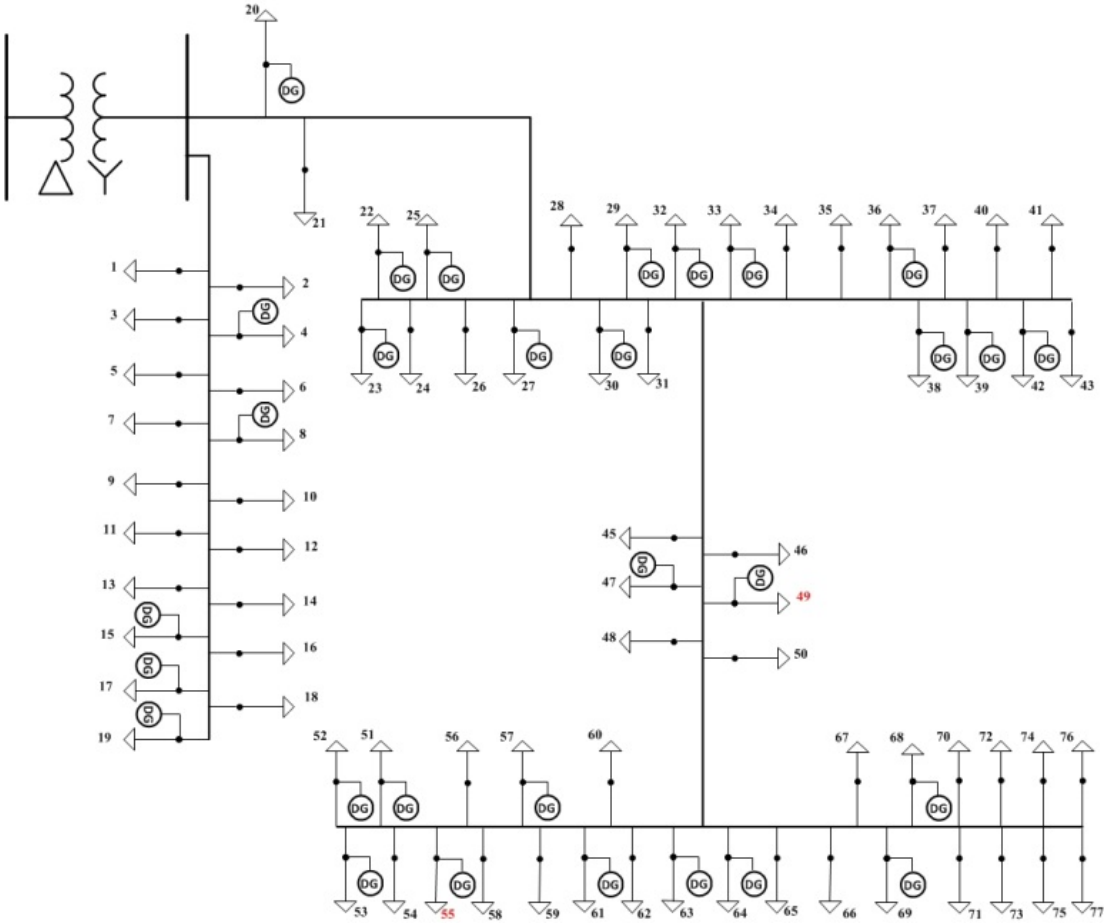

Figure 3-4. Pavetta feeder diagram

The feeder under study is an aerial, three-phase, multiple earthed neutral (MEN) construction (Figure 3-4). Load data, including energy consumption, voltage and current is recorded by smart meters on the Western Power network at the point of connection to each consumer switchboard in 15-minute intervals. Smart meter data has been collected since July 2011, and transformer data from a dedicated data logger system has been collected from July 2011 at 5-minute intervals. At the time of the recording there were 2 three-phase meters (49 and 55, highlighted in red in Figure 3-4) that were not active and no recording is available for these meters.

3.4 **Experimental Results**

Two different cases are evaluated in this section. In the first case, the phase identification technique is based on the availability of the voltage data from both

individual customers and the transformer phase voltages. The required data resolution is 15-minutes and the duration of the recorded data is one week. In the second case, it is assumed that no data is available from the transformer logger and only customers' voltage data is available for phase identification.

3.4.1 Phase Allocation Based on Transformer Data

The utility provider in the region (Western Power) did not confirm the correct phase of houses at the beginning of this study. In addition, there were eight units (Figure 3-4, loads 69-77), each with individual smart meters, connected to the distribution pole by a three-phase overhead consumer mains but for which the phase was not known. For these reasons, the phases of all meters had to be verified and confirmed. This task was achieved by attempting to profile the voltage of each individual house along the feeder and verifying phase voltages against known phase voltages of the transformer. To confirm that the correlation between the phases exists, an auto-correlation and cross-correlation have been performed on the voltage profile of the three-phase transformer over the period of one-week and the results are shown in Figure 3-5.

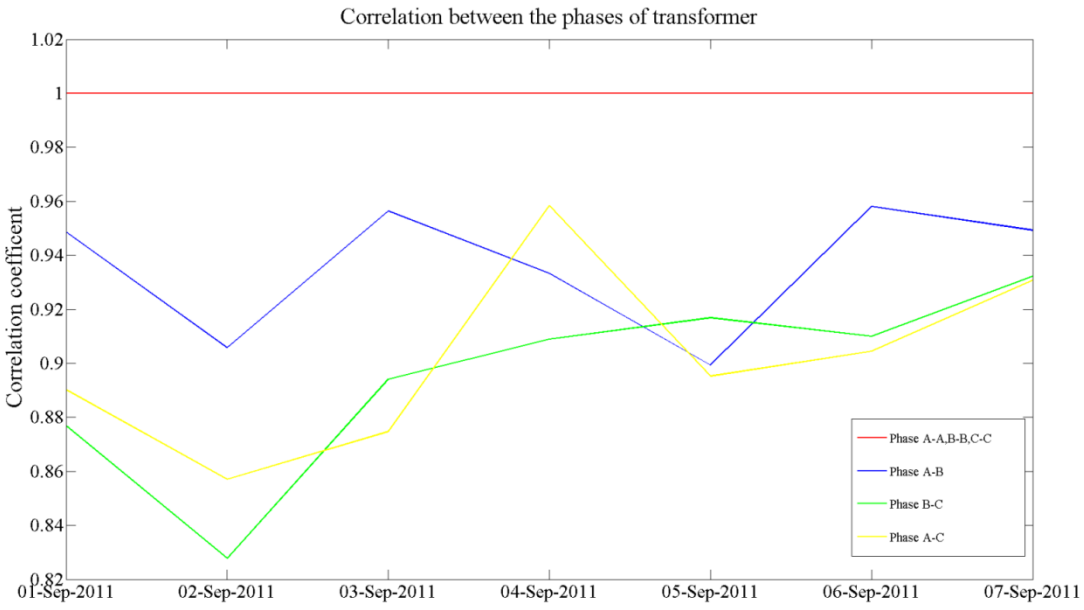

Figure 3-5. Auto-correlation & cross-correlation of transformer phase voltages 1st-7th September 2011.

In order to compare the smart meter and transformer voltage signal cross-correlation, the seven-day voltage profiles of the 51 single phase houses, 24 three-phase houses and the voltage profile on each phase of the distribution transformer were recorded. The average voltage for each phase of the transformer over the seven days is calculated, as well as their variance. Next, the signal segments that contain the transformer average voltage sequence are extracted from the simultaneously received smart meter voltage signals and are cross correlated with the variable signal of phases A, B and C of the transformer.

The amplitude of each sample in the cross-correlation signal is a measure of how much the received signal resembles the target signal, at that location. This means that a peak will occur in the cross-correlation signal for every target signal that is present in the received signal. The value of the cross-correlation is maximised when the target signal is aligned with the same features in the received signal. Figure 3-6 illustrates the procedure to perform the cross-correlation. For the single-phase load, it is a simple three-way correlation test with each phase of the transformer (Figure 3-7a). In the case of the three-phase load the cross-correlation will be performed on the six combinations shown in Figure 3-7b and the three combinations with the highest cross-correlation will be picked as the correct phases.

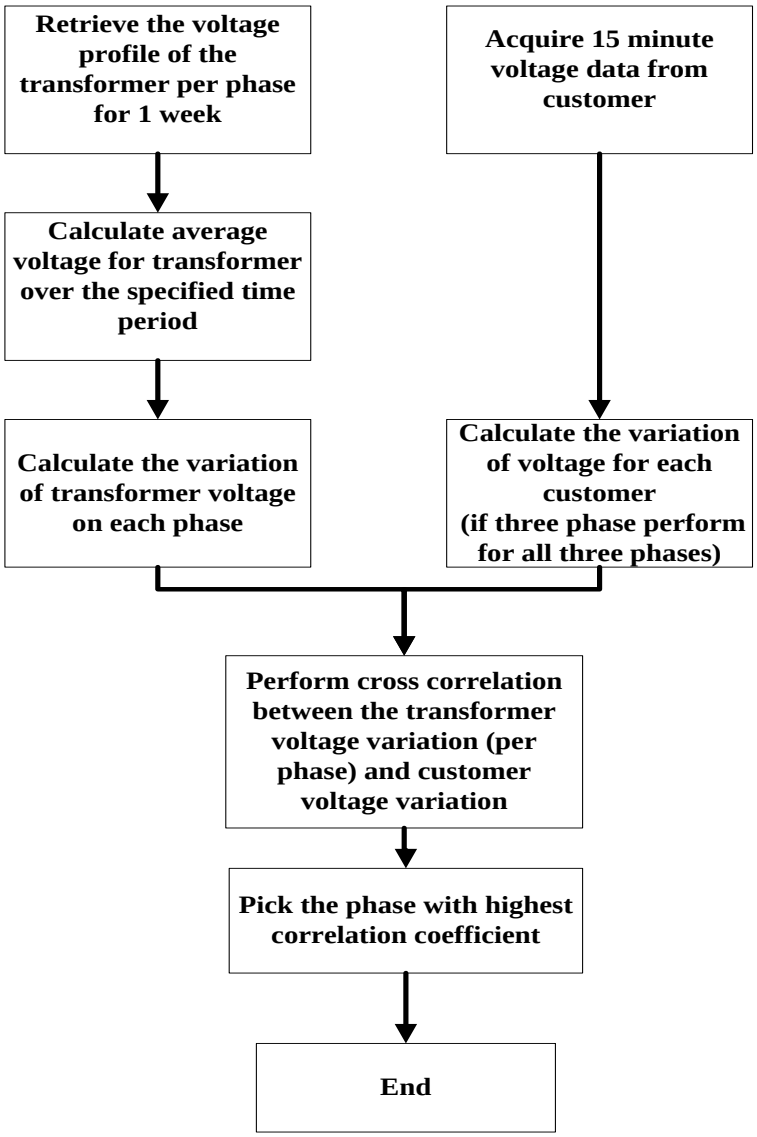

Figure 3-6. Flow chart of phase identification based on cross correlation

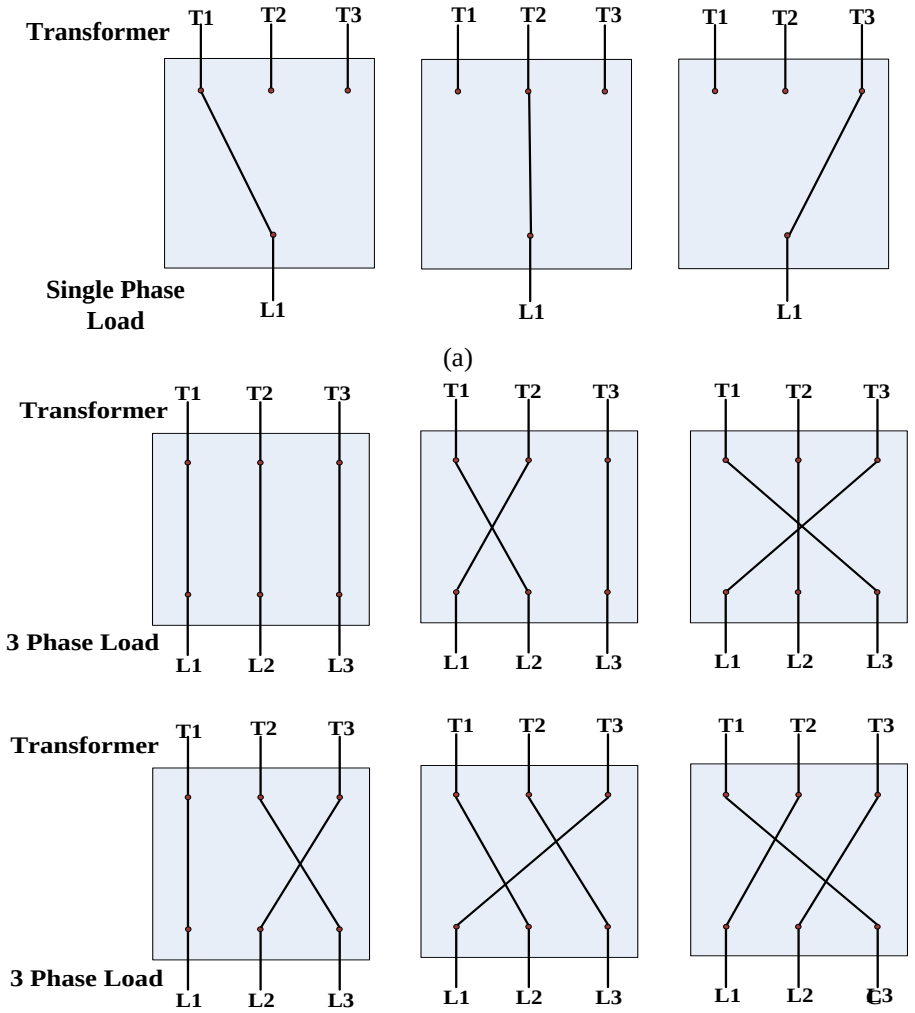

Figure 3-7. Cross-correlation of three-phase and single-phase house with transformer

3.4.2 Phase Allocation Based on Three-Phase Meter Data

The next step is to assess the ability of the introduced method to work based on grouping the houses with each other into three separate groups which then would be compared with the phases A,B and C of the transformer. In this case a reference three-phase house is selected (preferably with close proximity to the transformer). This three-phase meter is then used as the basis for identifying the phase connection of the rest of the three-phase houses. The average series voltage for each phase of the reference three-phase house over the seven days is calculated, as well as their variance. Next, the signal segments that contain the reference three-phase house average voltage sequence are extracted from the simultaneously received smart meter

voltage signals and are cross correlated with the variable signal of phases M1, M2 and M3 of the reference three-phase household. The amplitude of each sample in the cross-correlation signal is a measure of how much the received signal resembles the target signal, at that location. This means that a peak will occur in the cross-correlation signal for every target signal that is present in the received signal. The value of the cross-correlation is maximised when the target signal is aligned with the same features in the received signal.

The abovementioned procedures were performed on all of the 75 houses available (there are 77 houses connected to this feeder but at the time of this work, two meters were out of the trial and no data was available for them). Table 3-1 and Table 3-2 summarise the allocation of the 51 single- phase and 24 three-phase meters respectively. Table 3-3 shows installed PV capacity on each phase of the transformer as well as the penetration level on each phase. Smart meter load data on the Pavetta LV feeder and the result of the phase identification is shown in Figure 3-8 and Figure 3-9 for the period of one week (21 -27 January 2012), and one day (25 January 2012), respectively.

Table 3-1. Allocation of the single-phase houses

House No	Group	House No	Group	House No	Group	House No	Group
1	2	**17**	1	**37**	3	**59**	2
2	1	**18**	2	**39**	3	**60**	3
4	2	**19**	3	**40**	1	**62**	3
5	3	**20**	1	**41**	2	**65**	3
6	1	**22**	3	**42**	3	**70**	1
7	2	**24**	1	**43**	3	**71**	2
8	3	**27**	3	**45**	2	**72**	3
10	2	**28**	3	**48**	2	**73**	3
12	1	**29**	2	**50**	3	**74**	2
13	2	**31**	1	**51**	2	**75**	1
14	3	**33**	1	**54**	2	**76**	2
15	3	**34**	1	**55**	3	**77**	1
16	2	**36**	1	**57**	3		

Table 3-2. Allocation of the three phase-houses

House No	Phase A	Phase B	Phase C	House No	Phase A	Phase B	Phase C
3	1	2	3	**47**	1	2	3
9	1	2	3	**49**	1	2	3
11	1	2	3	**52**	1	2	3
21	1	2	3	**53**	1	2	3
23	1	2	3	**56**	1	2	3
25	1	2	3	**58**	1	2	3
26	1	2	3	**61**	1	2	3
30	1	2	3	**63**	1	2	3
32	1	2	3	**64**	1	2	3
35	1	2	3	**66**	1	2	3
38	1	2	3	**67**	1	2	3
44	1	2	3	**68**	1	2	3
46	1	2	3	**69**	1	2	3

Table 3-3. Solar PV system connections on LV network (Pavetta)

Customer Connection Phase	No of Customers	No of PV Customers	PV Capacity Installed (kW)	PV Penetration by Transformer Capacity
3 phase	26	15	26.3	13.1%
Phase A (Red)	26	6	11.8	5.9%
Phase B (Green)	26	5	9.45	4.7%
Phase C (Blue)	26	4	5	2.5%
1 phase	51	19	37.5	18.8%
Phase A (Red)	14	4	7.8	4.0%
Phase B (Green)	17	4	7.8	4.0%
Phase C (Blue)	20	11	18.4	9.2%
Total	77	34	63.8	31.9%

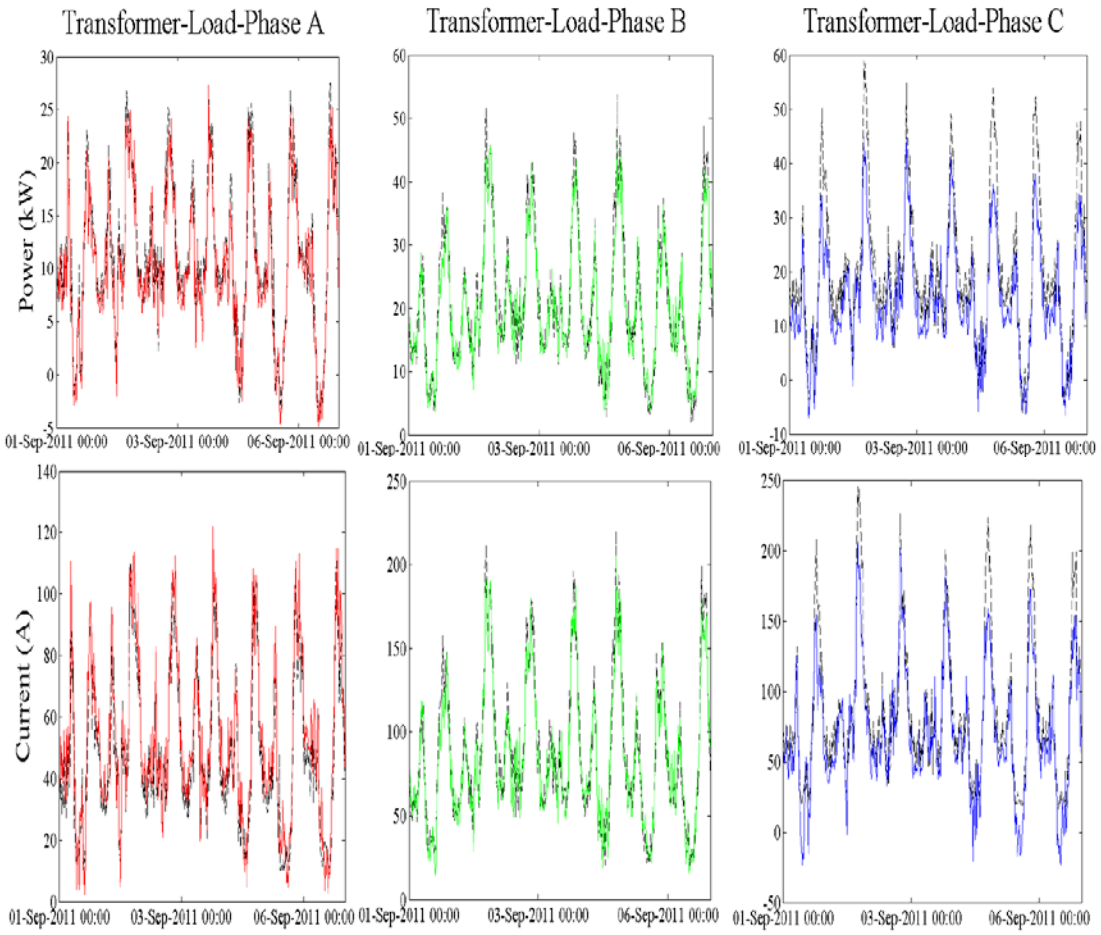

Figure 3-8. Comparison of aggregation of correlated meters with transformer reading, power and current (21-27 January 2012)

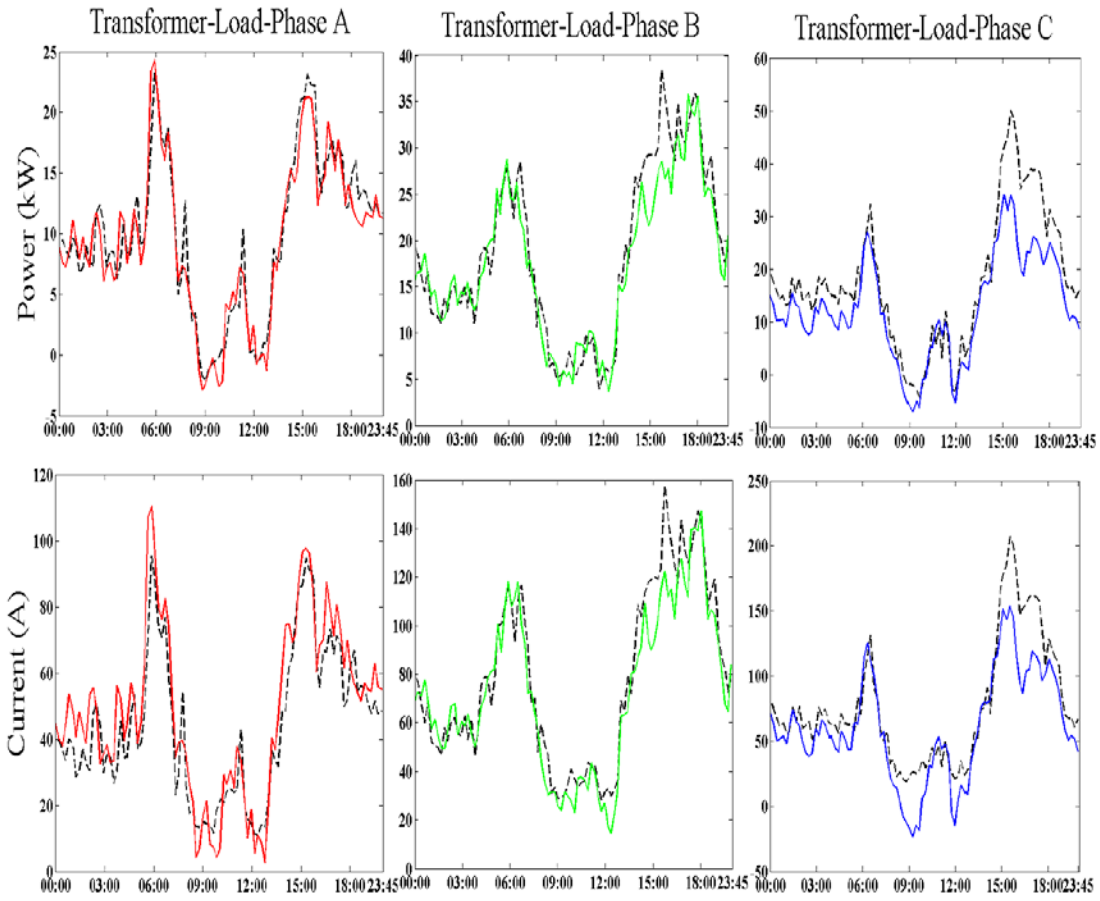

Figure 3-9. Comparison of aggregation of correlated meters with transformer reading, power and current (25 January 2012)

In Figure 3-8 and Figure 3-9, transformer actual phases A, B and C are illustrated in red, green and blue colours respectively, and the black dotted line shows the estimation of these phases based on the allocated phases assigned using the technique described in section 3.4.1 . The phase allocation that is achieved using the cross correlation method introduced in this chapter had a discrepancy with the phasing allocation supplied by the local utility provider (Western Power) for four of the 75 houses. These discrepancies were investigated during a subsequent site visit in June 2012. This showed that phase allocation determined in this work using the cross correlation matched the physical phase connection in the street for three of the houses. As for the fourth house, it was not possible to verify the historical phase connection due to recent power pole replacement (Figure 3-10). As mentioned earlier

it is very difficult in practice to maintain an accurate knowledge of the street phase connection due to normal network maintenance and recording errors.

Figure 3-10. Replaced wooden power pole

3.5 **Measurement Set-up and Errors**

Consumer smart meters can record and report periodic measurements of power consumed in watt-hours (Wh) over short time intervals of $\Delta t = 15$ minutes. Government regulations require that the watt-hours reported by consumer meters be accurate, typically of the order of 99.5% accuracy [72-74].

A meter records readings based on its internal clock and this clock may be out of synchronism with respect to the true clock. For example if a meter reports that 100Wh were consumed from 9:00:00 to 9:15:00 pm and its clock lags the true clock by 5 seconds, in reality the 100Wh were consumed from 9:00:05 to 9:15:05 p,. Therefore, even if all consumer meters are setup to report over the same time intervals, each may suffer from a different clock drift and report watt-hours consumed over a slightly different time interval.

Meters deployed at transformers are much more complex devices. Unlike consumer meters, they measure several parameters needed to monitor a transformer, such as voltage, current, power factor, active and reactive power, at a finer time resolution. Typically, the meters publish average values of parameters over small

time intervals. Therefore, the watt-hours computed from these parameters for each phase are estimates of the actual watt hours supplied and may contain errors. (The real power supplied by a phase can be computed as the time average of the instantaneous voltage and current product). In addition, similar to a consumer meters, clock synchronisation problems may occur at the transformer meter.

Another source of variation is line losses. These losses primarily vary with the load. On the highest load day in our data series, the network losses are calculated at 7.4 kW for a 172 kW peak load. In the network under study, there were also two properties with mechanical meters, which are excluded from the trial, and no recording was available for streetlights and two council loads (typically amenities lighting and public park loads) that were connected to this residential LV transformer.

Four cases have been developed and the Root Mean Square Error (RMSE) was calculated for each of them. These cases are:

Case 1. RMSE for the current on each phase of the transformer versus the aggregated current based on information supplied, at the trial commencement, by the local utility phase connection of the houses. No phase information was available for the block of eight home units.

Case 2. RMSE for the current on each phase of the transformer versus the aggregated current that used phase allocation based on cross correlation between the voltage profiles of the individual houses with transformer data logger voltage data.

Case 3. RMSE for the current on each phase of the transformer versus the aggregated current based on voltages of the houses with three-phase connections .Phase allocation is made without access to the transformer voltage data or the utility

has stated street phase connection. A cross-correlation method between single-phase houses and the reference three-phase house is applied.

Case 4. RMSE for the current on each phase of the transformer versus the aggregated sum of individual house currents based on our best knowledge of phase connections. This is a combination of the initial information provided by the utility, voltage cross-correlation using the distribution transformer logger as a reference and physical observations during site visit.

Efforts were made to account for known imperfections. In all of the above mentioned cases, the 2 three-phase properties that are excluded from the trial were allocated loads that are an average of the actual observed load of the other three phase houses. The phase connection of ten 250 W High Pressure Sodium (HPS) streetlights was identified by physical inspection. Table 3-4 and Figure 3-11 summarise the comparison between RMSE values of the above mentioned cases.

Table 3-4. Comparison between RMSE values of the four cases

RMSE	Phase A		Phase B		Phase C	
Case 1	15.81	18.63*	15.73	23.92*	19.53	20.72*
Case 2	15.58		15.39		17.06	
Case 3	15.74		15.58		17.93	
Case 4	15.04		16.85		16.93	

* The block of 8 units were not aggregated in this scenario of case 1

The rated secondary current of the distribution transformer under study is 289 Amps. Taking this value as the base of the per-unit RMSE for these four cases, we could calculate the percentage of RMSE (Table 3-5).

Table 3-5. Comparison between RMSE values of the four cases (percentage)

RMSE	Phase A		Phase B		Phase C	
Case 1	5.47%	6.45%*	5.44%	8.28%*	6.76%	7.17%*
Case 2	5.39%		5.33%		5.90%	
Case 3	5.45%		5.39%		6.20%	
Case 4	5.20%		5.14%		5.86%	

* The block of 8 units were not aggregated in this scenario of case 1

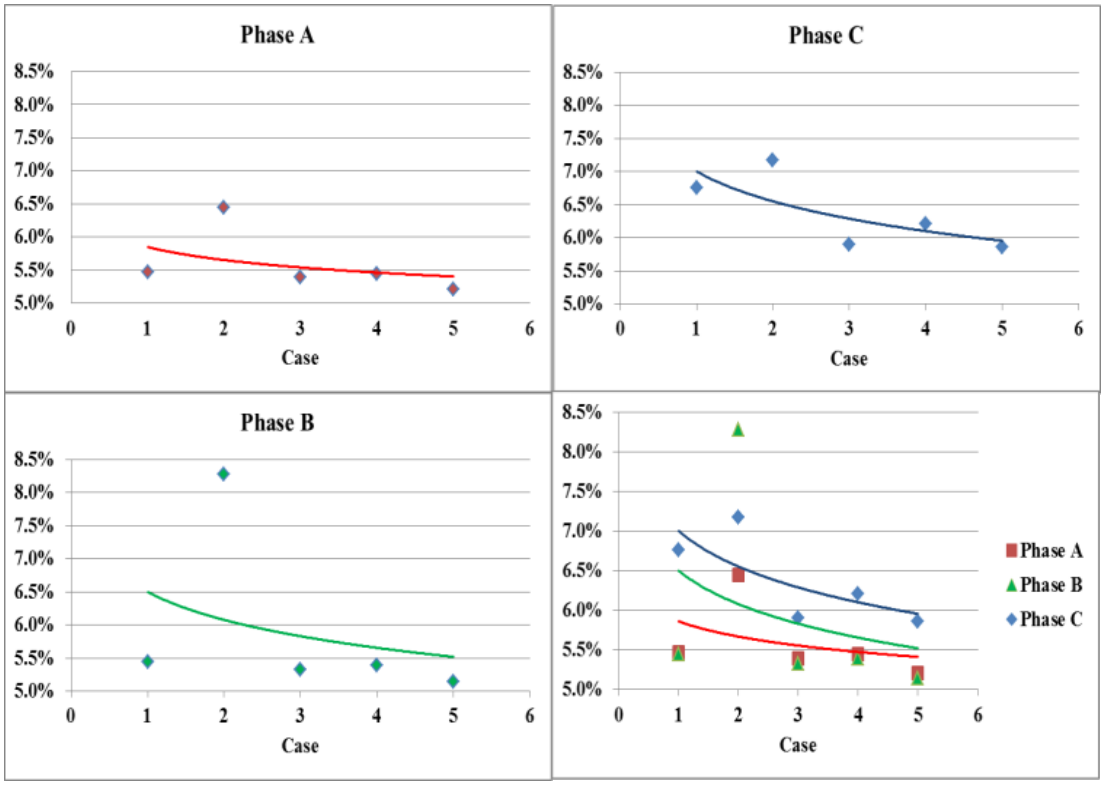

Figure 3-11. Comparison between the RMSE value of all four cases

3.6 **Summary**

This chapter demonstrates that the voltage profile of consumer is well correlated with the voltage profile on the same phase of the transformer and establishes a new method to determine the phase connection of consumer loads on a

LV distribution network from smart meter voltage measurements of the consumer and transformer log data. The initial field-testing was successful, with 51 single-phase meters and 24 three-phase meters correctly allocated on a residential LV feeder.

It should be noted that load and solar PV system generation are not optimally balanced across all three phases. As a result, customers connected to a phase with more generation exhibit a greater frequency of over-voltage. Conversely, customers connected to a more heavily loaded phase exhibit a greater frequency of under-voltages. Note that these two scenarios are not mutually exclusive. By undertaking a phase balancing exercise, customer phase allocation is changed in order to more evenly distribute generation and loads across the three phases, which reduces the occurrence and magnitude of over-voltage and under-voltage for customers. Phase identification is the first step towards solving the larger problem of phase balancing. We investigate this problem taking into account various costs associated with phase rebalancing.

Chapter 4 Impact of Load Unbalance and Rooftop PV on Transformer Life

The reliable operation of distribution systems is critically dependent on detailed understanding of load impacts on distribution transformer insulation systems. This chapter explores the impact of rooftop photovoltaic (PV) generation on a typical 200 kVA, 22/0.415 kV distribution transformer life under different operating conditions. The transformer loads and the phase distribution of the PV systems are significantly unbalanced. Oil and hot spot temperature and remnant life of a distribution transformer under different level PV penetration and load level (balance/unbalance) scenarios are calculated. The work can be separated into two main steps. The first step is to identify the consumer phase connection and to process smart meter data to allow two data sets to be established (chapter 2). These data sets are the actual transformer phase loading and the loading that would have resulted in the absence of the installed PV systems. The second step is to use these two data sets to calculate the transformer hot spot and oil temperatures under the different scenarios. The addition of PV has beneficial impacts with regard to hot-spot temperatures and reduces the transformer loss of life, (LOL).

Our study focuses on the ageing of a 200 kVA MV/LV transformer installed in Perth Western Australia. For this purpose, a thermal model to calculate the hot-spot temperature of windings is used; transformer life models used in this analysis are dependent solely upon thermal loading characteristics, as developed in IEC 60076 [75]. Harmonic currents are excluded from the thermal model and for more realistic simulation, one year of residential electric power load data and one year of ambient temperature data are integrated into the model.

4.1 **Introduction**

Modern distribution systems serve a variety of diverse customers. Three-phase four-wire systems, such as 400/230Vrms systems found in Europe, the United Kingdom and Australia, will typically serve 60 to 120 consumers with a single transformer. The customers may be three-phase or single-phase. Some efforts are made at construction to balance the phase loading but, as discussed in the previous chapter, significant unbalances develop during normal operation. While the systems are robust, unbalance has undesirable effects including reduced transformer life, increased losses and power quality problems due to phase voltage variations and negative sequence voltages.

Transformers operated under unbalanced conditions will suffer more extreme stresses than under balanced conditions. The transformer life is largely determined by the insulation life [76-78]. Mechanical, electrical and thermal stresses affect the oil-paper insulation system [79]. The main factors that determine the insulation life of oil-immersed transformers are the transformer load, ambient temperature, moisture content and the oxygen content of the oil [80]. For unbalanced loading the resulting increased loss, and the concentration of the losses in one or two phases, affects the insulation system of the transformer and reduces its lifetime [81, 82].

To maximize the return on their investment, utilities will take advantage of a full cyclic loading capability of transformers to achieve financial savings and reduce operating costs. Optimal utilisation of a transformer can be achieved by taking advantage of thermal time constant of transformer and the diurnal variation of the load and ambient temperature. It is necessary to have accurate models for predicting winding hot-spot temperature (HST) and top-oil temperature (TOT).

The development of accurate prediction models of the HST and TOT for substation, distribution and power transformers has been the subject of a substantial amount of research [82, 83]. IEEE Standard C57.91-1995 [84] and IEC standard 60076-7 [75] describe in detail methods to calculate the HST and offer guidance on temperatures that should not be exceeded at either winding or structural hotspots to avoid undue ageing failures from gassing. These standards, and recent publications, assume balanced loading of the transformer.

4.2 **Impact of Rooftop PV on Transformer Loading**

PV at the distribution level has become widespread. Previous studies [32, 85, 86]have identified many impacts that roof top PV may have on a local distribution network including changes in voltage profile and network power flows [32]. The problem of voltage fluctuations resulting from the passage of clouds is also addressed in [87]. In particular, variations of nodal voltages in small or weak electrical grids (e.g. SWER systems) have been reported to cause system instability [88]. Studies have also been conducted to explore the extent to which the geographical diversity of distributed PV mitigates the short-term output variability caused by rapidly changing weather conditions. Spatial distribution significantly reduces transients caused by clouds. Distribution systems are typically designed for a specific load profile based on consumption patterns. When rooftop PVs are deployed, the pattern of electric power demand will change. The addition of PV does not strongly reduce the peak load in the residential feeders but will reduce the energy served. As a result, the load factor (the ratio of average to peak load) is reduced.

4.3 **Unbalanced vs. Balanced Transformer Loading**

The network under study is significantly unbalanced but reflective of normal network conditions. The level of three-phase unbalance in the distribution feeder

Pavetta shown in Figure 4-1 was introduced because of the poor allocation of customer loading among the three phases. For instance, the loading on phase A is much less than on phases B and C during peak hours. It is possible that most of the over-voltage and under-voltage incidents would be mitigated by reallocation of PV and loads. Balancing of the network will reduce the occurrence of voltage drop and reduce the incidences of voltage rise at branches of feeder with high PV penetration.

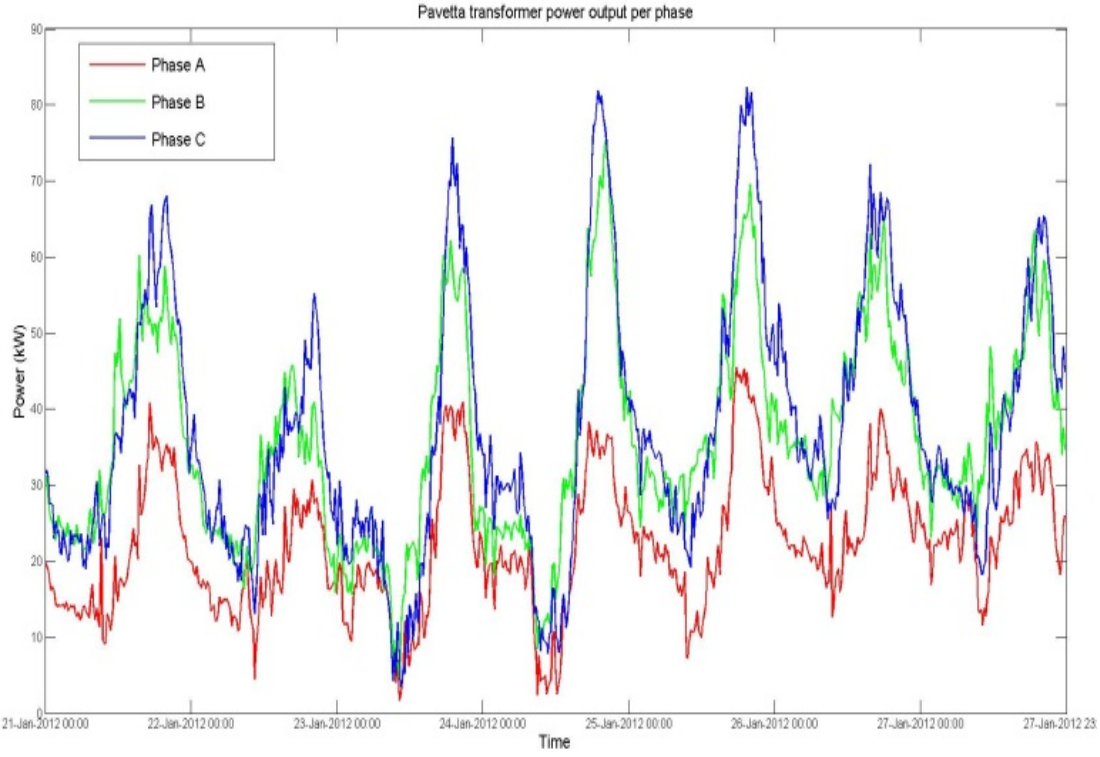

Figure 4-1. Pavetta transformer power output, 21-27 January 2012

4.4 **Distribution Transformer Thermal Model**

Transformers are operated within either manufacturer recommended or utility adopted maximum oil and hot-spot winding temperatures. These temperature limitations translate into the maximum loading levels that can be reached in emergency situations. In this section, the methods to calculate transformers losses and life duration are presented. A thermal model to assess the ageing of transformers is exposed. The characteristics of transformer used are also described.

4.5 **Transformer Thermal Diagram**

The thermal model investigated in this study is developed based on the basic thermal diagram, which describes the oil and winding temperature profile in a transformer's vertical direction. (Figure 4-2).

It should be noted that the figure is a simplified thermal diagram with the following assumptions made:

1. The oil temperature increases from bottom to top at any circumstance, regardless of the cooling mode or load.
2. The winding temperature increases linearly from bottom to top disregarding the cooling mode or load, and has a constant temperature difference from the oil temperature at the same vertical position. This is known as the winding to oil gradient (Gr).
3. The hot-spot temperature is higher than the temperature of the top winding as the result of extra stray losses build-up. It exceeds the top-oil temperature by a small fraction (the IEC loading guide defines this as Gr multiplied by the hot-spot factor; while the IEEE loading guide defines this as the hot-spot temperature rise over the top-oil as a whole).

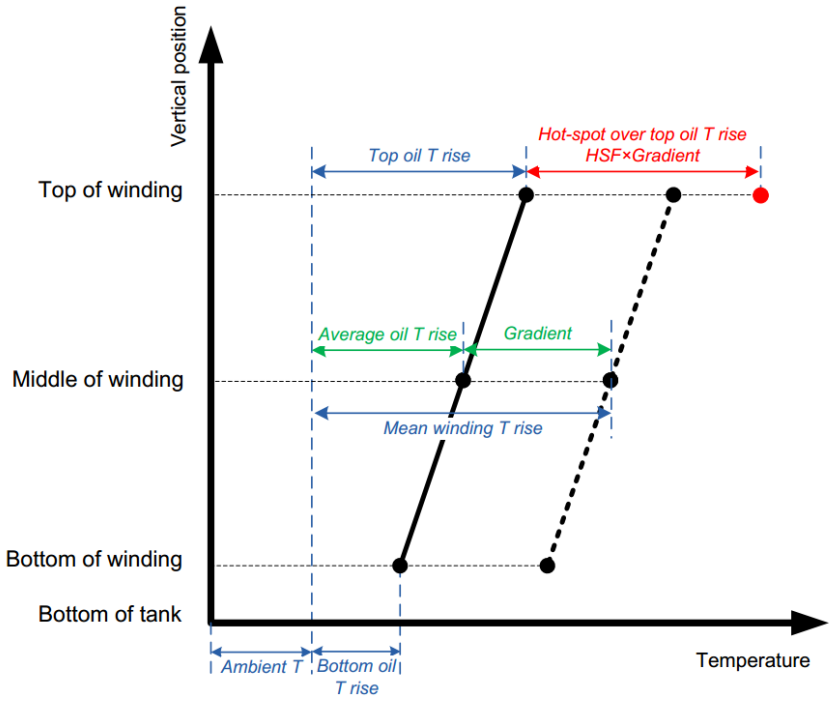

Figure 4-2. Thermal diagram of oil-immersed transformers

4.6 **IEC Thermal Model**

The transformer thermal modelling has been studied quite intensively in the earlier literature [78, 82, 89, 90],as well as in multiple standards; for example, IEEE guides [84], [91] and the IEC 60354 Loading Guide for Oil-immersed Power Transformers [92]. The fundamental of the thermal model published in the IEC 60076-7 loading guide is based on the thermal diagram of a transformer depicted previously in Figure 4-2. IEC 60076 develops the hotspot temperature equations in the following way:

$$\Delta\theta_{h_{(n)}} = \theta_{(n)} + \Delta\theta_{h_{(n)}} \tag{4.1}$$

Where θ_h is the HST in degrees Celsius, θ_o is the top-oil temperature at the current load, and $\Delta\theta_h$ is the total HST rise at the nth time step, where Δ is calculated:

$$\Delta\theta_{h_{(n)}} = \Delta\theta_{h1_{(n)}} + \Delta\theta_{h2_{(n)}} \tag{4.2}$$

$\Delta\theta_{h1_{(n)}}$ and $\Delta\theta_{h2_{(n)}}$ come from the difference equations for HST rise, and can be calculated:

$$\Delta\theta_{h1_{(n)}} = \Delta\theta_{h1_{(n-1)}} + \frac{Dt}{k_{22}\tau_{\omega}} \times \left[k_{21} \times \Delta\theta_{hr} \times K_a^{y} - \Delta\theta_{h1_{(n-1)}}\right] \tag{4.3}$$

where Dt is the time step in minutes, k_{22} and k_{21} are experimentally-derived constant related to the thermal recovery of the transformer. τ_w is the winding time constant in minutes, $\Delta\theta_{hr}$ is hotspot-to-top-oil gradient at rated current in Kelvin, K is the load factor (current load/rated load), and y is the exponential power of current versus winding temperature rise (winding exponent). Similarly, $\Delta\theta_{h2}$ can be evaluated:

$$\Delta\theta_{h2_{(n)}} = \Delta\theta_{h2_{(n-1)}} + \frac{Dt}{\tau_o/k_{22}} \times \left[(k_{21} - 1) \times \Delta\theta_{hr} \times K_a^{y} - \Delta\theta_{h2_{(n-1)}}\right] \tag{4.4}$$

where τ_o is the average oil time constant in minutes, the top-oil temperature must be calculated and substituted back into (4.2)

$$\theta_{o_{(n)}} = \theta_{o_{(n-1)}} + \frac{Dt}{k_{11}\tau_o} \times \left[\left(\frac{1+K_b^2 R}{1+R}\right)^X \times \Delta\theta_{or} - (\theta_{o_{(n-1)}} - \theta_a)\right] \quad (4.5)$$

where k_{11} is another experimentally derived thermal baseline constant of the transformer, R is the ratio of load losses at rated current to no-load losses, $\Delta\theta_{or}$ is the top-oil temperature rise at rated load, and θ_a is the ambient temperature in degrees Celsius. The winding time constant is as follows:

$$\tau_w = \frac{m_w \times c \times g}{60 \times P_w} \quad (4.6)$$

Based on "Appendix A" of IEC 60076-7, we could rewrite it as (4.7) for a transformer with aluminium conductor (this is the case with the transformer under study):

$$\tau_w = 1.15 \times \frac{g}{(1+P_e) \times s^2} \quad (4.7)$$

It means that the thermal capacity C for the ONAN cooling mode is:

$$C = 0.132 \times m_A + 0.0882 \times m_T + 0.4 \times m_O \quad (4.8)$$

where m_A is the mass of core and coil assembly in kilograms, m_T is the mass of the tank and fittings in kilograms and m_O is the mass of oil in kilograms.

$$\tau_o = \frac{C \times \Delta\theta_{om} \times 60}{P} \quad (4.9)$$

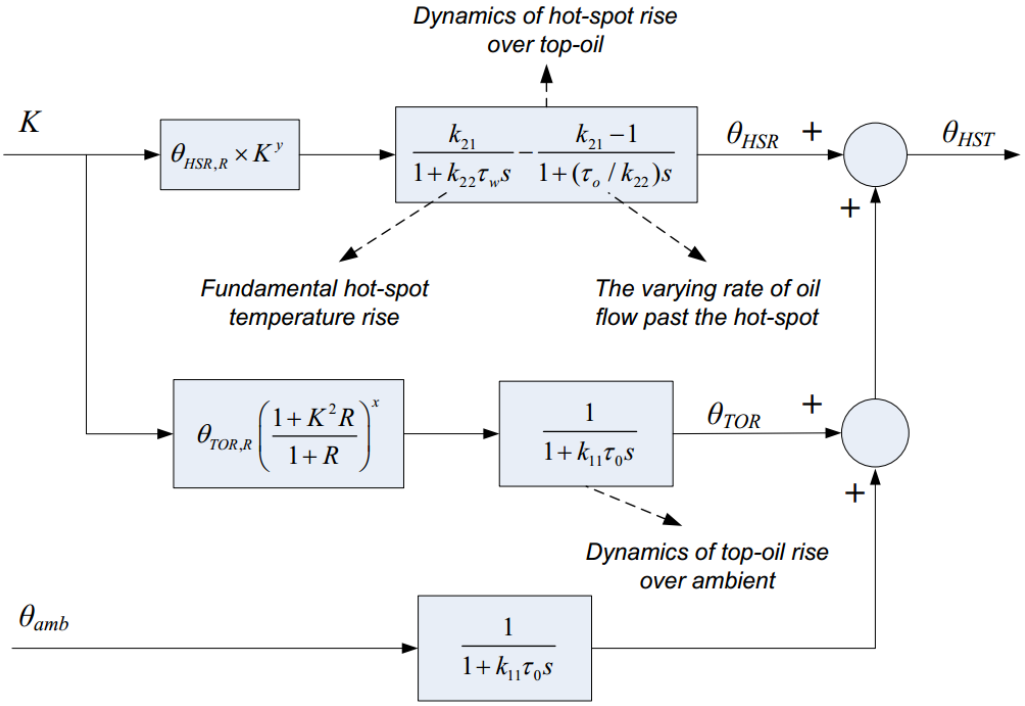

Figure 4-3. Block diagram representation of the differential equations

4.6.1 HST for Unbalanced Loading:

Equation (4.5) would be accurate if all legs of a three phase transformer are loaded identically or for single phase transformers which are commonly used in North America or in rural areas of Australia (e.g. SWER systems). However, the loads on the phases of the typical three-phase distribution transformer are not balanced. It is possible to derive an expression analogous to (4.3 and 4.4) for each phase if the time varying loads on each phase are known.

The phase currents of the transformer would determine the winding to oil temperature differential of that phase so (4.4) could be rewritten for each individual phase.

$$\Delta\theta_{h2_{(n)R}} = \Delta\theta_{h2_{(n-1)R}} + \frac{Dt}{\tau_o/k_{22}} \times \left[(k_{21}-1) \times \Delta\theta_{hr} \times K_R^y - \Delta\theta_{h2_{(n-1)}}\right] \quad (4.10)$$

$$\Delta\theta_{h2_{(n)W}} = \Delta\theta_{h2_{(n-1)W}} + \frac{Dt}{\tau_o/k_{22}} \times \left[(k_{21}-1) \times \Delta\theta_{hr} \times K_W^y - \Delta\theta_{h2_{(n-1)W}}\right] \quad (4.11)$$

$$\Delta\theta_{h2_{(n)B}} = \Delta\theta_{h2_{(n-1)R}} + \frac{Dt}{\tau_o/k_{22}} \times \left[(k_{21}-1) \times \Delta\theta_{hr} \times K_B^y - \Delta\theta_{h2_{(n-1)}}\right] \quad (4.12)$$

The current load (I_{cl}) that would impact on the top oil temperature would be the RMS value of each individual phase current at that given time:

$$I_{cl}(t) = \sqrt{\left(I_{RMS}^{R}(t)\right)^2 + \left(I_{RMS}^{W}(t)\right)^2 + \left(I_{RMS}^{B}(t)\right)^2} \tag{4.13}$$

$$K_{ub} = \frac{I_{cl}(t)}{I_{rated}} \tag{4.14}$$

$$\theta_{o_{(n)}} = \theta_{o_{(n-1)}} + \frac{Dt}{k_{11}\tau_o} \times \left[\left(\frac{1+{K_{ub}}^2 R}{1+R}\right)^X \times \Delta\theta_{or} - (\theta_{o_{(n-1)}} - \theta_a)\right] \tag{4.15}$$

As a suggestion, the IEC loading guide offers recommended values of x, y, k_{11}, k_{21} and k_{22}, as well as oil and winding time constants τ_o and τ_ω. The values of the thermal constants are shown in Table A-3 of the Appendix A.

4.7 **Loss of Life of Distribution Transformer**

Transformers are designed to handle cyclic load conditions, which include emergency and cold load pickup scenarios. With an increase in load, internal transformer temperature increases and the normal life expectancy of the transformer decreases accordingly. Life expectancy is defined as the calculated life of the transformer winding insulation, which deteriorates as a function of time and tem

Several models have been introduced to assess the life estimation of insulation in transformers [76-79, 93, 94]. A wide variety of methods have been presented for inferring loss-of-life for power and distribution transformers, such as those proposed in [91], Clause 7, and updated in [89]. When inferring the transformer loss of life (LOL) acceleration rate using these methods, the calculation of the winding hot-spot temperature (HST) is the most critical issue [78, 79].

Although deterioration of insulation is a function of temperature, moisture content, oxygen content and acid content, the model presented in this work is based

only on the insulation temperature [75]. Since the temperature distribution is not uniform, the part that is operating at the highest temperature will normally undergo the greatest deterioration. Therefore, the rate of ageing is referred to the winding hot-spot temperature. Equations (4.16) and (4.17) describe, respectively, the relative ageing rate V_T for a thermally upgraded paper (reference temperature of 110ºC) and non-thermally upgraded paper (reference temperature of 98ºC) [75]

$$V_T = 2^{\theta_h - 98\,/6} \tag{4.16}$$

$$V_T = e^{\left[\frac{15000}{110+273} - \frac{15000}{\theta_h+273}\right]} \tag{4.17}$$

The equivalent life at the reference temperature that will be consumed in a given time period for an actual temperature cycle can be calculated by (4.17) [84]. Where V_{EQA} is the equivalent ageing factor for the total time period, n is the index for the time interval t, N is the total number of time intervals, Δt_n is the time interval and Vn is the ageing acceleration factor for the time interval Δt_n.

$$V_{EQA} = \frac{\sum_1^N V_n \Delta t_n}{\sum_1^N \Delta t_n} \tag{4.18}$$

In this work, we chose the normal life as 180,000 hours (20.55 years). Under this normal life value, the normal loss of life percentage for operation at a rated hottest-spot temperature of 110°C for 24 hours is 0.0133%. The normal life expectancy is a conventional reference basis for continuous duty under normal ambient temperature and rated operating conditions

$$\%\ Loss\ of\ Life = \frac{V_{EQA} \times t \times 100}{Normal\ insulation\ life} \tag{4.19}$$

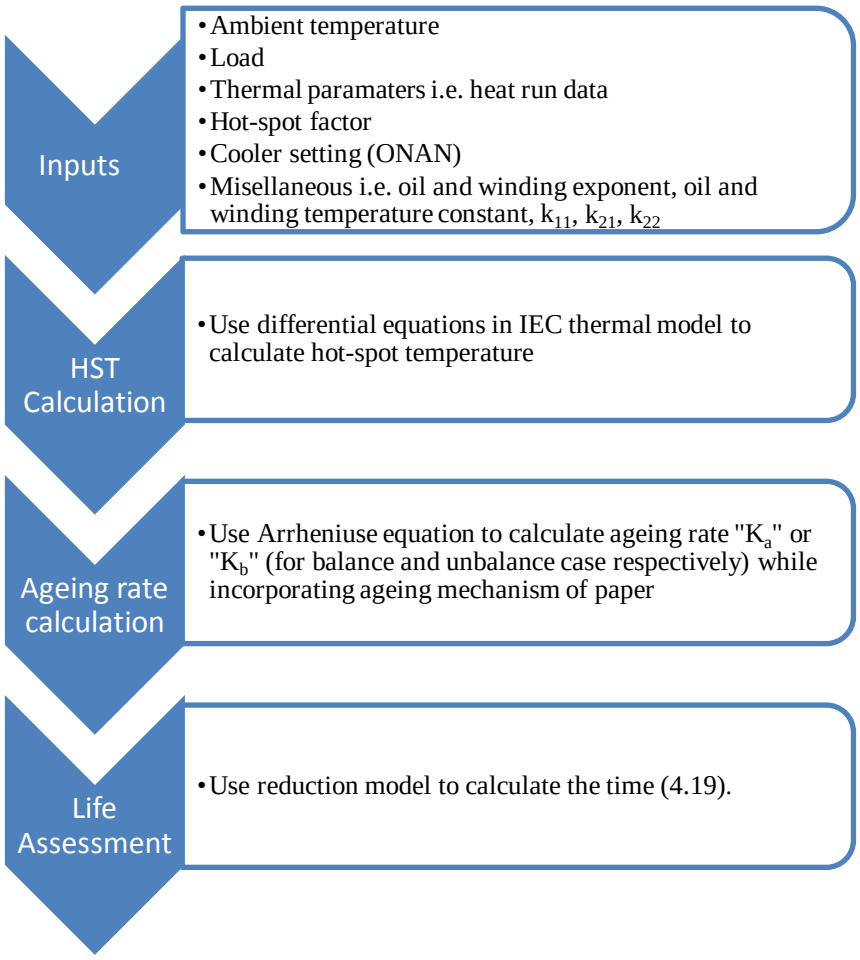

Figure 4-4. Flow chart of transformer life assessment using the thermal model

4.8 **Thermal Model Inputs**

4.8.1 Ambient Temperature and Rooftop PV Generation

As described in the thermal model (4.15) and in publications [93, 95], the ambient temperature affects the hot spot temperature and impacts the life duration and the ageing rate of a transformer. Therefore, as one of the inputs to the thermal model, one year of ambient temperature data (July 2011- July 2012) were collected from the Australian Bureau of Meteorology's Perth Airport weather station which is close to the high PV penetration trial area [96]. The ambient temperature and solar irradiance is obtained at a 15-minute rate to be consistent with the smart meter load data sampling times (Figure 4-5).

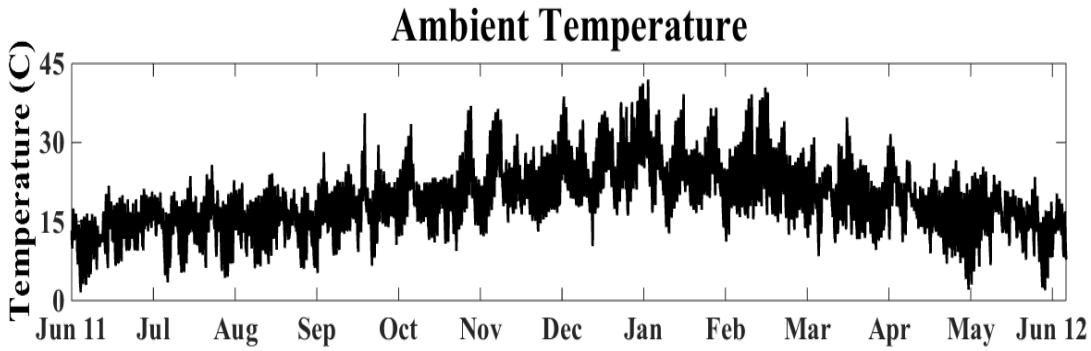

Figure 4-5. Ambient temperature from June 2011 - July 2012

4.8.2 Household Load Profiles

The transformer daily load curve is determined by the aggregated demand measured by the smart meters connected to individual consumers. In this work, 15-minute intervals are used, so a daily load curve is made up of 96 pairs of time and demand values. In order to guarantee a representative set of field data, a total of 365 days of measurements were collected from operating smart meters at the high PV penetration trial in Perth. To determine the loading of the transformer the previously introduced method using cross-correlation of consumer voltage profiles was implemented to identify their phase connection [97]. Using the known phase connections of the residential loads, the data collected from the smart meters was aggregated to determine the phase loading on the transformer. Figure 4-6 shows the predicted transformer loading (kW) during the 7-day window, that includes the annual peak day. The sampling rate is 15 minutes. The network under study is significantly unbalanced but reflective of normal network conditions. The unbalance results from the poor allocation of customer loading among the three phases. For instance, the loading of phase A is much less than that of phases B and C during daytime peak hours.

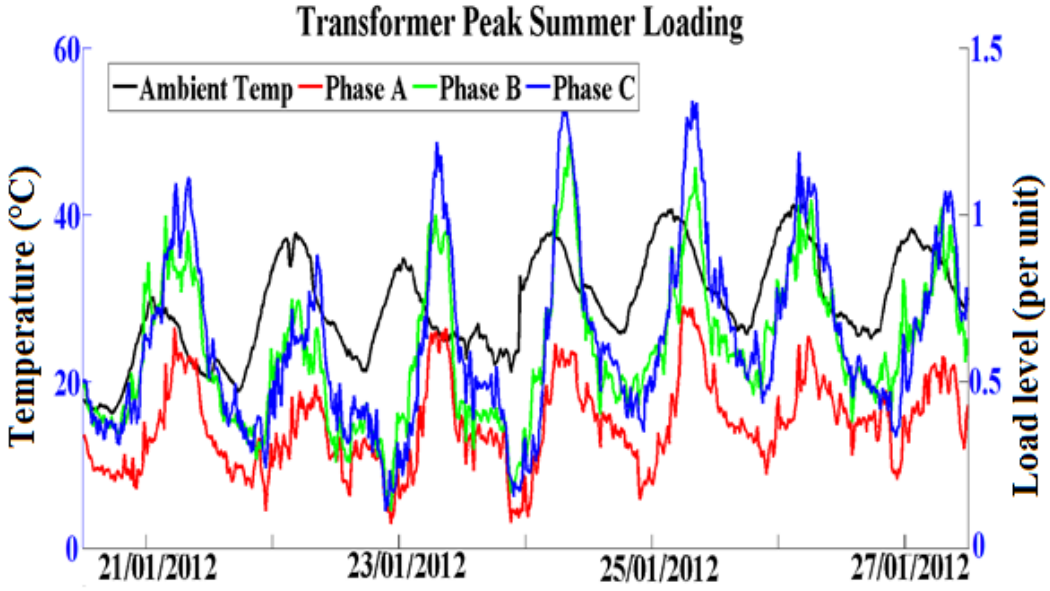

Figure 4-6. Pavetta transformer power output, 21-27 January 2012

4.8.3 Distribution Transformer Thermal Parameters

A 200kVA ONAN pole-mounted distribution transformer system supplies the residential low voltage feeder for this trial. This transformer complies with the prevailing Australian Standard AS2374. Within the Western Power service area, approximately 17,000 distribution transformers are in service. More than 3,000 of these are 200 kVA units. The insulation paper used in this transformer is made of non-thermally upgraded paper and its life duration is 30 years. Table A-1 and Table A-2 in Appendix A describe the characteristics and the values of parameters for the thermal model of the transformer, respectively.

4.9 **Results and Discussion**

Simulations investigating the interplay between transformer loading, PV array capacity, ambient temperature, transformer size, oil and winding temperature rise, peak load magnitude and loss of life, is show in this section. Trade-offs between PV array capacity and transformer overrating gains is assess, The impacts of PV

generation on the overrating potential of an actual 200-kVA distribution transformer of a high PV penetration trial in Perth, Western Australia is evaluated.

A generalised analysis framework was developed to investigate the simulated distribution transformer loss of life under proposed scenarios. In each scenario, the annual loss of life rate and the expected lifetime of the analysed transformers were determined. These scenarios are:

- Scenario 1-unbalanced operating conditions (no solar input)
- Scenario 2-unbalanced operating conditions (with solar input)
- Scenario 3-balanced operating conditions (no solar input)
- Scenario 4-balanced operating conditions (with solar input)

In the first two scenarios the transformer was significantly unbalanced. The last two scenarios examine the benefit of balanced operation with PV generation. Load balance could be achieved using a dSTATCOM or optimal phase swapping strategies with laterals or individual loads [41, 98, 99]. Phase identification systems, introduced in Chapter 3, can be combined with phase swap to improve voltage unbalance.

4.9.1 Unbalanced Operating Conditions (With Solar Input)

To investigate the impact of PV on the life of the transformer, a one year set of 15-minute measurements of transformer load and ambient temperature was assembled. Equations (4.1-4.15), together with transformer thermal parameters, were used to determine the transformer thermal response. Equations (4.16-4.19) were then used to obtain the loss of life (LOL) rate and total LOL accumulated by the transformer over the given year. The distribution transformer under study is substantially unbalanced. Out of 77 connected residential consumers, 13 are connected to phase A, 17 are connected to phase B while phase C is serving 21

customers and 26 of the premises have three-phase connections. Figure 4-6 shows the temperature profiles corresponding to one summer week during the trial that includes the annual peak day for the transformer. The peak demand day occurred on the second day of a heat wave[1] and immediately preceded the Australia Day public holiday. It is evident that phase C is heavily loaded. At the peak time, the loading on phase C is 360 A/90 kVA or 1.34 pu and this value is close to the allowable maximum cyclic loading. In Australia it is an acceptable practice to load a transformer up to 1.4 times its rating for short period of time in a given year [100]. In this instance, the utility company would not notice this overloading incident as the total energy sales from the transformer are used to predict peak loads. The energy sales are aggregated over the three phases, which at peak time was 196 kVA, and the individual phase loading was not available. Based on this approach, the transformer will be kept in service until the total loading on it would reach 1.4 pu or 280 kVA; this assumption has been used as a basis to create four test cases. These investigate the LOL of the transformer if the loading on the transformer increases in 10% increments until it reaches the set value of 280 kVA (1.4 pu).

Case 1 illustrates the transformer HST and LOL quantities that correspond to the current unbalanced state of the transformer with 64 kW of PV. The results are presented for the peak day in the summer (Figure 4-7(a) and Figure 4-8(a)), as well as for the day with lowest load in the winter (Figure 4-7(b) and Figure 4-8(b)), for each phase of the transformer. The horizontal axis is the time of day in 15-minute intervals.

[1] This discussion is based on the Bureau of Meteorology's definition of a heat wave as three or more consecutive days with daily maximum temperatures exceeding 35 °C

From Figure 4-7 it is clear that the unbalance has caused different hotspot temperatures in each leg of the transformer. For example on the peak day, the phase A; winding would reach 90 °C whereas the phase C winding exceeds 130 °C. This 40 °C temperature difference drives the rapid degradation of the phase C insulation. This temperature difference is much less at lighter loads (Figure 4-7 and Figure 4-8). As can be seen in Figure 4-8, in the summer the LOL is dominated by the higher transformer temperatures during the late afternoon and evening peak. Mention should be made of the high LOL rate of phase C; in fact, it exceeds the design rate of 1 day per 24 hours, by losing more than 3 days in 24 hours. On the contrary, in winter, the peak of the LOL rate is well below the designed value. This is due to the moderate loads combined with relatively low ambient temperature. To see how future load growth would affect the transformer hot-spot temperature, simulations were carried out and compared together with the base load case (cases 2-4). In addition to the present status (case 1) of the transformer four additional (labelled cases 2 to 5) cases were developed. For case 5, the worst-case scenario is investigated by increasing the load to 1.4 pu (280 kVA).

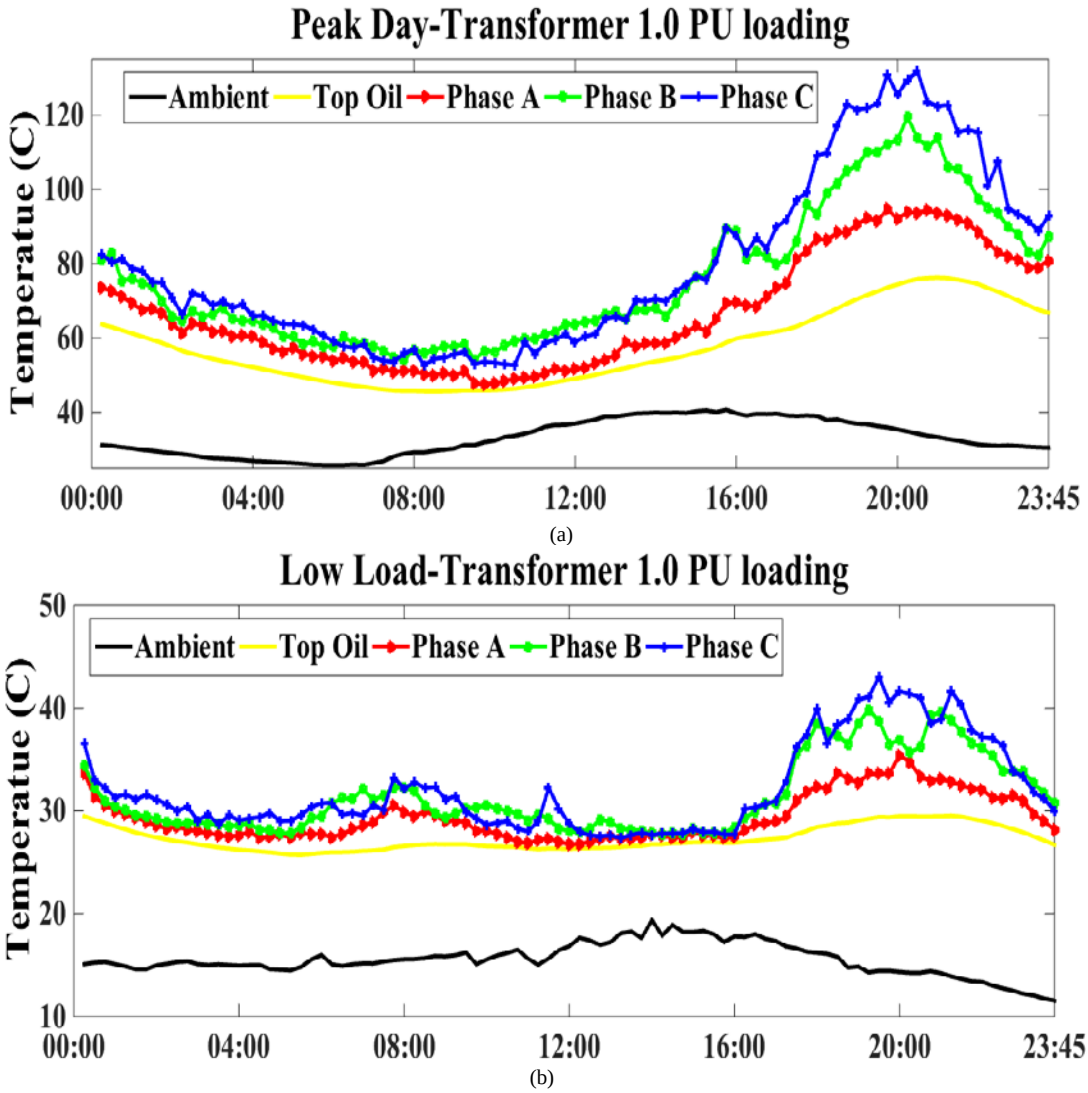

Figure 4-7. Comparison of the daily evolution of the hotspot, top oil and ambient temperature peak day (a) low load day (b)

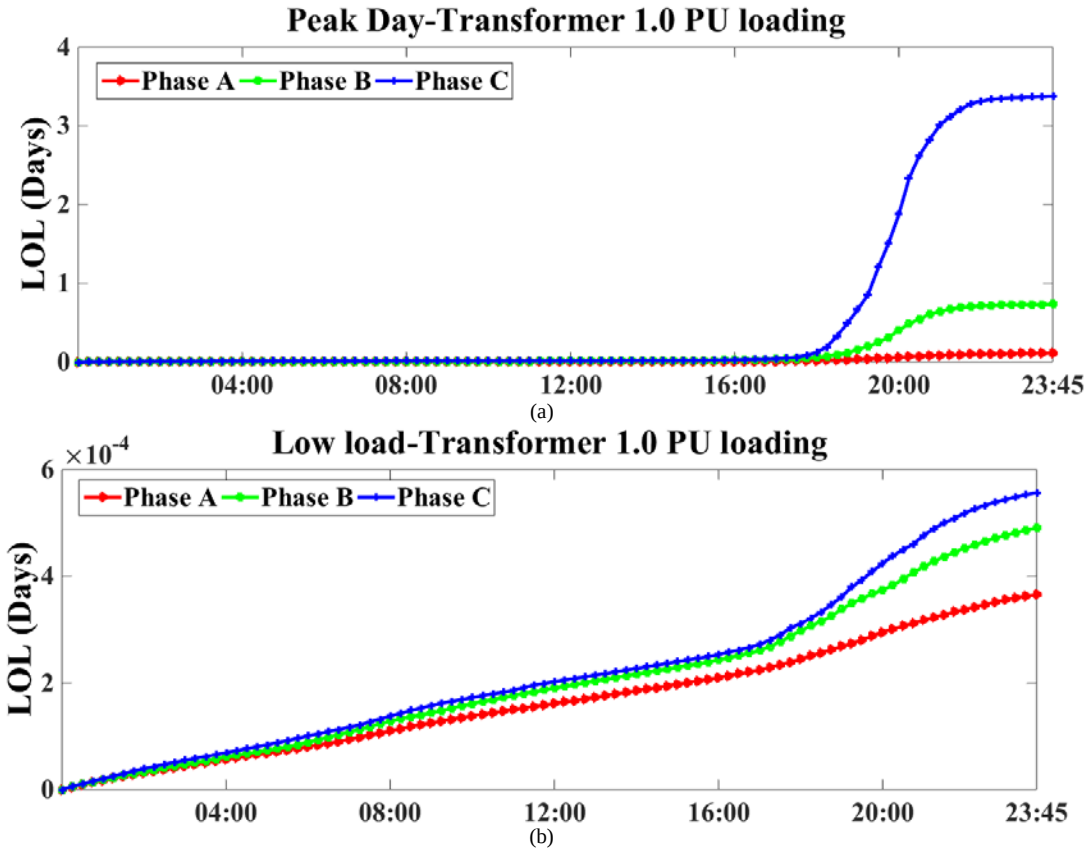

Figure 4-8. (a) Daily evolution of the loss of life on each phase of transformer, peak day (b) daily evolution of the loss of life on each phase of transformer lightly load day

Figure 4-9 shows the top oil temperature and HST on the peak summer day when the transformer is loaded 40% above the nameplate 200 kVA rating and compares them with the reference case. The oil reached 97 °C and hot-spot temperatures for each phase reached 126 °C, 162 °C and 185 °C respectively. The HST limit of 160 °C was violated for both phases B and C and rapid degradation was expected.

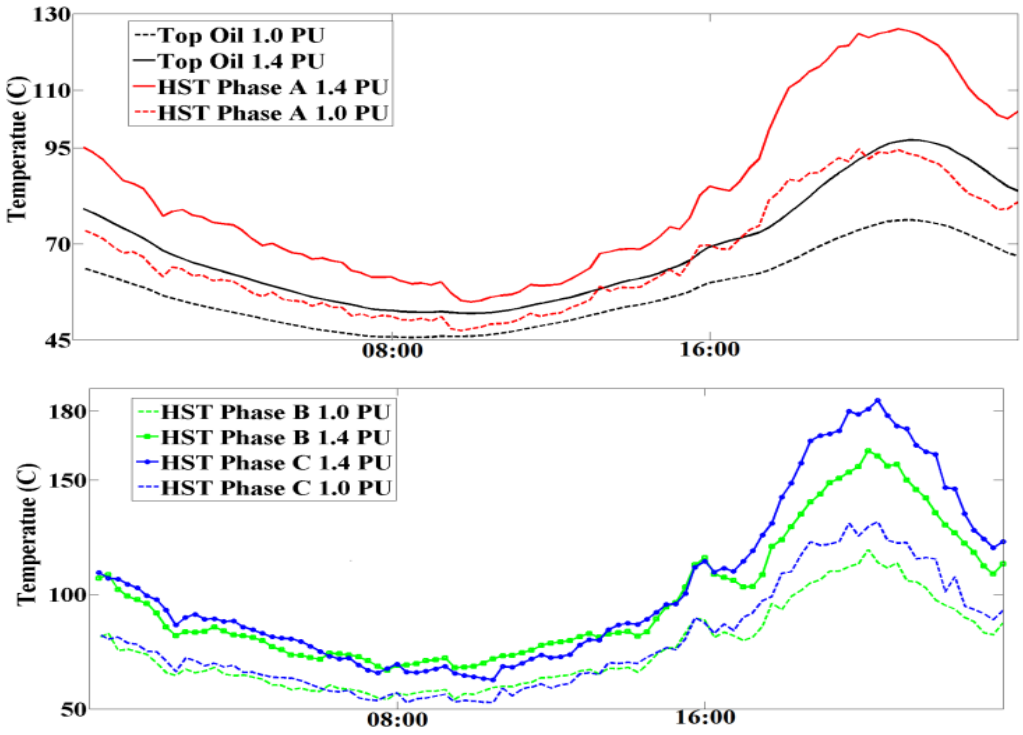

Figure 4-9. Effect of possible load growth on TOT and HST

4.9.2 Unbalanced Operating Conditions (No Solar Input)

In order to demonstrate the benefit that roof top PV could provide in reducing the transformer loss of life, the solar generation was removed from the system. The production pattern of PV units was obtained from the calculated and collected values using the solar irradiance measurements during the first three months of the trial (July - September 2011) and the smart meter data in 15-minute interval during the remaining period of the trial (October 2011-June 2012). For the first three months of the trial, only net household consumption data was available. In the last nine months of the trial, a two-channel record of household load and solar generation was available for all single-phase customers. The solar generation profile of the first three months was estimated using solar irradiance, ambient temperature and rating information for the PV modules and inverter.

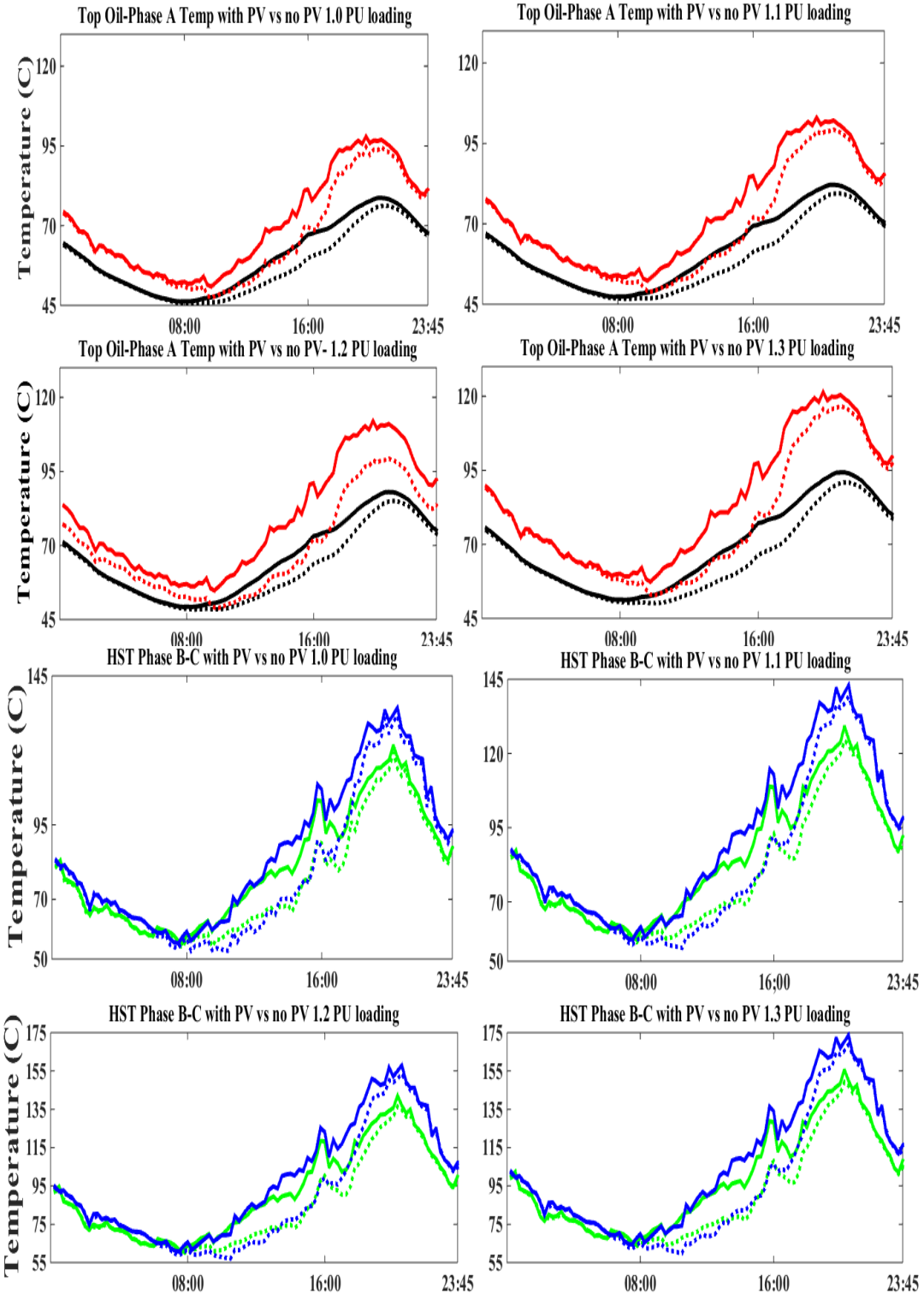

Figure 4-10. Improvement in top oil temperature and HST in presence of PV at different loading conditions

The method was confirmed by correlating with the generation pattern of the last nine months of the trial. Of the 34 premises with PV, 12 houses had dual reading meters that captured both the PV generation and consumption of the houses. The PV

generation for the other 22 houses, which only had net meter recording, could be calculated from these observations. The results for five operating conditions are shown in Figure 4-10. In each graph, the dotted line represents the system with PV and the solid line the system without PV. The first graph of this figure (top left side) is the reference case (current state of the transformer); cases for additional loadings to 1.3 pu are shown in this figure. The final case, with 1.4 pu loading, will be considered separately. Figure 4-11 shows the temperature profiles corresponding to a peak transformer overload of 1.4 pu.

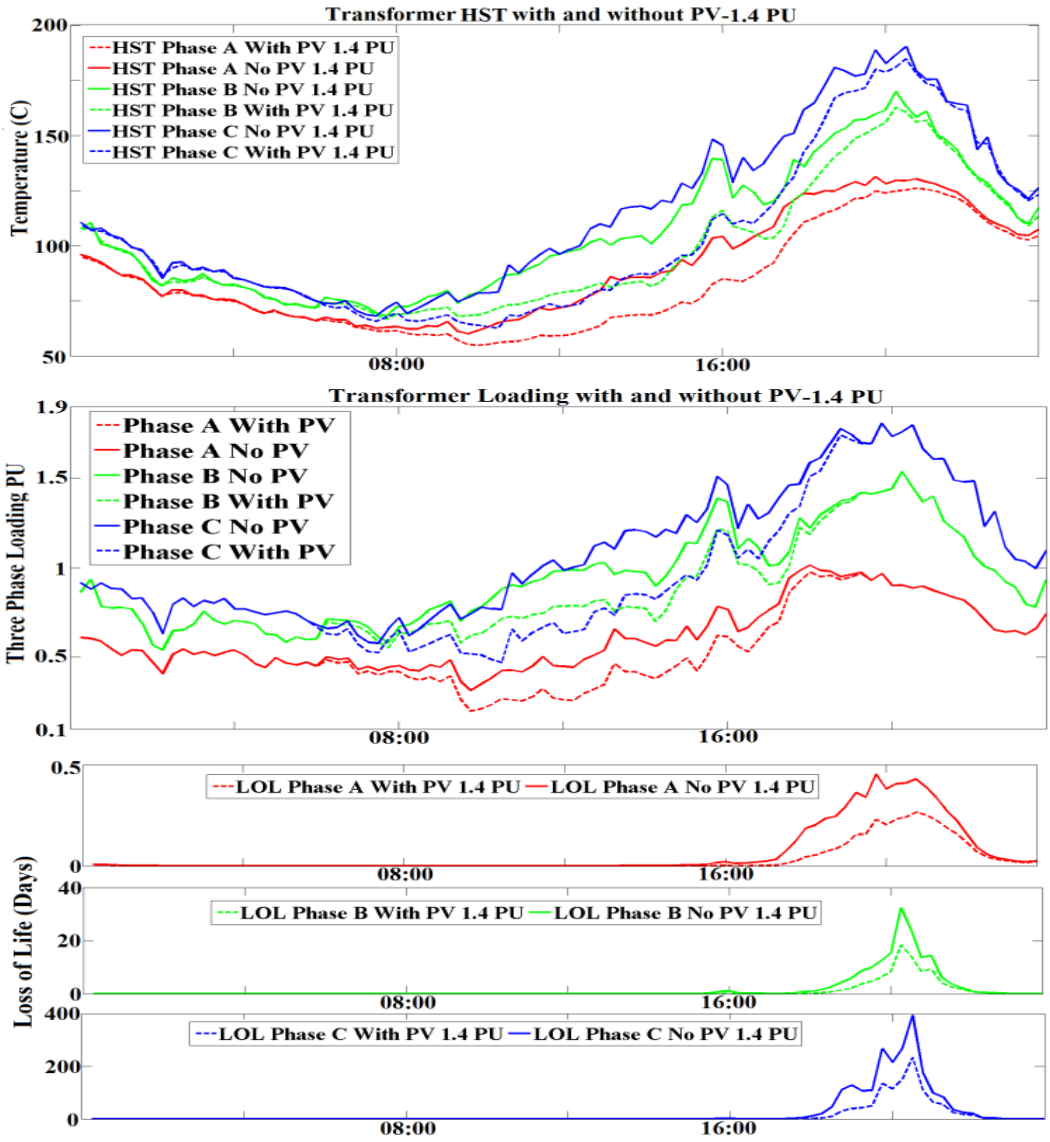

Figure 4-11. Temperature difference in hot spot and oil of transformer and reduction in LOL as a result of PV generation

Table 4-1. Top oil and HST comparison under different loading conditions

Case condition	HST (ºC)			Top Oil (ºC)
	Phase A	Phase B	Phase C	
Solar-1.0 pu	94.4	117.3	128.9	76.1
No solar-1.0 pu	97.6	120.3	133.6	78.7
Solar-1.1 pu	99.3	124.4	137.9	79.5
No solar-1.1 pu	102.1	127.7	142.3	82.1
Solar-1.2 pu	107.7	136.5	151.7	85.0
No solar-1.2 pu	111.0	140.3	157.2	88.0
Solar-1.3 pu	116.7	149.3	166.8	90.9
No solar-1.3 pu	120.3	153.7	172.8	94.3
Solar-1.4 pu	126.0	162.7	180.7	95.1
No solar-1.4 pu	130.2	167.6	189.2	100.9

Without PV generation, the oil and hot spot temperatures reached 100 °C and 190°C respectively. The addition of 64 kW of PV generation lowered this to 180 °C for the HST and 95 °C for the top oil. These values are still extremely high. The PV benefit occurs during the time leading up to the peak. Lower loadings in the afternoon allow the transformer to enter the peak period with lower oil temperatures. In this example the LOL saving for phases A, B and C is 0.2, 14 and 160 days, respectively. Except for cases where the PV installations are larger than the peak load, PV will decrease the daily top oil temperature and HST and extend transformer life. The extent of the improvement depends on the loading ratio of the transformer and the PV penetration level.

Table 4-2 provides a summary of each phase of transformer LOL and the benefit that roof top PV could provide to improve the transformer ageing process based on its current and future loading. The first conclusion from Table 4-2 is that regardless of the operation scenario, the LOL rate of the transformer is far higher in summer. This may be due to the combined effect of higher ambient temperature and electricity use driven by cooling loads in this season. It further implies that rooftop PV could provide a higher LOL reduction in the summer and is a suitable option for extending the life of distribution transformers. The targeted installation of rooftop

PVs along the feeder, and even on a specific phase, could be considered as a life extension strategy. There are voltage rise limitations on the number and location of the installed roof top PVs. Considering this 7 additional PVs (with average rating of 1.88kW) were randomly allocated to consumers on Phase C. Table 4-3 shows the corresponding life improvement.

Table 4-2. Seasonal variation in LOL of transformer

Transformer Loss of Life (Days)											
		Solar 1.0 pu	No Solar 1.0 pu	Solar 1.1 pu	No Solar 1.1 pu	Solar 1.2 pu	No Solar 1.2 pu	Solar 1.3 pu	No Solar 1.3 pu	Solar 1.4 pu	No Solar 1.4 pu
Winter	Phase A	0.1	0.1	0.1	0.1	0.1	0.1	0.2	0.2	0.3	0.3
	Phase B	0.1	0.1	0.1	0.1	0.2	0.2	0.3	0.3	0.5	0.5
	Phase C	0.1	0.1	0.2	0.2	0.3	0.3	0.6	0.6	1.3	1.2
Spring	Phase A	0.1	0.1	0.1	0.1	0.1	0.1	0.1	0.1	0.1	0.2
	Phase B	0.1	0.1	0.1	0.2	0.2	0.2	0.3	0.4	0.4	0.7
	Phase C	0.1	0.2	0.2	0.2	0.3	0.4	0.5	0.8	0.4	1.7
Summer	Phase A	0.7	1.2	1.1	1.8	2.1	3.8	4.5	8.8	10.3	22.1
	Phase B	3.9	6.8	7.3	13.2	22.6	43.5	79.9	161.7	318	670
	Phase C	9.8	18.5	20.9	41.5	81.8	173.3	365	820	1838	4350
Autumn	Phase A	0.2	0.3	0.2	0.4	0.3	0.8	0.6	1.6	1.2	3.8
	Phase B	0.5	1.1	0.8	2	1.9	6	5.2	19.4	1.2	69.1
	Phase C	0.7	1.6	1.1	3	3	9.6	8.8	34.1	28.5	133
Annual	Phase A	1.1	1.7	1.5	2.4	2.6	4.8	5.4	11	12	26
	Phase B	4.6	8.1	8.3	15.5	25	50	86	182	320	741
	Phase C	11	20	22	45	85	184	375	855	1868	4486

Table 4-3. Loss of life improvement with PV growth

Transformer Loading/ Phase C PV installation	TOT (Max) **(ºC)**	HST (Max) **(ºC)**	LOL (Days)
1.1 PU-26kW PV	79.5	137.9	22
1.1 PU-35 kW PV	77.1	130.6	14
1.2 PU-26kW PV	85.0	151.7	85
1.2 PU-40 kW PV	82.1	141.9	40

As revealed by Figure 4-10, Figure 4-11 and Table 4-3, regardless of the installed PV there is a significant decrease in the LOL rate of this transformer under the proposed scenarios when compared to the reference scenario. The extent of the reduction largely depends on the PV penetration level and their ability to produce power when most needed (i.e. the time periods at which the transformer loses its life at a high rate), as well as paper material and loading ratio of the transformer.

4.9.3 Balanced Operating Conditions (With Solar Input)

In the first two scenarios, the transformer was significantly unbalanced. In the last two scenarios, the benefit of balanced operation with and without PV generation is investigated. Load balance can be achieved using a distribution STATCOM (dSTATCOM) or optimal rephasing strategies with laterals or individual loads [41, 98]. Phase identification systems introduced in Chapter 3 can be combined with rephasing to improve voltage unbalance'. Figure 4-12 compares the transformer peak day when the transformer is balanced, to the current unbalanced case. The lower phase C current reduces the peak time HST to 115 °C from 130 °C. A reduction of 15 °C in HST translates into a reduction in LOL of approximately 2 days. It should be noted that in Figure 4-12 phase A and B would have experienced higher temperatures and therefore would age faster. The benefit is that whole transformer will age at the same rate.

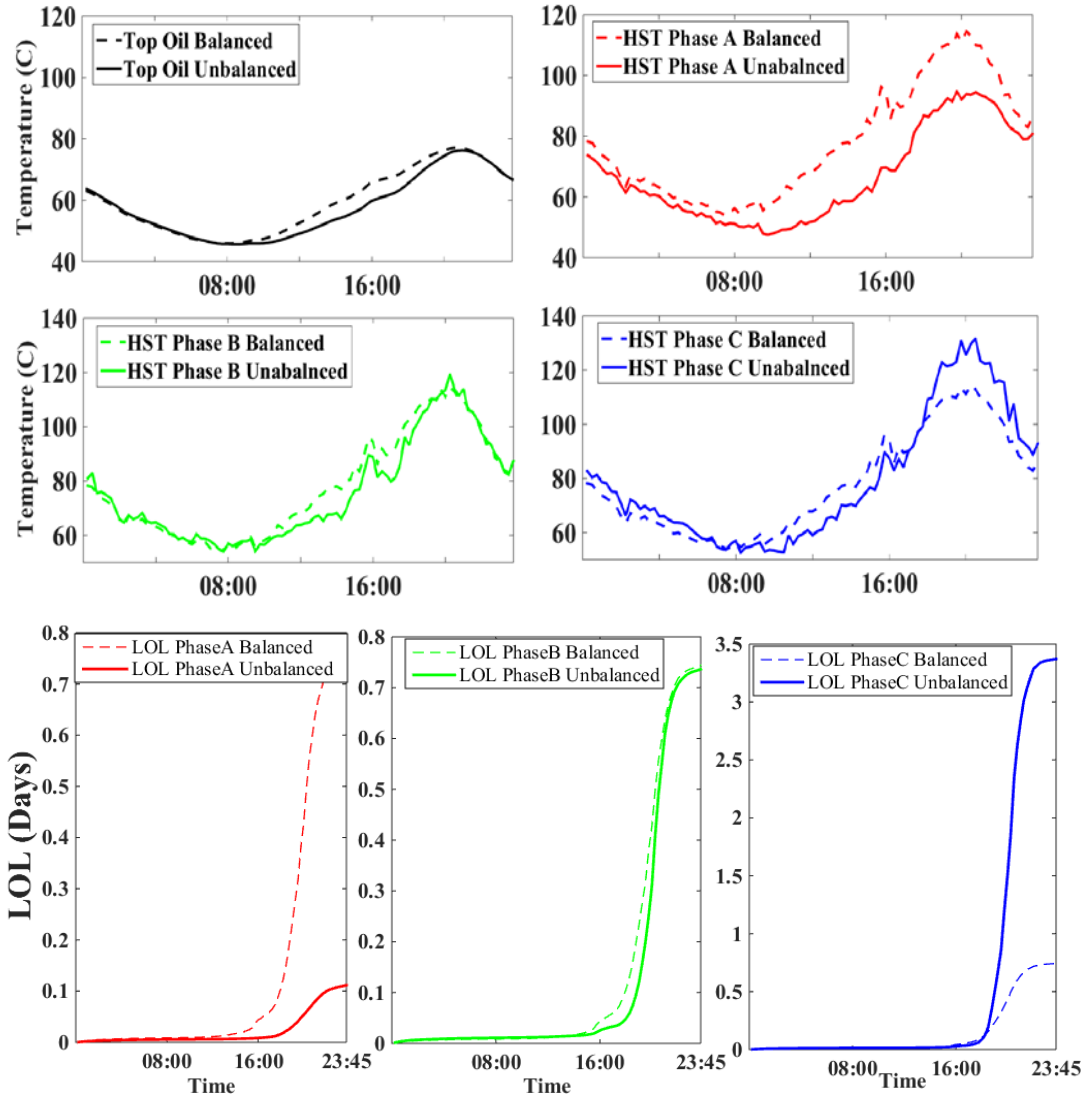

Figure 4-12. Balanced vs unbalanced loading, HST, TOT and LOL

4.9.4 Balanced Operating Conditions (No Solar Input)

The 200 kVA distribution transformer under study already has 32% (64 kW) of rooftop PV connected to its LV side. To extract the solar component, the production pattern of PV units was obtained from the calculated and collected values using the solar irradiance measurements during the first three months of the trial (July-September 2011) and the smart meter data in 15-minute intervals during the remaining period of the trial (October 2011-June 2012), corresponding to 96 data points per day.

For the first three months of the trial, no separate recordings were available on the houses with rooftop PV, therefore PV generation patterns were generated based on the solar irradiance, ambient temperature and information from the data sheets of the PV modules and inverter. To make sure the correct result has been achieved for the first three months, the solar generation profiles of these months were correlated with the generation pattern of the next 9 months and a high level of correlation was observed. Out of the 34 premises with PV connection, 12 houses were equipped with dual reading meters that enabled us to capture the generation profile of the PV separately from the consumption of the houses. Based on these generation patterns, as well as the PV and inverter rated power, efficiency and orientation of each individual PV, the generation profile for the other 22 houses, which only had net meter recording, were simulated.

The LV distribution system is investigated for five operating conditions to validate distribution system behaviour if there was no roof top PV connected to it. Case 1 illustrates the transformer hot spot temperature and loss of life quantities that correspond to the balanced loading of the transformer with no roof top PV. The purpose of this illustration is to capture the effect that ambient temperature might have on the distribution transformer LOL rate as well as establishing a reference case.Cases 2-4 explore the transformer hot spot temperature and its impact on transformer life under higher than rated current output during 12 months (1st July 2011- 30th June 2012). For case 5, a worst case is investigated by increasing the load to 1.4 pu (280 kVA).

To conduct a comprehensive comparison, the daily HST and annual LOL rates were calculated when the transformer was balanced and had no PV connection. Table 4-5 shows that the transformer will suffer from rapid loss of life when the winding is

under excessive stress. Balancing the phases will assure excessive LOL does not occur in one phase. Important benefits may be realised due to the life extension of distribution transformers brought about by customer-owned PV units even when the transformer is balanced.

Table 4-4. Loss of Life under different scenarios

Normal Paper					
	Loss of life 1.0 pu loading (days)	Loss of life 1.1 pu loading (days)	Loss of life 1.2 pu loading (days)	Loss of life 1.3 pu loading (days)	Loss of life 1.4 pu loading (days)
No Solar	4.6	12.2	36.9	125.2	471.7
32% Solar	2.6	6.6	19.2	63.0	232.4
Thermally upgraded Paper					
	Loss of life 1.0 pu loading (days)	Loss of life 1.1 pu loading (days)	Loss of life 1.2 pu loading (days)	Loss of life 1.3 pu loading (days)	Loss of life 1.4 pu loading (days)
No Solar	1.2	3.0	7.9	20.9	55.8
32% Solar	0.7	1.7	4.3	11.5	30.9

Table 4-5. LOL under different loading scenarios (balanced vs. unbalanced)

Transformer Loading	Scenario 1 Unbalanced (PV)	Scenario 2 Unbalanced (No PV)	Scenario 3 Balanced (PV)	Scenario 4 Balanced (No PV)
1.0 pu	11	20	2.6	4.6
1.1 pu	22	45	6.6	12.2
1.2 pu	85	184	19.2	36.9
1.3 pu	375	855	63	125.2
1.4 pu	1868	4486	232	472

It should be noted that under scenario 2, with a loading of 1.4 pu, the transformer would lose more than 12 years of its life in one year. If the transformer was not upgraded it could reach its end of life within 1-2 years of continuous operation.

4.10 **Summary**

A thermal model was developed to assess the transformer temperatures over a 12 month cycle allowing a cumulative measure of loss of life to be determined for various scenarios. This work is based on 15-minute field data and captures the impact of solar and load variability at these time scales.

The principal concept that was introduced in this chapter is that PV generation can delay and reduce the temperature rise of large oil-immersed transformers even when peak demand continues well after sunset. The time lag due to thermal inertia and ambient temperature decline allow overloading of the transformer beyond its normal rating without significant loss of life. PV generation will extend the life of oil-immersed distribution transformers even when the peak demand occurs well after sunset. The variations in irradiance produced by changes in cloud cover can cause faster fluctuations in the power generated by roof top PV. The short fluctuations (less than 15-minutes) would not have a significant effect on oil temperature (with time constant of 180 minutes) but could change the winding temperature in a magnitude of 2 °C to 3°C (the winding time constant is 10 minutes). This will not significantly contribute to the aggregated loss of life given the short duration. Finally, the general trend of life improvement will increase with PV penetration until power flow reversals, comparable to the peak demand, occur. At this point, the additional winding losses become significant.

The impact of PV on a single-phase distribution transformer (in the US, or SWER in Australia) is similar to the case where the three-phase transformer is balanced (scenarios 3 and 4). It is expected that as the coincidence of PV with commercial load is higher, better life extension will result for commercial load transformers. These results are specific to parts of the Western Power metropolitan

system. Differences in load shape, weather, and number of houses per transformer vary substantially depending on region, as well as within the same region.

Chapter 5 Voltage Balance Improvement in Urban Residential Feeders

Phase balancing problems are becoming more important in the deregulated environments because balancing can improve power quality with minimum cost. The main contribution of this chapter is to propose transferring the single-phase residential loads from one phase to another, within a three-phase system based on their annual billing data, to reduce voltage unbalance along the feeder and power mismatch among phases. The method can be further refined using any standard optimisation method such as particle swarm optimisation (PSO). The methodology is validated using data from a real Australian distribution network with considerable unbalance.

5.1 **Introduction**

Voltage Unbalance (VU) is one of the main power quality problems in distribution networks [101]. The unbalance is more common in Low Voltage (LV) feeders due to phase load inequality, especially where large single-phase loads are used. Three-phase four-wire LV systems, such as 400/230V systems found in Australia, Europe and the United Kingdom, will typically serve 60 to 120 consumers with a single transformer. Some efforts are made at initial connection to balance the phase loading but significant unbalances develop during normal operation because of the random phase allocation of customers, diversity of consumption among the houses and phase connection changes made by line workers when performing repairs on the lines and poles. The network configuration and length also has impact on the VU in the feeder. A major cause of voltage unbalance is the uneven distribution of

single-phase loads that can be continuously changing across a three-phase power system [101].

Single-phase loads are indirectly affected by unbalance if the unbalance causes over-voltages or under-voltages that exceed statutory limits. Based on Australian Standard, 60038-2000, the Australian low voltage network voltage is 230 V with a tolerance between +10% and –6% [102]. Voltage unbalance spreads through the network as zero sequence and negative sequence apparent powers are injected from loads and untransposed lines and cables. Negative sequence currents flow through the network in the same way as positive-sequence currents, while zero sequence currents are interrupted by network components such as Δ-Y transformers.

As mentioned, unbalanced loads are one of the main causes of unbalanced voltages on distribution circuits and, thus, a great deal can be gained by attempting to distribute single-phase loads equally across all three phases. There are practical options for balancing the three-phase electrical systems. One is to reconfigure the feeders at system level and the other is phase swapping at the feeder level [103]. The purpose of these approaches is to balance loads among feeders; therefore, it is not an effective technique to settle the unbalance problem in the distribution system at the LV level. Under normal operating conditions, the network is reconfigured to reduce the losses of the system and/or to balance load in the feeders.

The network reconfiguration consists of modifying the topology of the system by switching locally or remotely controlled sectionalising switches. In this process, the nodes can be energised through different paths through the interconnection with other feeders (substations) and/or interconnection of nodes belonging to the same feeder. Usually, distribution systems operate with a radial topological structure; consequently, the opening and closing of sectionalising switches must be made while

considering this constraint. The problem consists of determining an ordered switching list that allows reduction of losses or balancing the load of the system without infringing operational and topological constraints [11].

Phase swapping is an effective way to balance a feeder in terms of its phase load, and consists of change the connection of the loads or lateral branches among the phases of the line. Carrying out the appropriate swapping can reduce the unbalance level of the network, since the main causes of unbalances in an electric network are the single-phase and two-phase loads connected to a three-phase network.

It is necessary to determine the preferred phase swap that minimises voltage unbalance. A phase swap at any bus will result in the voltage magnitude and angle changes in all phases and all connected buses to some degree. In reality, it is quite possible that the voltages at any bus are already unbalanced due to other loads connected to the upstream side of the feeder. In addition, the problem is further complicated by the diversity and unequal distribution of the loads along the feeder. A method is developed in this chapter, which is not computationally intensive, is very straightforward and easily implemented. The method also has the following characteristics:

- effectiveness. The scheme should reduce the voltage unbalance along the feeder.
- scalability. The scheme should be easily scalable to larger networks.
- low cost. The hardware and labour costs should be minimal.

5.2 **Structural Modifications of Single-phase Loads**

One of the main objectives in this study is to mitigate the voltage/current unbalance through the most cost-effective process. Structural rearrangement is one of

those cost effective processes. For instance, the rearranging or redistributing of limited single-phase loads equally among all three phases can mitigate asymmetry. This refers to the distribution of the supply to individual homes or alternating connections in row of houses in residential subdivisions, per floor supply in commercial buildings or street lights [35].

5.3 **Case Study Networks**

The main advantage of working with real networks instead of synthetic ones is the possibility of capturing their particularities. For example, load unbalance, cable characteristics (direct in ground, drawn into ducts, copper conductor, etc.), and network characteristics (length, number/type of customers) are all implicitly captured from real data. Historically, utilities have mainly worked with synthetic (or generic) LV networks in order to assess the corresponding requirements of the planning stage. Given that operational aspects are typically not considered for LV networks, it is still uncommon for utilities to have accurate data and software packages that can be used for power flow analyses at LV level. In this work, 2 three-phase four-wire LV networks (Figure 3-4 and Figure 5-2) are modelled based on network connectivity data, considering the original network topology, conductor characteristics, customer locations/types and phase connectivity (when available). The first case study network represents a sub-urban Australian radial LV distribution network. The second case study network represents a typical UK radial suburban underground LV network [104].

The modelling presented in this thesis is based on an unbalanced load-flow analysis of a complete LV network, using load and generation data with 15-minute time resolution. It is much more detailed than the modelling used in typical design

studies for such networks, and could well be used for a broad range of network studies, providing detailed insight into network operation.

5.3.1 Australian LV Distribution Network

The modelled network in this work consists of an LV (suburban) distribution network incorporating 77 domestic homes facilitated by 23 pole-top connections and supplied by a 22 kV/400V transformer (200 kVA). Of these 77 dwellings, 34 consumers have rooftop PV systems that have average ratings of 1.88 kW. The total installed PV capacity is 64 kW representing a penetration of 32%. In Australia the nominal voltage on the LV network is 400/230V and the voltage range tolerance is +10% -6%. The modelled network is radial in structure with the sub-distribution and consumer connection cabling being modelled as overhead cabling employing the approach discussed in [85]. These sub-main cables are 7X3.75 AAC (MARS) and 7X4.5 AAC (MOON) whereas the connections from the pole-top to the respective consumers is through 6 mm^2 hard drawn copper insulated service lines, which again is modelled as overhead cable (Table B-1). Load data, including energy consumption, solar power generation, voltage and current is recorded by smart meters on the Western Power network at the point of connection to each consumer switchboard at 15-minute intervals. Smart meter data has been collected since July 2011. The network under study is significantly unbalanced but reflective of normal network conditions. The unbalance results from the poor allocation of customer loading among the three phases and the development of PV connection driven by customers.

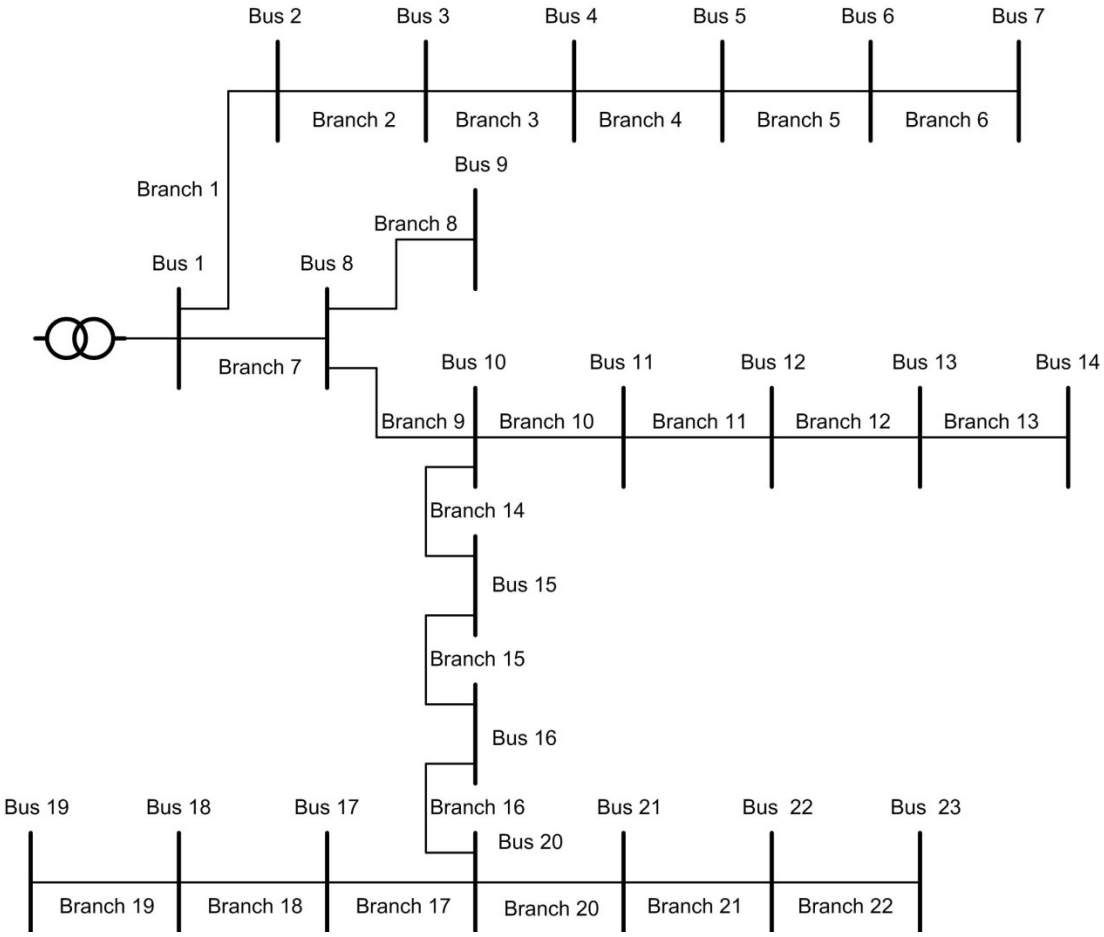

Figure 5-1 Australian LV aerial network

5.3.2 UK LV Network

The existing public UK network studied is depicted in Figure 5-2. It represents a suburban underground cable LV distribution. The network comprises a single 11/0.4 kV 500 kVA distribution transformer and four 400 V outgoing feeders with a total length of 1,588 m. The remote end of the second feeder has an open link point to a feeder from another LV network, which in the event of a fault may be closed. For the purposes of this work, however, the network is assumed to be radial. In total, there are 198 single-phase customers taken from 400 V three-phase street mains; each customer is assumed to use a 30 m long service cable. The total load (customer loads and public street lighting) is measured at approximately 450 kVA during maximum and 75 kVA during minimum loading conditions. For the purposes of this

work, all demand is attributed to customer loads. Detailed network data can be found in the Appendix B– Table B-2 [104].

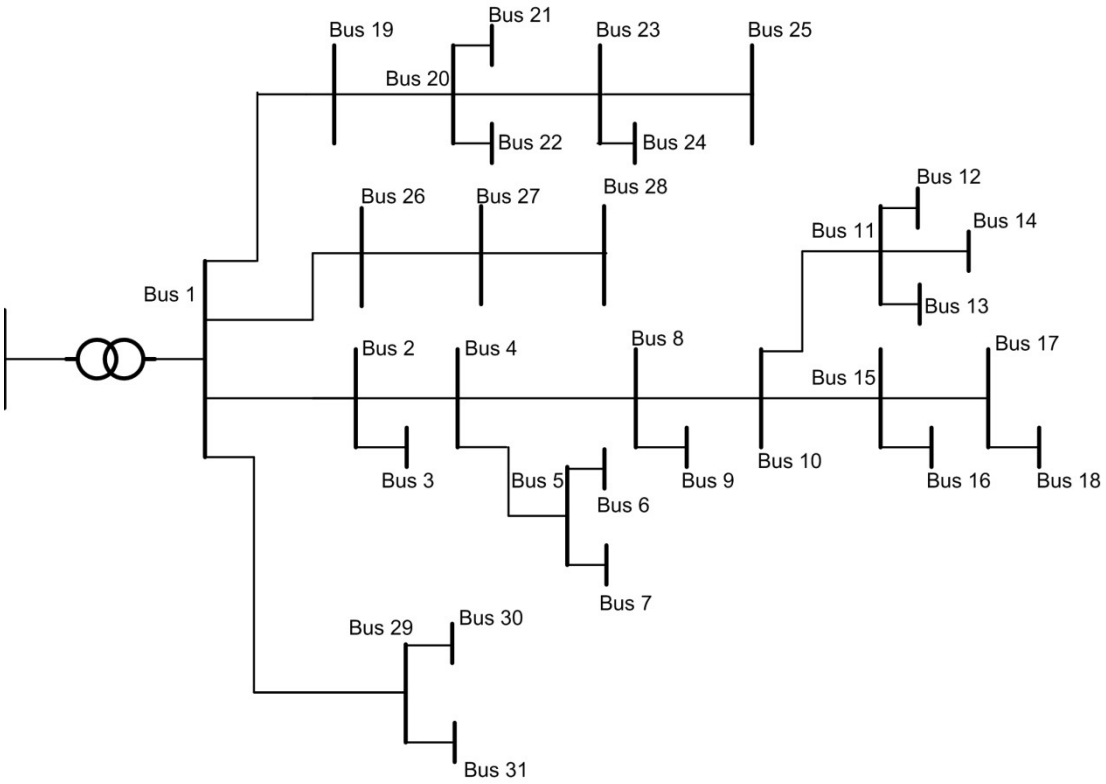

Figure 5-2. Existing public UK LV underground network

5.4 **Voltage Unbalance in the Australian LV Network**

As described in Chapter 3, for the network under study the transformer load and generation per phase is unbalanced. Figure 5-3 shows the individual phase loading as well as the aggregate three-phase load on each bus of the Australian LV network. It is apparent the blue phase (phase C) is the most heavily loaded phase, while the red phase (phase A) is the least loaded phase. In addition, the largest amount of solar PV system generation occurs on the blue phase. Note that, for visibility reasons, the white phase (phase B) is plotted in green in this thesis. This unbalance is likely to have implications for customer level voltage compliance as well. Figure 5-4 shows one of the instances when the voltage unbalance in some bus bars had exceeded the allowable limit on 25 November at 18:30. Inspection of the graph clearly shows that several of the buses are in violation of the acceptable limits

of voltage unbalance factor in a distribution network (2%)[2]. However, the important factor for these violations is their duration and frequency of occurrence in any given week (Table 2-1).

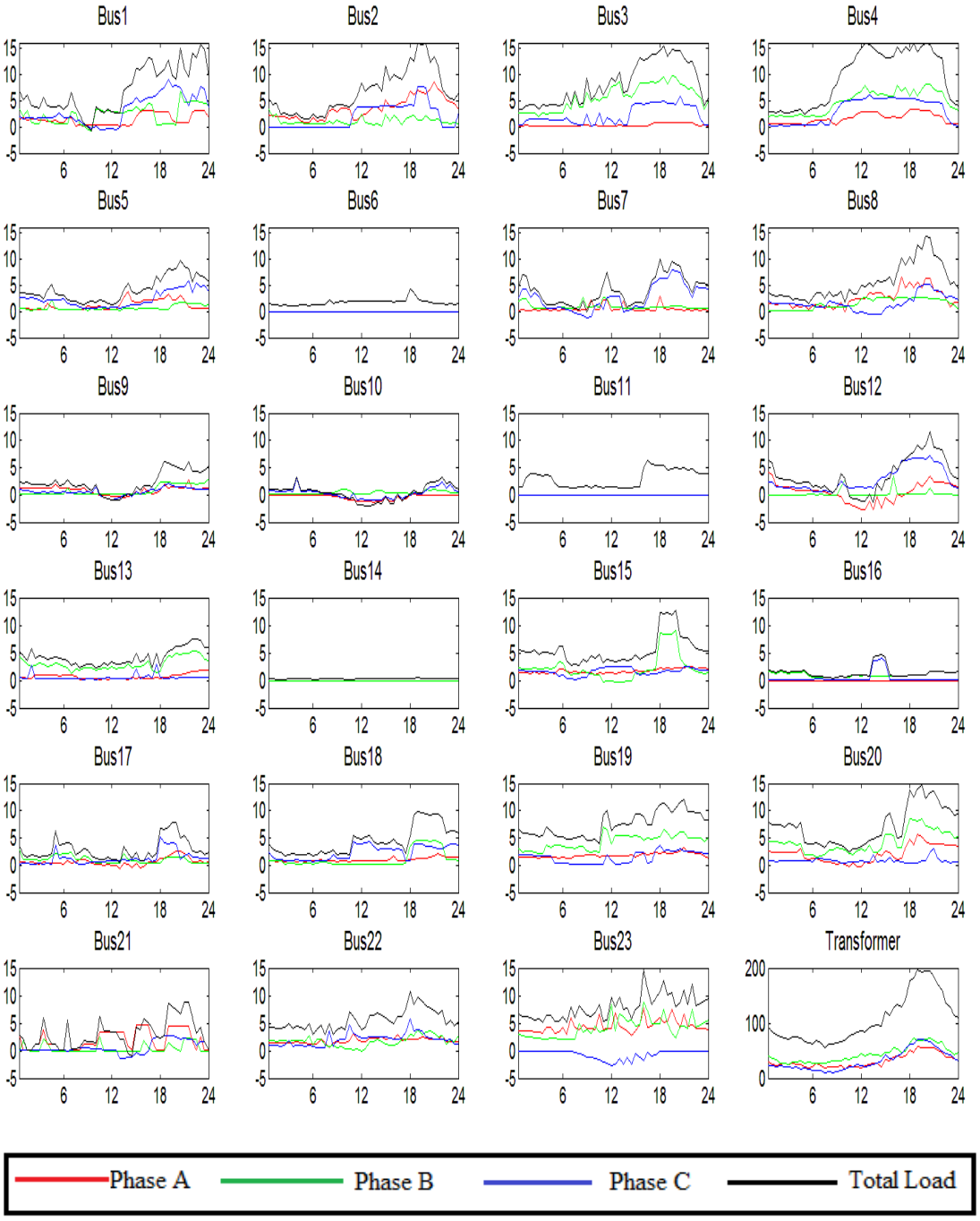

Figure 5-3. Individual phase loading on 23-bus LV network

[2] 61000-3-12 recognises that VUF can reach 3% in LV networks

A load flow analysis has been performed for the entire network for every half an hour for the period of one year (17,520 three-phase load flows).

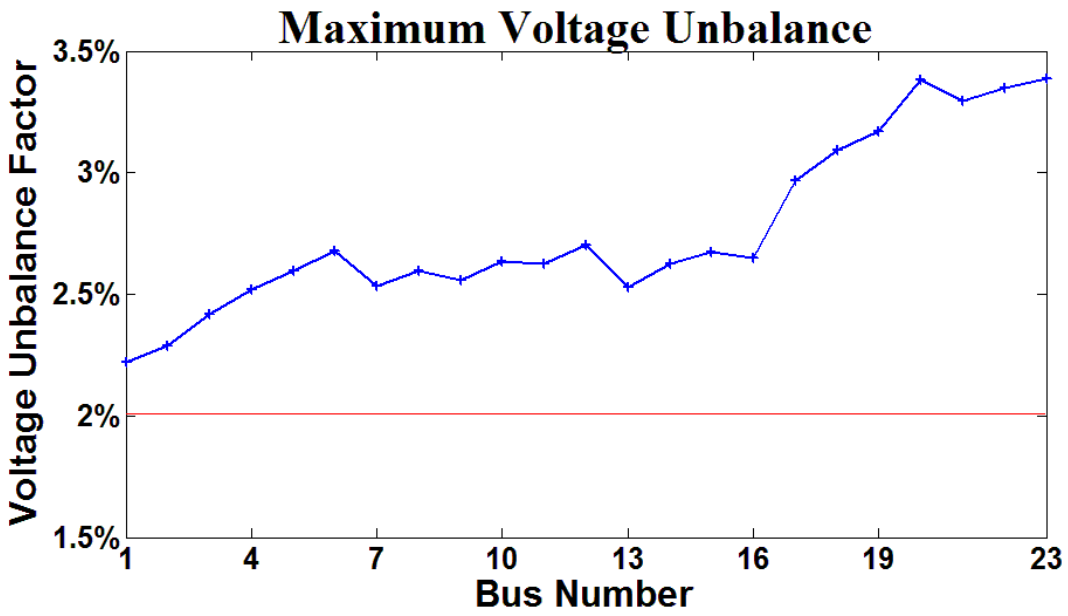

Figure 5-4. Voltage unbalance in base case

Figure 5-5 shows the histogram of voltage unbalance factor of all 23 buses in the network. This will be used to compare the improvement in voltage unbalance through different phase swap strategies and will be used as a basis for fail/pass criteria for each week [102].

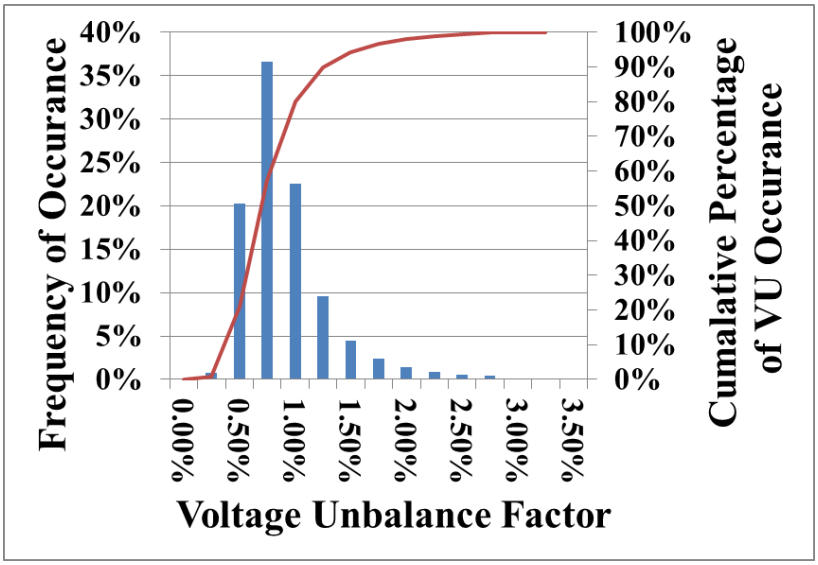

Figure 5-5. Australian LV feeder VUF histogram

In order to mitigate the voltage unbalance in this system it is important to understand which phase is contributing the most to the unbalance that is seen in the network. This task can be achieved by analysing the voltage unbalance angle at the worst affected buses.

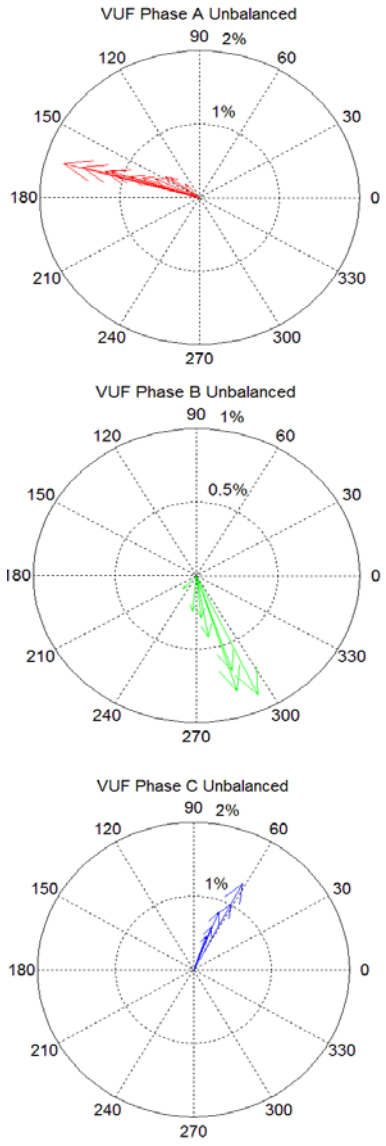

Figure 5-6. Vectorial distribution of VU (magnitude and angle)-each phase loading is varied while the other phases loadings are maintained constant.

Figure 5-6 shows the vectorial distribution of complex voltage unbalance factor when the loading on two of the phases on each bus is the same and the loading on the third phase is increased in 10% increments. It shows that when phase A is the phase contributing to voltage unbalance due to excessive loading on that phase the voltage

unbalance angle is in the range of 150-180°, while the unbalance angle would be in the range of 270-300° when phase B was the most heavily loaded phase. In the case of phase C being the phase with the most load consumption, the voltage unbalance angle would be shifted to the first quarter and would be in the range of 60-90°.

As seen in Figure 5-6, there is a spread of angles for each case that one phase is the dominating phase. This could be due to interaction between the phasor angles that is caused by load unbalance and the voltage unbalance that is due to line mutual impedance difference. What is presented in this figure is the summation of all sources of unbalance (i.e. load unbalance and line unbalance). Due to the fact that line unbalance (Z_{21} in the symmetrical component domain) stays the same for the three cases (load unbalance caused by different phases), the main contribution to voltage unbalance is the current demand caused by the dominant load.

The vectorial distribution (complex voltage unbalance) for the 23-bus network is shown in Figure 5-7. These phasor diagrams illustrate the VU magnitude and unbalance and show that the majority of the voltage unbalances that are above 2% can be attributed to a dominant load on phase C. The unbalance phasors are mainly concentrated in the region of 30-90°. There is a larger spread of angles for CVUF as they are the summation of voltage unbalance sources at different times of the day and year. There are nearly 200 instances when voltage unbalance exceeds the 2% limit (red inner circle) in the one-year period that data was collected.

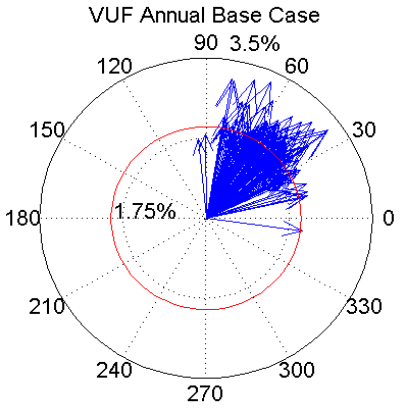

Figure 5-7. Vectorial distribution of VU (magnitude and angle) base case

5.5 **Phase Swapping Scheme**

To derive a phase swapping strategy for houses to improve the three-phase voltage and power balance of the distribution network and transformers, the phase voltages and currents of all primary line sections, laterals and transformers have been simulated using the three-phase load flow analysis that was discussed in Chapter 2. The voltage balance improvement is achieved by transferring the load from the highly loaded phase to the lightly-loaded phase at that bus. The number of phase swaps would be limited to three houses as this would spread single-phase customers evenly on the three phases (Table 3-3). The main aim of this method is VU reduction in the network; however, it indirectly improves the voltage variations and the power mismatch amongst the phases. This method does not result in the globally optimum condition; however, its main advantage is that only a few phase swaps are required. Although voltage rise and drop and three-phase power mismatch problems will be improved, they are not included in the primary concern. Phase swaps would be mainly based on three levels of knowledge about the distribution system:

1. phase swap based on billing data. In this case, the utility does not have detailed information about customer daily usage and only its quarterly and annual billing data is available.

2. phase swap based on billing data and PV generation. In this scenario the utility has knowledge about the separate consumption and generation billing data of the customers.

3. optimisation based phase swaps. A PSO based optimisation with a limited number of customer phase swaps is implemented to compare the results with previous cases. This case assumes complete knowledge of the distribution feeder in terms of customer phase connection and availability of the smart meter data at 15-30 minute intervals (voltage, current, real and reactive power)

5.5.1 Case 1-Billing

The customer phase swap in this case is solely based on the customers' annual billing data. Under this scenario, the top three single-phase customers with the highest annual energy usage that are initially connected to the heavily loaded phase (phase C) would be transferred to the least loaded phase (phase A). No other information would be required to choose the right candidates for the phase swap. The improved voltage unbalance profile is shown in Figure 5-8; it is evident after 3 phase swaps that the voltage unbalance in the feeder is reduced considerably.

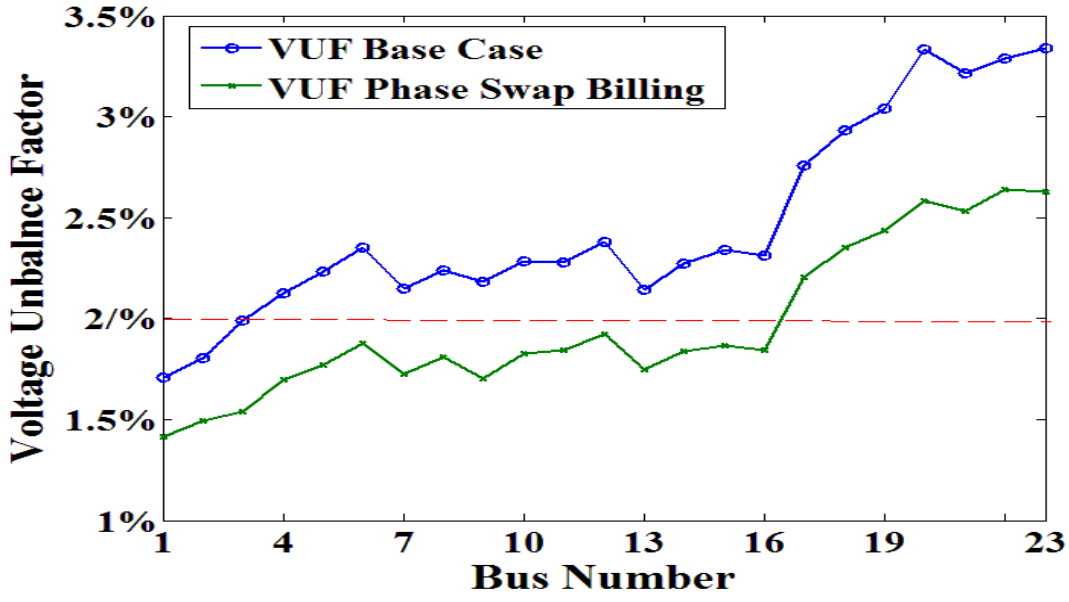

Figure 5-8 Improvement in VUF- phase swap based on billing

Now, the analysis is carried out for one 24-hour period, using the actual residential load profile and transformer voltage data. The maximum of voltage unbalance factor along the feeder is shown in Figure 5-9 before and after applying the proposed phase swaps. This figure shows that the phase swaps are effective in reducing the voltage unbalance along the feeder. The maximum network voltage unbalance factor was 3.27% which is reduced to 2.8% after three costumer phase swaps.

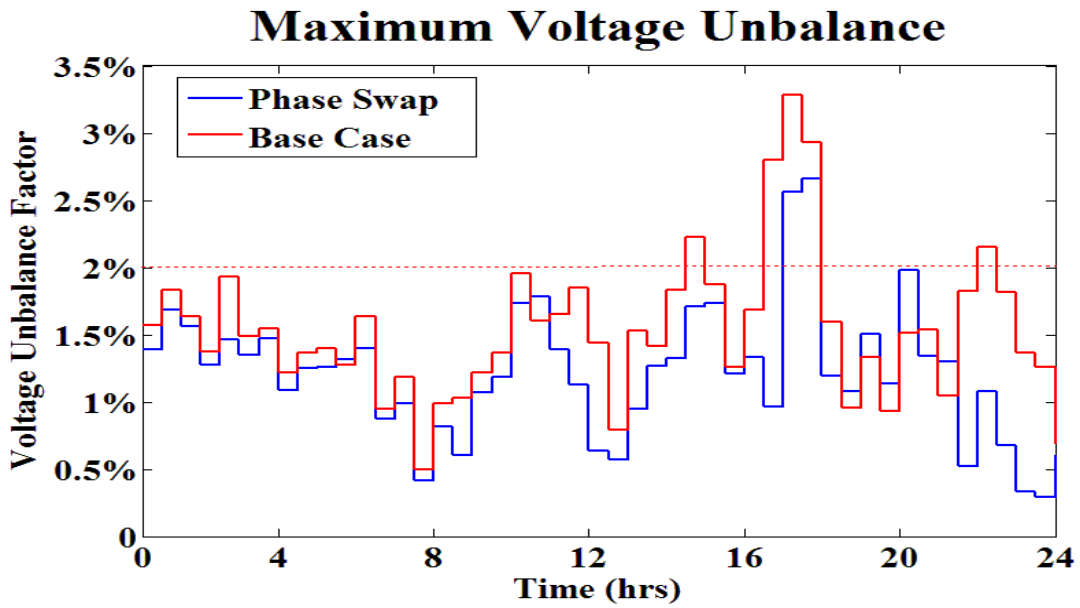

Figure 5-9. Maximum VU in the feeder before and after phase swaps

The important factor when considering changing customers phase connection is that these load transfers should improve the balance of the system not only for an instant or for a day but for the entire year. As a result, the load flow analysis based on the new phase connections has been performed for the entire year. In addition to the improvement to voltage balance in the system phase swapping could improve the voltage profile across the three phases, Figure 5-10 and Figure 5-11 show the change in the two minimum and maximum voltage extremes that the feeder experienced based on the available data. It can be seen that, as a result of customer phase swaps, the voltage profiles of all three phases have improved and voltages of customer at end of the feeder are clustered closer together.

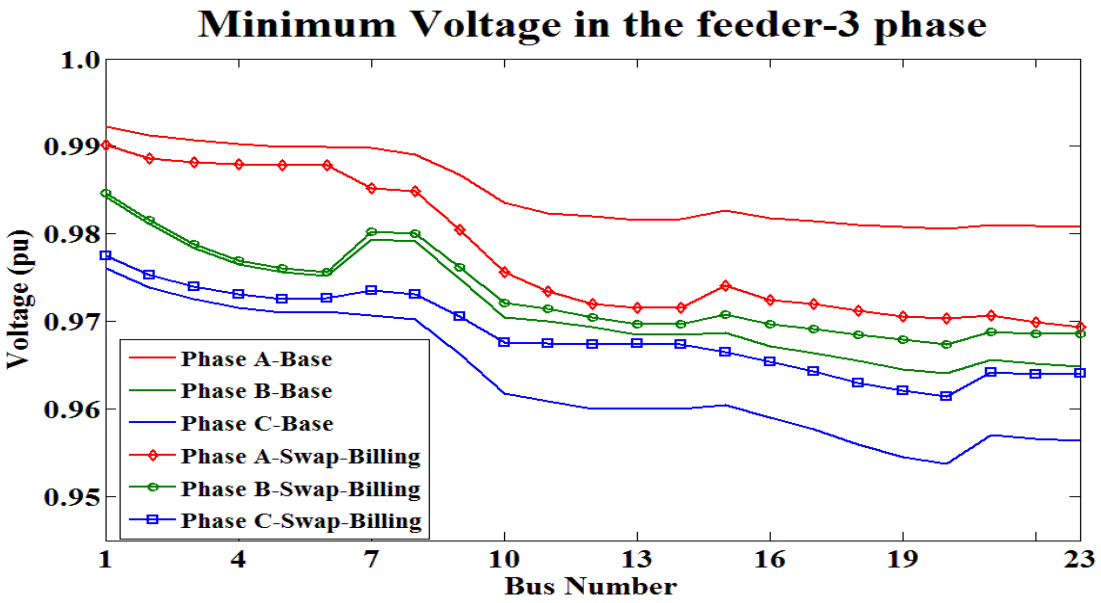

Figure 5-10. Minimum phase voltage at 23 buses, base case vs phase swap (across the year)

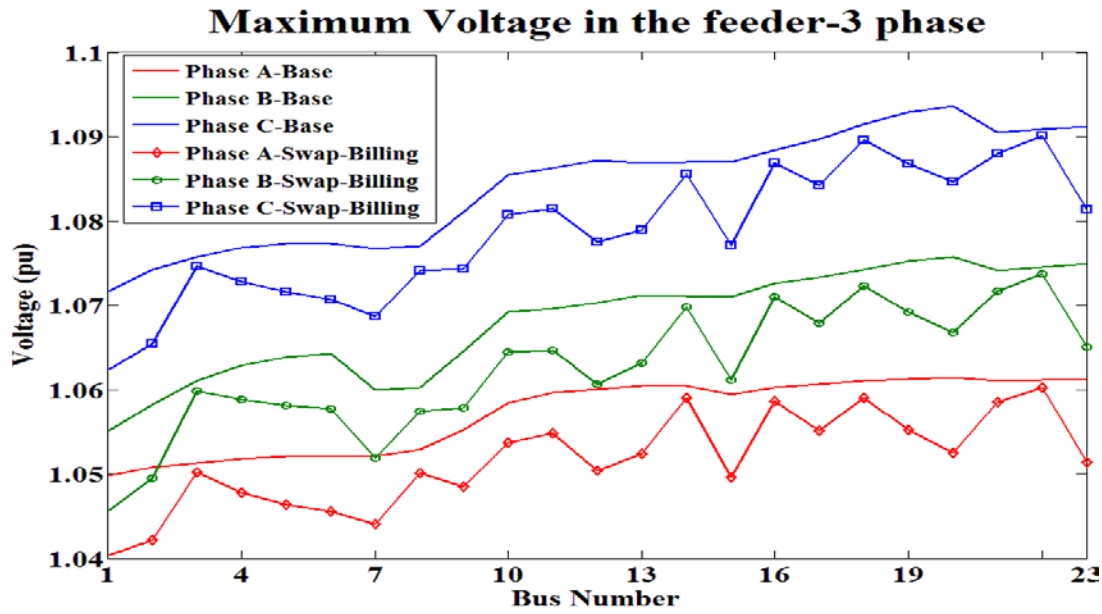

Figure 5-11. Maximum phase voltage at 23 buses, base case vs phase swap (across the year)

The phasor diagram for the 100 instances that the voltage unbalance factor is above 2% is shown in Figure 5-13. Comparing the phase angles of the complex VUF before and after phase swaps (Figure 5-12) shows that the voltage unbalance angle is becoming less influenced by phase C and more by phase B as phase B becomes the dominant phase.

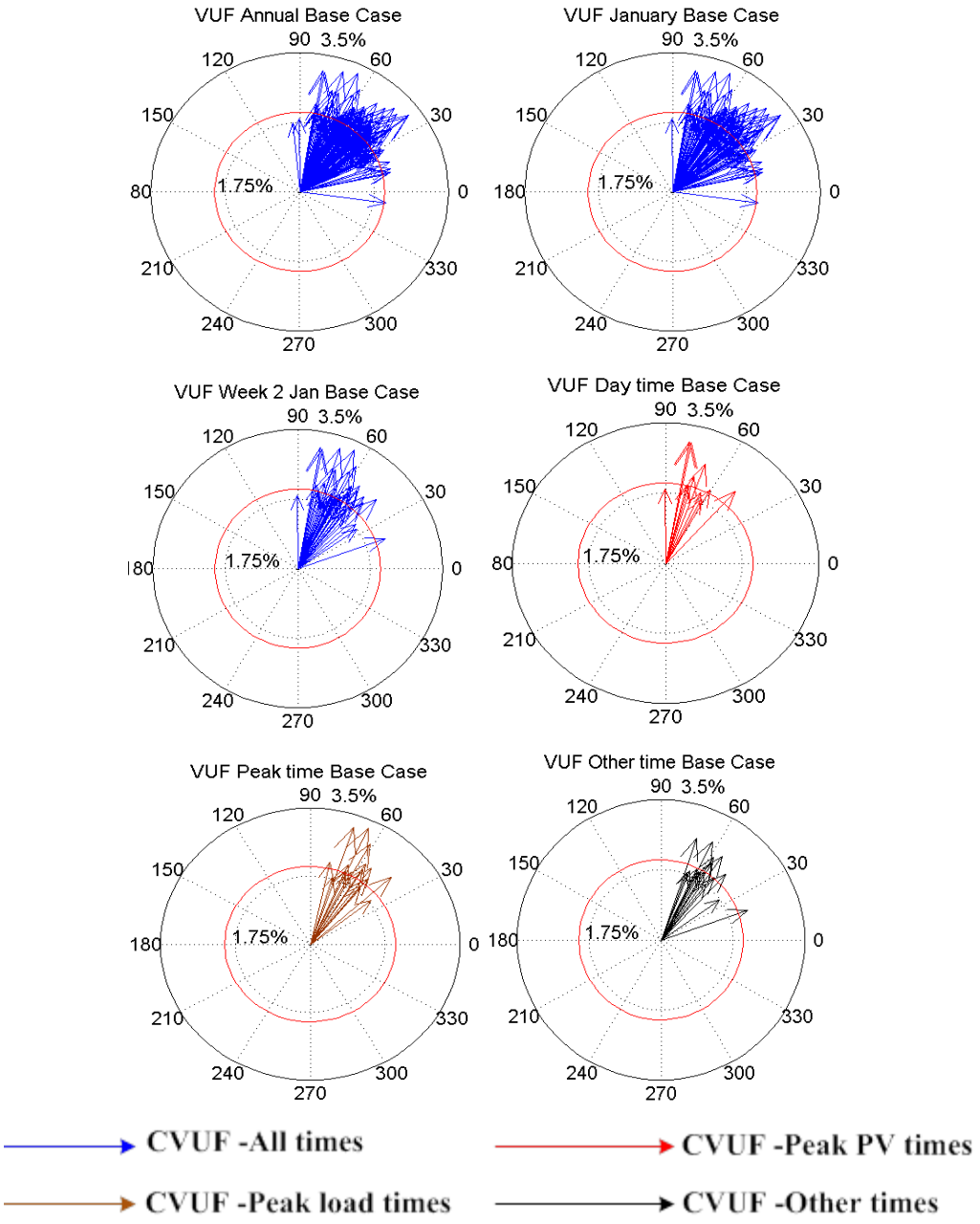

Figure 5-12. Complex voltage unbalance-base case

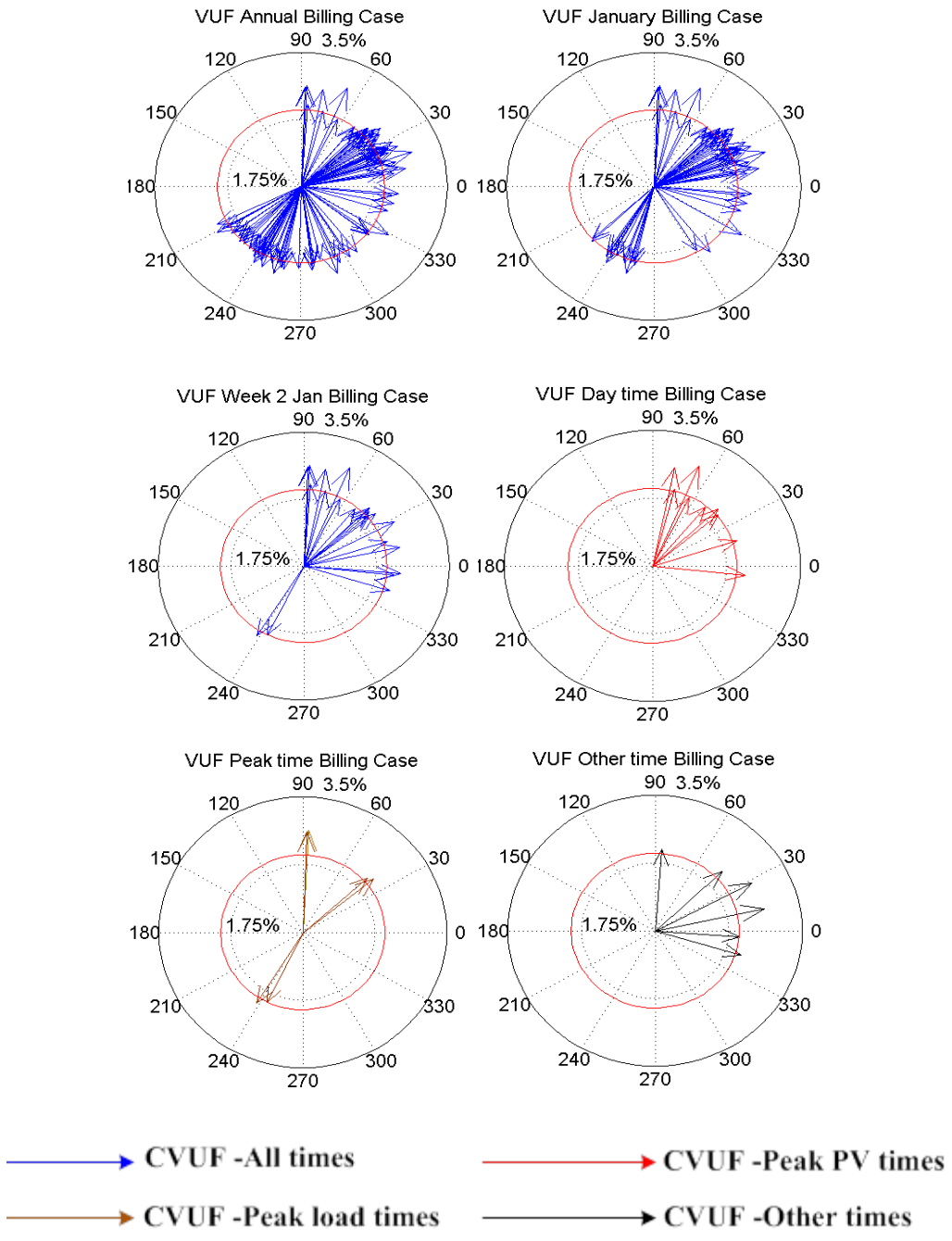

Figure 5-13. Complex voltage unbalance-phase swap-billing

Table 5-1 and Table 5-2 summarises the beneficial impact that the limited number of customer phase swaps based on a minimum level of information delivers to the LV feeder. These improvements are not only in terms of a reduction in the number of instances that are above the acceptable limit of 2% (reduction of more than 50% from 190 instances to 100) but in terms of also eliminating the extreme cases where VUF in some of the buses could have exceeded 3%. The other important

benefit that this limited phase swap brought to this LV network is in reducing the duration and continuity of instances where voltage unbalance is above 2%. This achievement could reduce the losses in induction motors and prevent premature motor failure caused by extra heating associated with unbalanced currents. It should be noted that the presence of three phase induction motors in a residential LV distribution network is not so common.

Table 5-1. Comparison of VUF occurrences in different cases (1 year)

	VUF > 2.0%	VUF 2.0-2.5%	VUF 2.5-3.0 %	VUF 3.0-3.5%
No PV	186	148	16	2
Base Case	190	166	20	4
Phase Swap based on Billing data only method	100	90	10	0

Table 5-2. Voltage unbalance duration

	No PV	Base Case	Phase Swap-Billing
VUF >1.5% lasting 1 hour or more	140	160	37
VUF >2% lasting 1 hour or more	91	30	4

5.5.2 Case 2-Billing and PV

As discussed earlier in section 5.3.1, the network under study has significant number of rooftop PV installations (34 houses, 32% penetration level). As a result of this, the phase swap method could be further modified and improved to include changing a customer's PV connection based on their phase attribute, PV power rating, the annual generation and exported energy in the year (the smart meters installed in the network are dual channel meters that log consumption and generation separately). To minimise the cost of labour, and to allow comparison with other cases, only three phase swaps are allowed under this scenario. These three customers were chosen based on their annual billing and energy export data. Priority of the phase swap is given to three houses that have PV installations and are consuming more than the average consumption of that phase. The selected houses should also

have a high in respect to energy exports to the grid. The vectorial distribution of all 23 buses of the Australian LV network with highest voltage unbalance (above 2%) for the entire year is shown in Figure 5-14 after the three phase changes based on billing and PV generation.

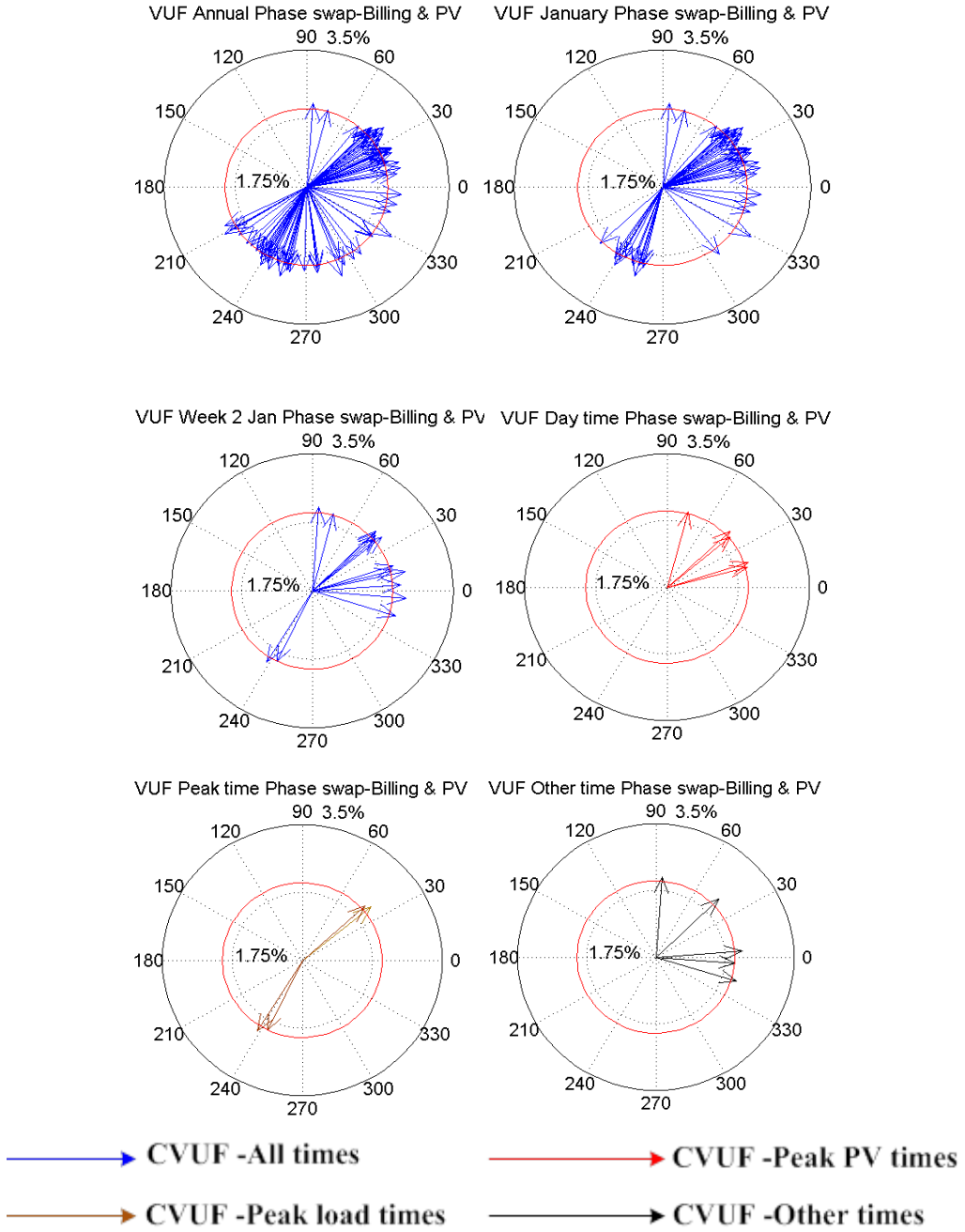

Figure 5-14. Complex voltage unbalance-phase swap-billing & PV

Figure 5-15 shows the change in the loading of the three (3) buses that had customers with phase swaps based on different levels of information.

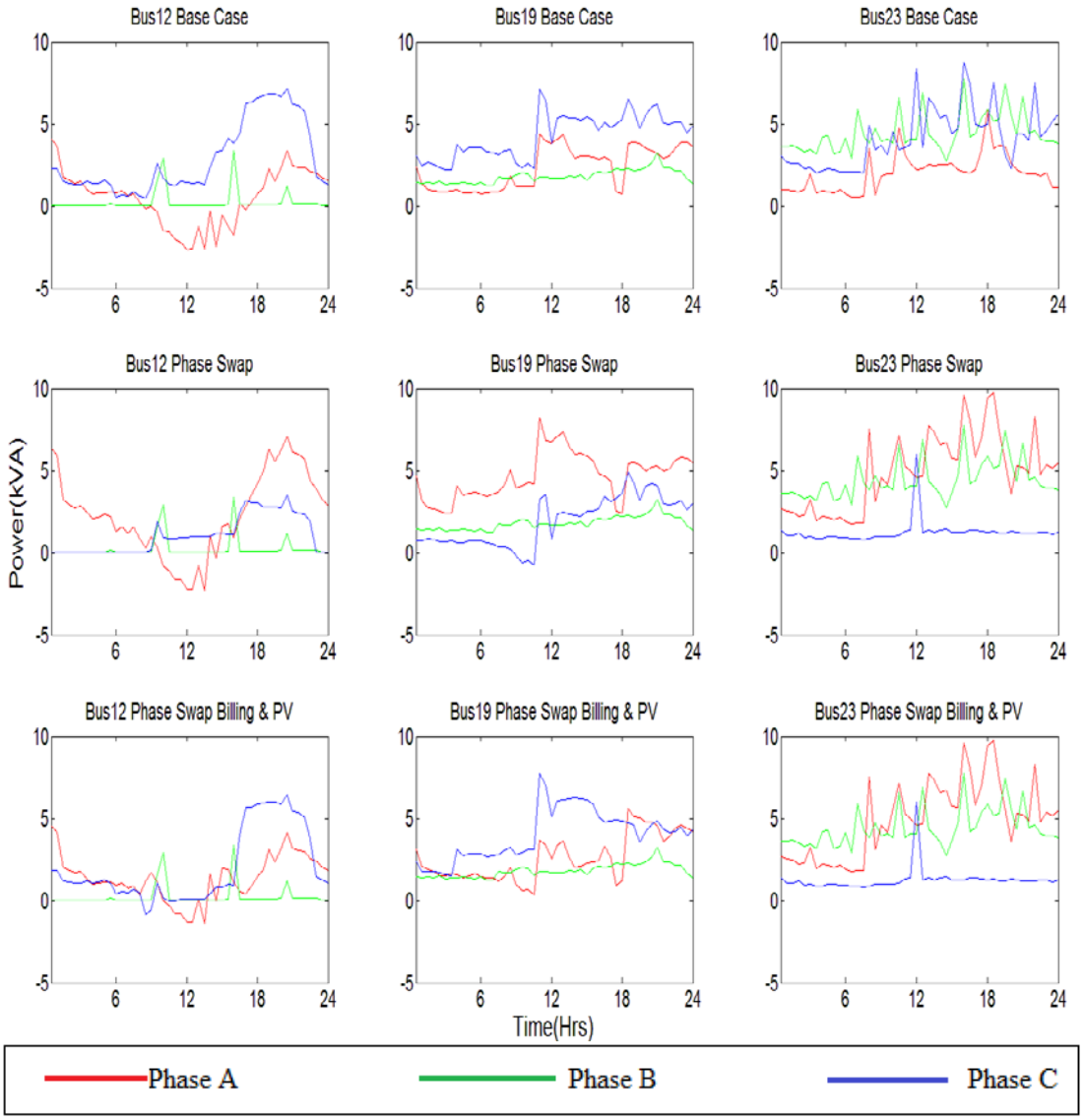

Figure 5-15.Load profile-phase swap cases 1 and 2

As mentioned earlier the Australian LV feeder (Pavetta) has 32% penetration of rooftop PV. This level of penetration was one of the highest at the time that the trial was undertaken (2011-2012). However, with the current rate of installation of distributed generation in Australia and around the world it is expected that there are LV systems that have higher PV penetration levels. In order to test the capability of the billing only and billing with PV methods for voltage unbalance mitigation in the case of higher PV penetration levels, the number of roof top PVs in the system has been gradually increased up to the level that penetration of PV capacity has reached

64% rating of the transformer. The allocation of additional rooftop PV will follow the same historical distribution between the phases as is depicted in Table 3-3, which will result in more rooftop PV installations on phase C of the network. Figure 5-16 shows the maximum voltage of the LV feeder as a result of increasing the PV penetration on the network based on the abovementioned routine. It is evident that as the PV penetration reaches 60-70% capacity of the transformer peak the voltage of most of the buses at the end of the feeder are above the acceptable limit of 1.1 pu.

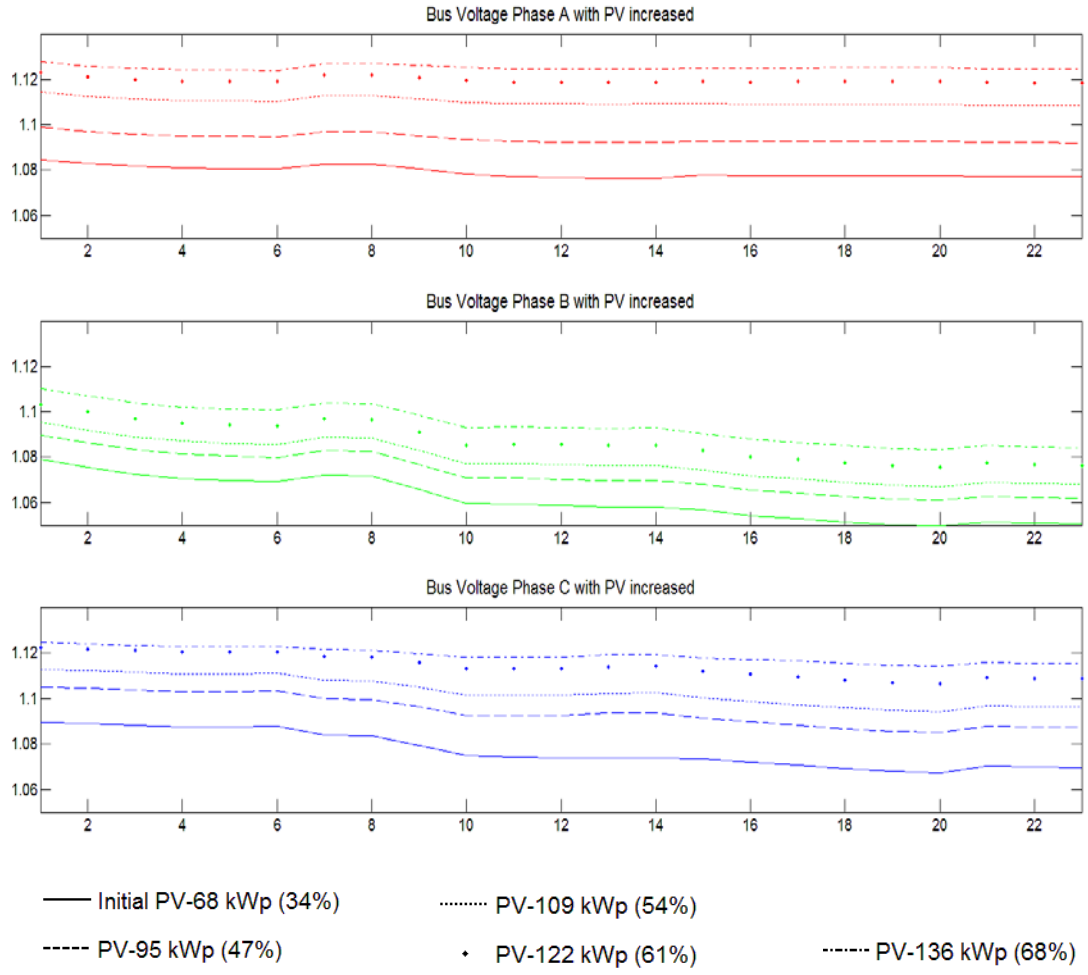

Figure 5-16. Maximum voltage with increase in PV penetration

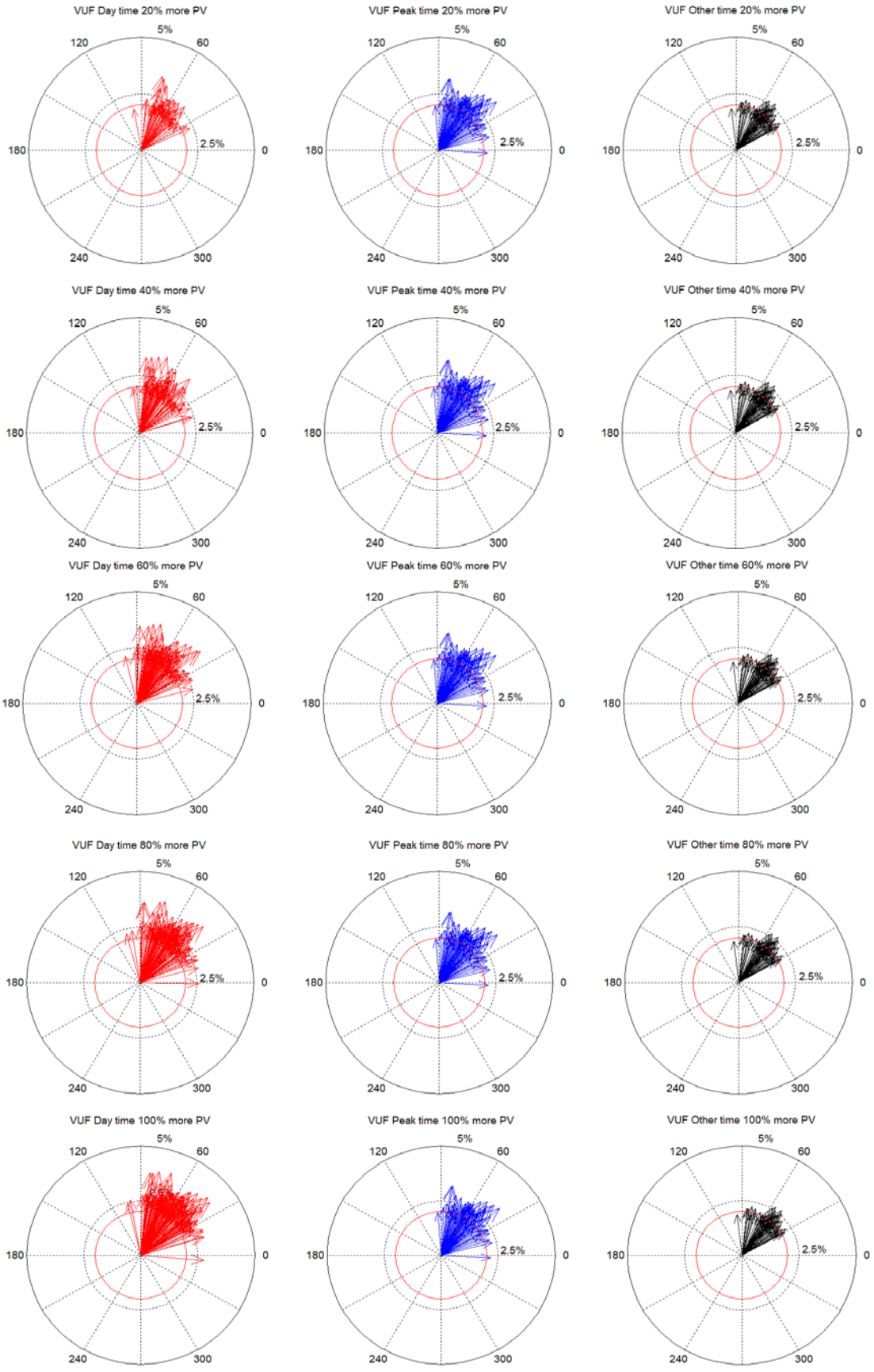

Figure 5-17. Voltage unbalance factor with increase in PV penetration

The voltage unbalance factor for different increments of PV penetration is shown in Figure 5-17. The figure shows that as the penetration increases the voltage unbalance becomes more and more of a problem during day time (peak PV generation time). First, the phase swap method based on billing only strategy was applied to pick the correct candidates for phase changeover, but, by looking at Table 5-3 we can see that phase swap based only on billing information cannot mitigate the voltage unbalance as PV penetration increases.

Table 5-3. Voltage unbalance mitigation by billing only phase swap in presence of more PV

Increase in PV capacity compared to base case	Number of instances VUF above 2%	Maximum VUF	Number of instances VUF above 2% after phase swap (Billing only)	Maximum VUF after phase swap (Billing only)
0	190	3.3%	100	2.8%
20%	210	3.4%	115	2.8%
40%	260	3.5%	150	3%
60%	300	3.7%	200	3.1%
80%	330	3.8%	260	3.3%
100%	400	4.0%	300	3.5%

In order to mitigate the excessive voltage unbalance that the network experiences due to the increase in PV generation, the billing plus PV phase swap method was applied, and, as a result of incorporating the information from PV export power to the grid, better voltage unbalance mitigation results in comparison with the previous method could be achieved. Table 5-4 summarises the results achieved under this scenario.

Table 5-4. Voltage unbalance mitigation by billing and PV phase swap in presence of more PV

Increase in PV capacity compared to base case	Number of instances VUF above 2%	Maximum VUF	Number of instances VUF above 2% after phase swap (Billing and PV)	Maximum VUF after phase swap (Billing and PV)
0	190	3.3%	90	2.5%
20%	210	3.4%	105	2.5%
40%	260	3.5%	120	2.6%
60%	300	3.7%	140	2.6%
80%	330	3.8%	160	2.7%
100%	400	3.8%	175	2.8%

5.5.3 Case 3-Particle Swarm Based Optimisation Phase Swap

Voltage unbalance can be reduced even further if more data is available for making a decision and a general optimisation is applied. Any optimisation tool can be used for this purpose. In this study, a particle swarm optimisation (PSO) based method is chosen. Unlike classical optimisation techniques such as gradient search methods, the PSO based optimisation does not get stuck at a local minimum but will normally converge to a global minimum, if it exists at all within a limited number of iterations and particles. This algorithm can work as long as fitness values for the optimisation model can be calculated. Compared with the genetic algorithm, the advantage of PSO is that it is simple in terms of mathematical expression and understanding. PSO is very fast in converging to a solution when compared to genetic algorithms because of its mathematical simplicity. The PSO performance is represented by an exploration of an optimum and limited phase rearrangement to minimise the voltage unbalance on the feeder. The benefit of this approach is that many phase arrangement patterns can be examined by PSO.

This optimisation is based on assuming a vector with column number equal to the number of the houses in the network. The value of each vector array (cell) can be 1, 2, or 3 which represents, respectively, the phase A, B, or C connection for each single-phase house. Each cell must have a value between one (1) and three (3), at any time, to indicate that it is connected to one phase. To be able to compare the result of the PSO with previous cases, only three phase swaps are allowed in any iteration. After each iteration, the three phase load flow program that was introduced in section 2.8 will calculate the voltage unbalance factor, and maximum and minimum voltage of three phases for all the 23 buses in the entire year. The objective of the PSO is to eliminate any instances where the voltage unbalance factor is above 2% as well as reducing the number of the weeks that 95 percentile criteria as discussed in section 2.2 would not be met. Table 5-5 provides a summary of all the cases and scenarios that were investigated in this chapter.

Table 5-5. Comparison of all cases

Case	VUF > 1.5%	VUF > 2%	Maximum VUF	Number of weeks failing 95% Criteria	Time of the year VUF is less than 2%
No PV	890	186	3.1%	8	93.8%
Base Case	1026	190	3.3%	9	93.2%
Phase Swap (Billing)	640	100	2.8%	4	96.1%
Phase Swap (Billing and PV)	120	90	2.5%	2	97.8%
Doubling the PV Penetration (32% to 64%)	1200	400	3.8%	10	89.2%
Doubling the PV- Phase Swap (Billing and PV)	539	175	2.8%	7	94.1%
Optimisation (Existing PV Penetration)	198	61	2.2%	1	98.6%
Optimisation (Doubling PV penetration)	455	101	2.3%	2	97.6%

Table 5-6. Impact on voltage boundaries in one year: (base 230 V, +10%, -6%)

Case	Maximum Voltage 3 phases (pu)	Minimum Voltage 3 phases (pu)
No PV	1.08	0.93
Base Case	1.10	0.95
Phase Swap (Billing)	1.09	0.96
Phase Swap (Billing and PV)	1.08	0.96
Doubling the PV Penetration (32% to 64%)	1.13	0.95
Doubling the PV- Phase Swap (Billing and PV)	1.10	0.96
Optimisation (Existing PV Penetration)	1.09	0.97
Optimisation (Doubling the PV Penetration)	1.10	0.97

5.6 **Impact of Phase Swap on VUF in UK Network**

To investigate to what extent the method introduced in this chapter could improve the voltage unbalance in networks with different topology and/or impedance, an existing UK underground LV network that was discussed in section 5.3.2 was chosen for this analysis. As the UK network has eight (8) more buses than the Australian LV network, it was decided to allocate customer loads to the 31-bus underground feeder randomly but with the intention to keep the loading on phase C of the network greater than the other two phases.

Under the base case scenario (with no phase swap) the UK network under study is expected to have lower voltage unbalance factor compared to the Australian LV feeder. This is due to the fact that the UK feeder is an underground LV feeder whereas the Australian LV feeder is aerial and has higher voltage variation due to the load/PV variation. Figure 5-18 shows the maximum VUF that is observed in the UK underground LV feeder. As expected, the VUF is lower in this case (2.4% in

comparison with 3.3%) nevertheless the unbalanced load and PV generation in the system cause the VUF to be in violation of the voltage unbalance criteria for 3 weeks of the year (the load flow was performed based on Australian load profile for one year).

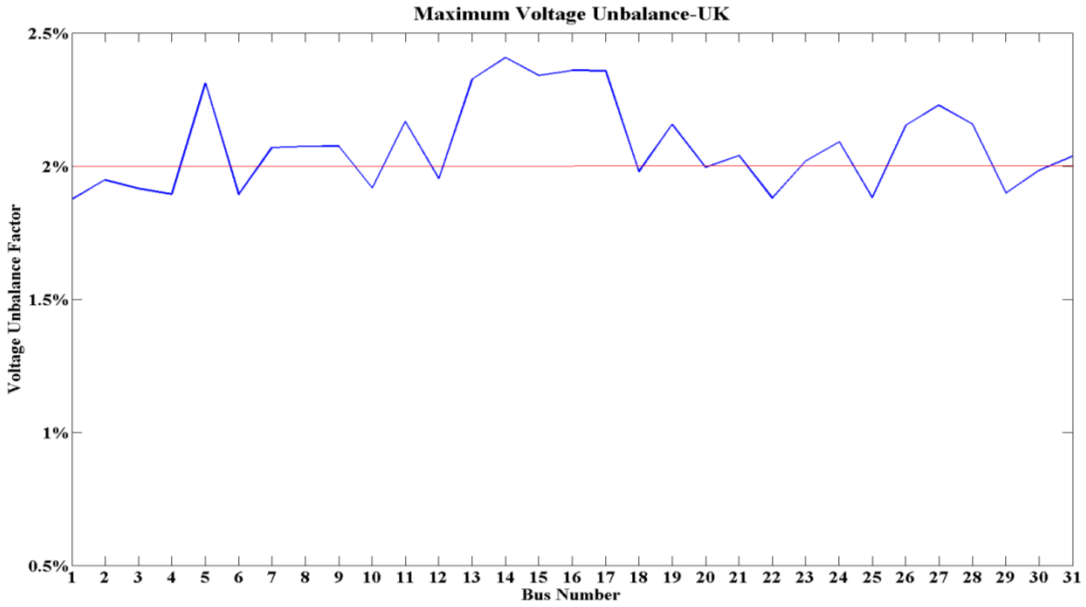

Figure 5-18. Maximum VUF in UK LV feeder-31-buses, base case

Figure 5-19 shows the effectiveness of the proposed method of phase swap (billing only as well as billing with PV). In the case of phase swap based on billing only information the maximum VUF in the network over the one-year period was reduced to 2.1% with only one week that the network voltage unbalance was in violation of the 95% criterion. When the phase swap based on billing and PV information is applied the VUF network is always less than 2% and within standard (Table 5-7).

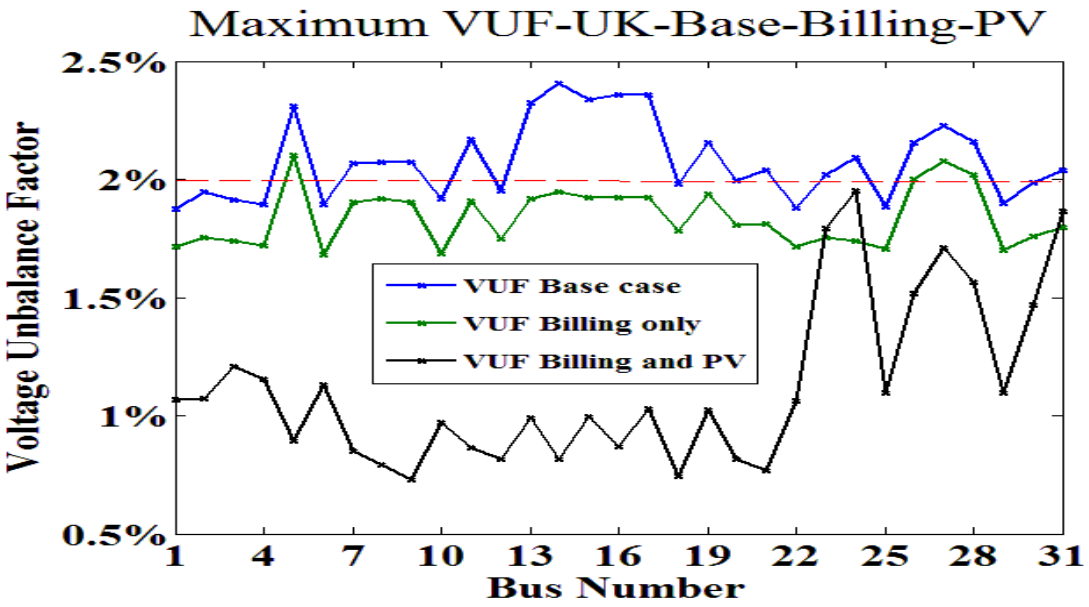

Figure 5-19. Maximum VUF at UK LV feeder-31-buses, base case vs billing vs billing and PV

Table 5-7. Comparison of three main cases for UK network

Case	VUF > 1.5%	VUF > 2%	Maximum VUF	Number of weeks failing 95% Criteria	Time of the year VUF is less than 2%
Base Case	96	58	2.4%	3	96.2%
Phase Swap (Billing)	54	25	2.1%	1	98.1%
Phase Swap (Billing and PV)	11	0	1.95%	0	98.8%
Optimization	8	0	1.96%	0	99.1%

5.7 **Summary**

An effective residential phase swap method is proposed in this chapter. Customers can be transferred from one phase to another based on their annual billing data and/or PV generation. A PSO can be applied for voltage unbalance and power mismatch reduction among the three phases. The effectiveness of the proposed method has been verified through MATLAB analyses of a typical Australian and UK LV distribution feeder using the load profile data available from smart meters. The analysis results for a 24-hour period showed how effectively the voltage unbalance is reduced by applying the customer phase change schemes developed. Similarly, the

results for a one-year period showed that the method is effective and does not cause adverse impacts at other times both in terms of voltage magnitude and unbalance.

Chapter 6 Distribution System Wide Voltage Balancing Methods

6.1 **Introduction**

The thesis identifies that the feeder voltage profile and unbalance are two main concerns in planning distribution networks. These two can be improved by employing distributed static compensators (dSTATCOMs) and limited phase swaps. In this chapter, the size and location of dSTATCOMs are determined for minimising the voltage unbalance and improving the voltage profile when the load level is time varying. Furthermore, the impact of a dSTATCOM placed in a LV network, upon its neighbouring LV feeders, is investigated.

6.2 **dSTATCOM**

Different methods are proposed for unbalance reduction in LV feeders such as feeder conductor cross-section increase or capacitor installation [34, 85]. In [41], the application of custom power devices such as Distribution Static Compensator (dSTATCOM) has been proposed. dSTATCOMs can compensate for power quality problems such as unbalanced loads, voltage sags, voltage fluctuations and voltage unbalance [105]. The dSTATCOM is a power electronic-based compensator capable of providing rapid and uninterrupted capacitive and inductive reactive power supply. It is functionally similar to a Static VAR Compensator (SVC) in this regard. In this balancing application, the dSTATCOM phases have additional degrees of independence in comparison to the SVC. Real and reactive power can be provided on each phase, subject to some constraints that will be investigated shortly. It is shown that such devices can balance voltages at their connection terminals [106, 107]. If the terminal voltage is forced into balance by injecting suitable reactive and real currents, the current drawn from the upstream network will be balanced, provided

that the supply voltage is balanced. The current to be injected by the dSTATCOM will add to the downstream current so that the total upstream current is balanced. This will prevent the flow of any unbalanced current from the upstream network in the ideal case of 100% compensation.

6.3 **Optimal Sizing and Location of dSTATCOM**

6.3.1 Problem Formulation

The problem has two mutually conflicting objectives. The first and foremost objective is to compensate the buses in such a way that none of the buses are above standard voltage unbalance factor. The second objective is to minimise the cost of compensation. The objective function for minimisation of voltage unbalance factor of the LV network is the total cost dSTATCOMs including fixed and variable costs and a weighted cost related to voltage unbalance. The optimisation is subject to additional voltage criteria as constraints.

In our study, the objective function is defined as a sum of three terms with individual criteria. The first part of the objective function concerns the voltage unbalance level in all of the buses. It is necessary that voltage unbalance factor in all buses to be less than 2%. The second part of the objective function concerns the voltage levels. It is favourable that the voltage magnitude of all of buses (per phase) be as close as possible to 1.0 pu The desired voltage profile required [5]:

$$0.94 \leq V_i \leq 1.06 \qquad i: 1 \rightarrow nb \text{ (number of buses)}$$

Each solution that does not satisfy the above two restrictions is considered not feasible, thus its fitness function value is set to infinity. Finally, in order to limit the size of the dSTATCOM units a size restriction is applied to the particles (20 kVA per phase). If the summation of the real power component of the dSTATCOM is not zero a battery installation cost penalty is applied.

$$Min\ f(\bar{X}) = S_{dSTATCOM} \times price_{dSTATCOM} + S_{battery} \times price_{battery} + Penalties$$

$$Penalties = |VUF - 2\%| \times Penalty_{VUF} + (|V_i - 1.0| > 0.06) \times Penalty_V + Penalty_{battery}$$

6.3.2 Candidate Location of dSTATCOMs

In order to reduce the search space, a voltage unbalance analysis is conducted to obtain the most important candidate buses. For this analysis, the load flow equations used in a direct approach solution are utilised (section 2.8). This approach uses the BIBC, BCBV, and DLF matrices as (with dimension of 69x69):

$$DLF = BCBV \times BIBC$$
$$\Delta V = DLF \times I$$

where: DLF is the distribution load flow; BCBV is the branch-current to bus-voltage; BIBC is the bus-injection to branch-current; ΔV is the error of voltage matrix; I is the bus current vector. The outcome of the load flow is used to calculate the voltage unbalance factor at each instance of the time for all the buses of the network. The direct load flow is used to reduce computational load during the PSO search.

Candidate locations of dSTATCOMs are determined after analysis of the existing network. The candidate location should be downstream from the buses whose voltage unbalance is above the standard limit (VUF > 2%)

6.3.3 Applying Modified PSO to Problem

The first step in an optimisation procedure is identifying the variables. In this problem the variables are the size and the placement of dSTATCOMs. Figure 6-1 shows the structure of particles in the employed MPSO. As observed, the particle is composed of N cells with the value of Di. Each candidate bus for installing dSTATCOM is assigned 7 cells. The first cell locates the dSTATCOM, and the

three-phase active and reactive power rating of the dSTATCOM at the relative candidate bus is the value of the remaining 6 cells.

Figure 6-1. Structure of a particle

For example, D_i is the rating of the dSTATCOM installed at bus *i*. If all buses are candidates for installing dSTATCOM, *N* will be the number of buses. Therefore, the number of variables is at most equal to the number of buses. If the value of a cell, the dSTATCOM size, is more than a specific threshold, it indicates that a dSTATCOM is installed at that bus. Otherwise, no dSTATCOM is placed at the relavant bus. This specific threshold is the minimum size of the available dSTATCOM.

Step 1: (Input System Data and Initialisation)

In this step, the distribution network configuration, network and load data and the number of available dSTATCOMs are input to the analysis. The input data include the line impedances and bus data (load power i.e. real power and reactive power). The maximum allowed voltage unbalances, and rated currents, are also specified as constraints. The PSO parameters, number of population members and iterations, as well as the PSO weight factors, are also selected. The random-based initial population of particles X_j (sizes of the dSTATCOMs) and the particles velocity V_j in the search space are also initialised.

Step 2: (Calculate the Objective Function)

Given the dSTATCOM size determined in the previous step, the admittance matrix is reconstructed. Using the new admittance matrix, a load flow program is run

and the bus voltages as well as the voltage unbalance factor are calculated. After that, the objective function is evaluated. The constraints are also tested in this step and any violations are included in the objective function with a penalty factor. This means that if a constraint is not satisfied, then a large penalty factor is added to the objective function to exclude the relevant solution from the search space.

Step 3: (Calculate Pbest)

The component of the objective function value associated with the position of each of the particles is compared with the corresponding value in the previous iteration and the position with lower objective function is recorded as Pbest for the current iteration.

$$Pbest_j^{k+1} = \begin{cases} Pbest_j^k & if\ OF_j^{k+1} > OF_j^k \\ x_j^{k+1} & if\ OF_j^{k+1} < OF_j^k \end{cases} \quad (6.1)$$

where *k* is the number of iterations and *OFj* is the objective function component evaluated for particle *j*.

$Pbest_j^{k+1}$ is the personal best position of particle in dimension found from initialization through time.

Step 4: (Calculate Gbest)

In this step, the lowest objective function among the Pbest values associated with all particles in the current iteration is compared with the corresponding values in the previous iteration and the lowest value at any iteration labelled as Gbest.

$$Gbest_j^{k+1} = \begin{cases} Gbest^k & if\ OF^{k+1} > OF_j^k \\ Pbest_j^{k+1} & if\ OF^{k+1} < OF_j^k \end{cases} \quad (6.2)$$

$Gbest_j^{k+1}$ is the global best position of particle in dimension found over the elapsed simulation time.

Step 5: (Update Position)

The position of particles for the next iteration can be calculated using the current Pbest and Gbest. Equations (6.3) and (6.5) describe the velocity and position update equations with the inertia weight included. Equation (6.3) calculates a new velocity for each particle (potential solution) based on its previous velocity, the particle's location at which the best fitness so far has been achieved, and the population global (or local neighbourhood, in the neighbourhood version of the algorithm) location at which the best fitness so far has been achieved. Equation (6.5) updates each particle's position in the solution hyperspace. The two random numbers are independently generated. The use of the inertia weight ω, which typically decreases linearly from about 0.9 to 0.4 during the course of the simulation, has provided improved performance in a number of applications.

$$V_i^{k+1} = \omega V_i^k + c_1 rand * \left(Pbest_i^k - X_i^k\right) + c_2 rand * \left(Gbest_i^k - X_i^k\right) \quad (6.3)$$

Work done by [111] indicates that use of a constriction factor may be necessary to ensure convergence of the particle swarm algorithm. Comparing between two PSOs using an inertia weight and using a constriction factor, the best approach is to use the constriction factor [112]. Therefore, in this work, PSO using a constriction factor is applied. Three models of constriction factor is presented in [113], but a simple version (Type 1″) is selected here, because this type requires the least number of adjusting coefficients with no increase in time or memory resources [113].

$$V_i^{k+1} = X\left(V_i^k + c_1 rand_1 * \left(Pbest_i^k - X_i^k\right) + c_2 rand_2 * \left(Gbest^k - X_i^k\right)\right) \quad (6.4)$$

$$X_i^{k+1} = X_i^k + V_i^{k+1} \quad (6.5)$$

where V_i^k is the velocity of particle i at iteration k, c_1 and c_2 are constants known as acceleration coefficients, and rand1 and rand2 are two separately generated, uniformly distributed random numbers in the range (0, 1). X_i^k is the position of particle i at iteration k, $Pbest_i^k$ is the best position of particle i at iteration k, and $Gbest^k$ is the best position among all particles at iteration k.

In order to control the system's convergence, explosion, and stability of the PSO, the constriction coefficient (X) is calculated from (6.6) as:

$$X = \begin{cases} \sqrt{\frac{2\kappa}{\varphi - 2 + \sqrt{\varphi^2 - 4\varphi}}} & \varphi > 4 \\ \sqrt{\kappa} & else \end{cases} \qquad (6.6)$$

$$\varphi = c_1 + c_2$$

In (6.6), $\kappa \in (1, 0)$ is a coefficient that allows control of exploration versus exploration. This results in slow convergence but thoroughly searches the space before collapsing into a solution point. However, for smaller values, particles care more for exploitation and less for exploration [113].

Step 6: (Apply Crossover and Mutation Operators)

Conventional PSO algorithm can find quickly a good and locally optimum solution; however it often remains around such a solution for a great number of iterations without any considerable improvement. Therefore, in order to control such behaviour and break through the stagnation of particles, a mutation function was applied in the proposed MPSO algorithm [114]. The mutation function is conceptually equivalent to the mutation in genetic algorithms. The mutation function is executed when Gbest is not improving with an increasing number of iterations. The mutation function selects a particle randomly and then adds a random perturbation to a randomly selected modulus of the velocity vector of that particle by

a mutation probability. In this work, if the Gbest after 25 iterations does not improve, a mutation function with the mutation probability of 0.7-0.85 will be applied.

Step 7: (Check convergence criterion)

If *Iter* = *Itermax* or if the output does not change for a specific number of iterations, the program is terminated and the results are printed, otherwise the program goes to step 2.

6.4 **Implementation of Proposed Work**

To reduce the number of load flows in each scenario, only the top 20 instances with highest voltage unbalance factor would be analysed in the MPSO for placement and sizing of dSTATCOM. These instances are chosen to be reflective not only of the highest voltage unbalance factor but also to be representative of maximum voltage unbalance caused by each phase (A, B and C) and different times of the day (peak PV time, peak load time, other times). The reason for this selection is to make sure the outcome of the optimisation would be correctly placed and adequate in size for compensating voltage unbalance caused by different sources (load, PV) because of different phases.

The PSO-based approach for solving the optimal placement and sizing of dSTATCOM to minimise the voltage unbalance and improving the voltage profile has been applied to Australian LV network under three different scenarios.

6.4.1 Scenario 1: dSTATCOM with Battery Storage

In Australia, the typical LV feeders can be more resistive than inductive with an R/X ≈ 1–2 with values up to 5 in rural areas. Under such conditions, it is possible that the dSTATCOM cannot effectively control its PCC voltage to the desired value by only exchanging reactive power with the feeder. Normally a STATCOM or

dSTATCOM is thought of as a purely reactive device. However, it is possible to allow real power flows on the phases in two operating modes. In the first mode, real power is effectively transferred from one or two phases to the other phases. If the total real power across the phases is zero then the dSTATCOM DC bus voltage can be controlled using only a suitably rated capacitor, which will carry some 100Hz or 120Hz current (depending on system frequency).

In the second mode, the sum of the real phase powers is not zero and some energy storage is required. This problem can be addressed if the dSTATCOM utilises a DC source (e.g. a battery) instead of a DC capacitor in such scenarios, to facilitate active power exchange with the feeder. Under the first scenario, it is assumed that the dSTATCOM will be equipped with a small battery and it is capable of absorbing or injecting real power as well as reactive power. As the optimisation is obtained at a specific loading condition, it is assumed that the battery can be brought to an adequate state of charge at an earlier point in the day. The actual management and optimization of charge and discharge cycle of the battery is out of scope of this thesis. In this work, it is assumed that the battery is in the desired state of charge at the time of need, i.e. the battery can absorb or inject the required active power at the instance of the time that is commanded by the dSTATCOM controller.

In this example after the initial load flow analysis, the MPSO algorithm identified 20 buses as candidate locations for the placement of dSTATCOM. The rating of the dSTATCOM is limited to 10 kVA per phase (with the ability to inject or absorb real and reactive power). The result of MPSO for the worst voltage unbalance factor in the feeder (3.27%) is a three-phase 6 kVA dSTATCOM. It is connected to Bus 16. As shown in Figure 6-2, after the dSTATCOM is connected the voltage

unbalance factor in all the buses is reduced to less than 2%, and all the voltages in the system are within the maximum voltage deviation limits of ± 5%.

Note also that the voltage value of the bus to which the dSTATCOM is connected is marginally sufficient to keep all other voltages between the limits and keep the dSTATCOM size as small as possible. In other words, the size and location of the STATCOM are optimal.

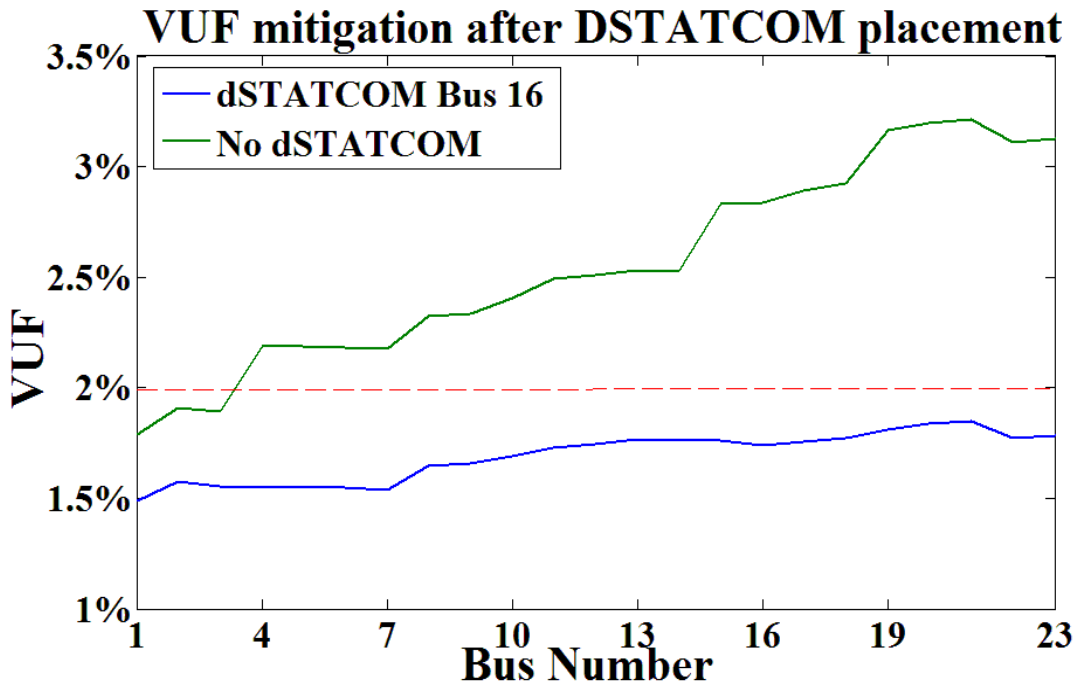

Figure 6-2. VUF mitigation after dSTATCOM placement

The MPSO analysis was then further used to investigate the adequacy of the selected dSTATCOM for voltage unbalance mitigation at the other instances with unacceptable voltage unbalance factor. Table 6-1 shows the results for the voltage unbalance mitigation after connection of dSTATCOM at Bus 16 for all the significant instances with high voltage unbalance factor caused at different times of the day (peak time, PV peak time, other times) as well as voltage unbalance contribution made by different phases.

Table 6-1. Results of dSTATCOM-battery

Maximum VUF	Time of Day	Contributing Phase	dSTATCOM Location	dSTATCOM Size (kVA) Per phase	VUF after dSTATCOM
3.30%	Peak	C	16	6	1.98%
3.11%	Peak	C	16	6	2.00%
2.99%	PV	C	16	6	1.98%
2.95%	PV	A	16	5	1.99%
2.90%	Peak	B	16	5	2.00%
2.84%	Peak	A	16	5	2.00%
2.79%	PV	A	16	5	1.96%
2.62%	Other	A	16	4	2.00%
2.57%	Other	B	16	4	2.00%
2.56%	Other	C	16	4	2.00%

6.4.2 Scenario 2: dSTATCOM without Battery Storage

Under the second scenario, it is assumed that the dSTATCOM can circulate the power between the phases and does not require a battery system. Under this scenario, the sum of active power injected by dSTATCOM in three phases is set to be zero to avoid the need for absorption or injection of extra real power. This constraint is added to the objective function of the MPSO as a penalty with significantly high cost so the MPSO will not choose a particle where the sum of its three phases is not equal to zero. As is summarised in Table 6-2, under this case the size of the dSTATCOM is increased but the extra kVA rating and associated cost of it would be less than the cost of a dSTATCOM that requires a battery system and the avoided cost of battery maintenance.

Table 6-2. Results of dSTATCOM-no battery

Maximum VUF	Time of Day	Contributing Phase	dSTATCOM Location	dSTATCOM Size (kVA) Per phase	VUF after dSTATCOM
3.30%	Peak	C	16	9	1.98%
3.11%	Peak	C	16	9	2.00%
2.99%	PV	C	16	8	1.96%
2.95%	PV	A	16	8	1.98%
2.90%	Peak	B	16	7	2.00%
2.84%	Peak	A	16	7	2.00%
2.79%	PV	A	16	7	1.97%
2.62%	Other	A	16	6	2.00%
2.57%	Other	B	16	6	1.99%
2.56%	Other	C	16	6	2.00%

6.4.3 Scenario 3: Phase Swap and dSTATCOM

In the third scenario, the phase swap method introduced in the previous chapter would be used in conjunction with the dSTATCOM optimisation. The phase swap based on billing and PV generation can reduce the maximum voltage unbalance from 3.3% down to 2.5% (Table 5-5) by swapping three customers from phase C to phase A. This level of voltage unbalance factor is still above the allowed limits. The updated loading profile on each bus of the network would be used as an input to the MPSO for determining the optimum dSTATCOM size and location. The result of this case is summarised in Table 6-3. It is evident that by applying the phase swap method a smaller dSTATCOM could be used (reduction of 50% rating). This is a significant reduction in cost even when considering the extra cost of labour for performing the phase swap in the beginning.

Table 6-3. Results of phase swap-dSTATCOM-no battery

Maximum VUF	Time of Day	Contributing Phase	dSTATCOM Size (kVA) Per phase	VUF after dSTATCOM
2.50%	Peak	B	5	1.98%
2.61%	Peak	B	5	2.00%
2.59%	PV	C	5	1.99%
2.55%	PV	A	5	1.98%
2.44%	Peak	B	5	2.00%
2.40%	Peak	B	4	1.96%
2.29%	PV	A	4	1.97%
2.22%	Other	B	4	2.00%
2.17%	Other	C	3	1.99%
2.06%	Other	A	3	1.96%

The other point that could be derived from Table 6-3 is the change in the contributing phase to voltage unbalance. After performing the phase swap phase C is no longer the dominant phase, but phase B is now the main contributing phase to voltage unbalance in the system.

6.5 **Impact on Neighbouring LV Feeders**

In this section the impact that mitigation of voltage unbalance in one LV feeder could have on other LV feeders connected to the same MV line is investigated. The Australian LV network introduced previously is replicated 5 times to create a 1 MVA distribution network (Figure 6-3). The LV feeders are identical in terms of topology and the number of single-phase and three-phase customers but the loading on each bus is different as they are randomly allocated.

The 5 LV systems are connected by 5 MV lines in a radial MV network. These MV lines are each 1km long and create a 5km feeder. Each of the 5 MV/LV

transformers has fixed tap settings. The tap ratio of these $\Delta - Y$ transformers has been chosen in such a way that the voltage profile in all of the LV feeders is within acceptable limits under all load scenarios and the last LV feeder voltage is identical to voltage measurements of the Australian LV network (Pavetta) under study.

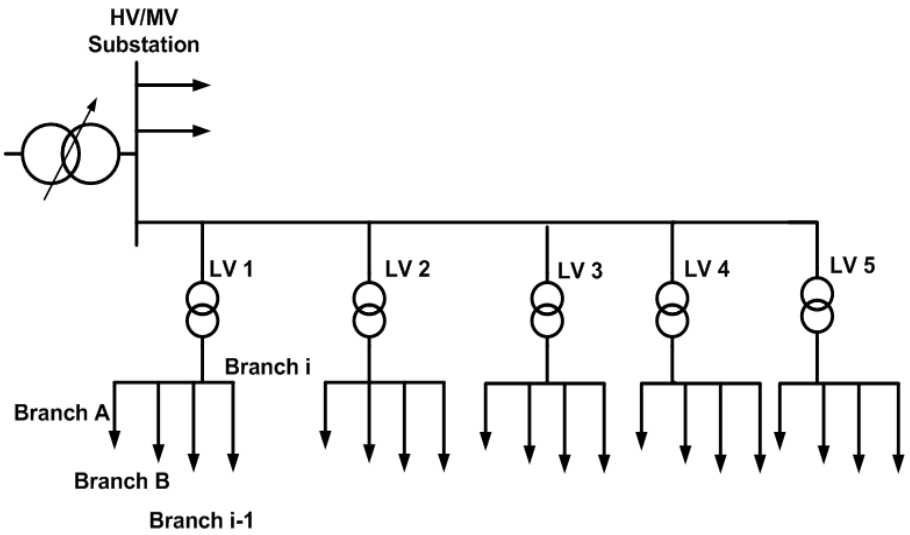

Figure 6-3. MV/LV distribution network

6.6 **Simulation Results**

The following section presents the simulation results obtained upon implementation of the above MPSO algorithm. The simulations are carried out using MATLAB. The first set of simulations is carried out on the Australian LV feeder. In the next set of simulations, the potential of multiple distribution static synchronous compensators (dSTATCOMs) to improve the voltage unbalance factor of radial distribution networks is analysed.

6.6.1 Identical Loading

Figure 6-4 shows the result of the load flow on all of the five identical LV feeders. In running the load flow, the first scenario is selected as a base case. It is assumed that all five feeders are identical in terms of topology and loading on all the buses. To improve the voltage unbalance of all the feeders it is possible to install a large dSTATCOM in one of the LV feeders to improve the VUF in all of the feeders.

This task is performed using the MPSO developed in this thesis and the result of the placement and sizing of the dSTATCOM is shown in Figure 6-5 and summarised in Table 6-4 and Table 6-5.

From a circuit theory perspective a dSTATCOM will reduce the negative sequence voltage at the point of connection. While the complete elimination of the unbalance at the PCC is the target, it is useful to consider an idealised case where the connected dSTATCOM acts as a negative sequence short circuit at the point of connection. The overall network response is that the negative sequence voltages are depressed at every other node. If multiple dSTATCOMs are applied, effectively multiple negative sequences short circuits are dispersed across the network and these will reinforce the reductions in voltage at every other uncontrolled node.

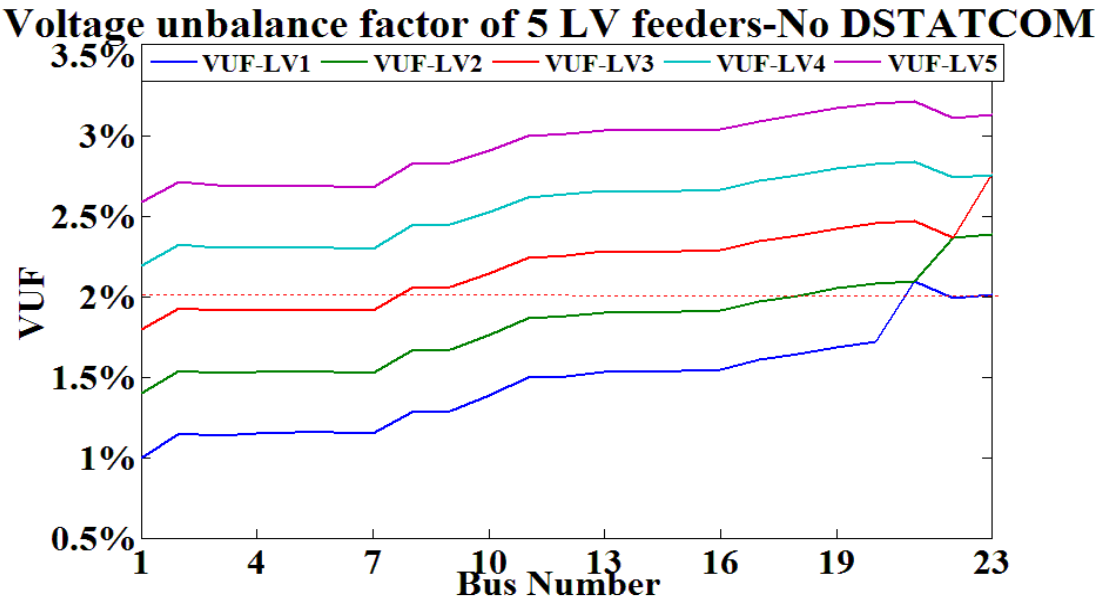

Figure 6-4. Maximum VUF of all 5 LV feeders

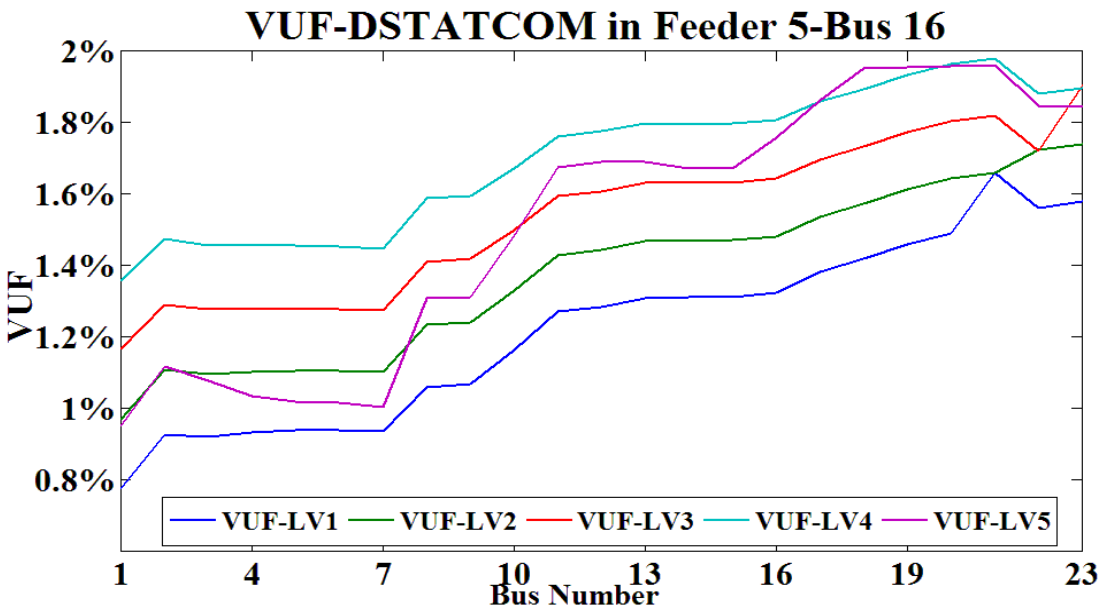

Figure 6-5. Improvement in VUF of all feeders

Table 6-4 Rating and placement of dSTATCOMs in LV 5

Feeder Number	Bus Number	Phase A Power (kW)	Phase B Power (kW)	Phase C Power (kW)	Phase A Reactive-Power (kVar)	Phase B Reactive-Power (kVar)	Phase C Reactive Power (kVar)
LV5	16	-10	20	-10	-20	20	20

Table 6-5. VUF improvement in all feeders

Feeder Number	Max VUF Before	Number of Buses in violation Before	Max VUF After	Number of Buses in violation After
LV-1	2.09%	3	1.66%	0
LV-2	2.39%	6	1.75%	0
LV-3	2.77%	16	1.91%	0
LV-4	3.14%	22	1.94%	0
LV-5	3.27%	23	1.96%	0

It is possible to provide voltage unbalance mitigation more efficiently by installing smaller dSTATCOMs in multiple LV feeders. From a circuit theory

perspective, multiple dSTATCOMs will be mutually supportive and the results support this conclusion. Figure 6-6 shows the result of MPSO after installing dSTATCOMs on two of the LV feeders. It is clear that the installation of dSTATCOMs was successful in reducing voltage unbalance factor in all of the LV feeders. The MPSO output is summarised in Table 6-6. The results are in line with the previous section in terms of the rating of the dSTATCOMs as well as the possibility of the real power circulation across phases within the dSTATCOM.

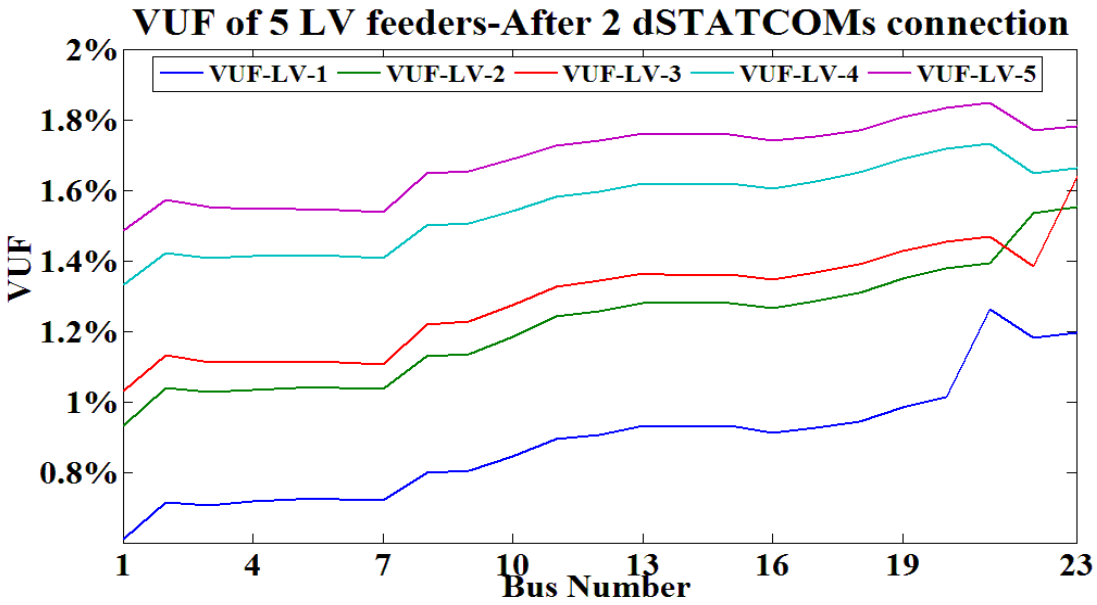

Figure 6-6. VUF mitigation after dSTATCOM in LV3 & LV5

Table 6-6 Rating and placement of dSTATCOMs in LV 3 & LV5

	DSTATCOM Location (Bus)	Phase A Power (kW)	Phase B Power (kW)	Phase C Power (kW)	Phase A Reactive-Power (kVar)	Phase B Reactive-Power (kVar)	Phase C Reactive Power (kVar)
LV-3	16	0	6	-6	-4	3	4
LV-5	17	-6	6	0	-4	5	4

6.6.2 Random Loading

The possibility of all the LV feeders having identical loading on all their buses is minimal so for a more realistic simulation the phase connection of the 77

residential customers for each LV feeder has been randomly allocated. The random allocation of the houses is done in the same manner as the initial phase connection (phase C would have more customers and loading).

Figure 6-7 shows the result of the load flow on all of the five LV feeders when the loading on each of LV feeder are generated randomly. Figure 6-8 shows the result of MPSO after installing dSTATCOMs on two of the LV feeders (LV4 and LV5). It is clear that the installation of dSTATCOMs was successful in reducing voltage unbalance factor in all of the LV feeders. The MPSO output is summarised in Table 6-7.Table 6-8 shows the ability of the power circulation ability of the dSTATCOM to bring the VUF, to under 2%.

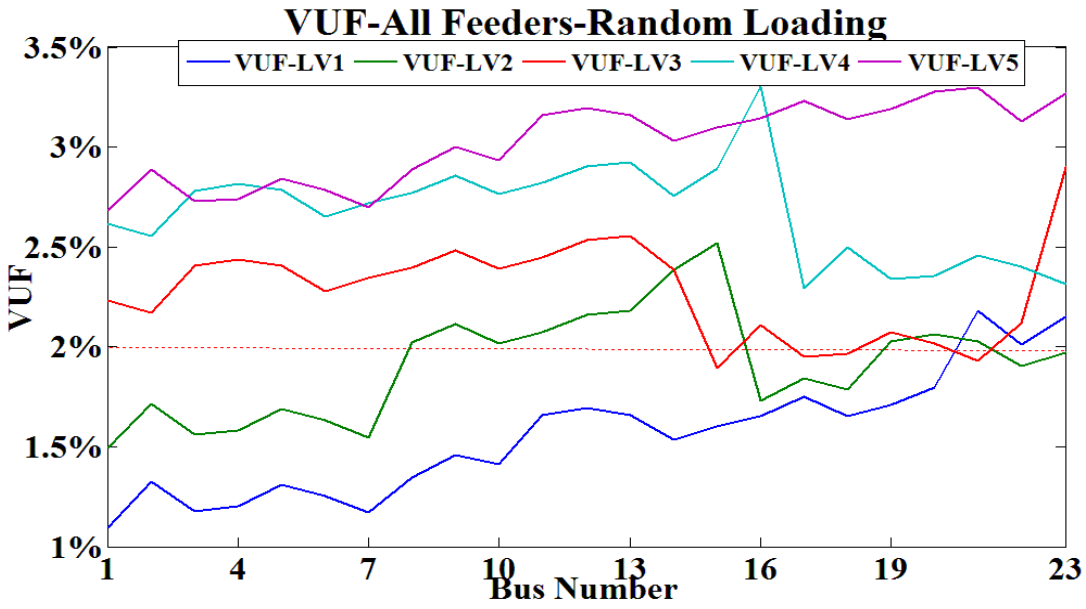

Figure 6-7. Max VUF of all 5 LV feeders with random loading

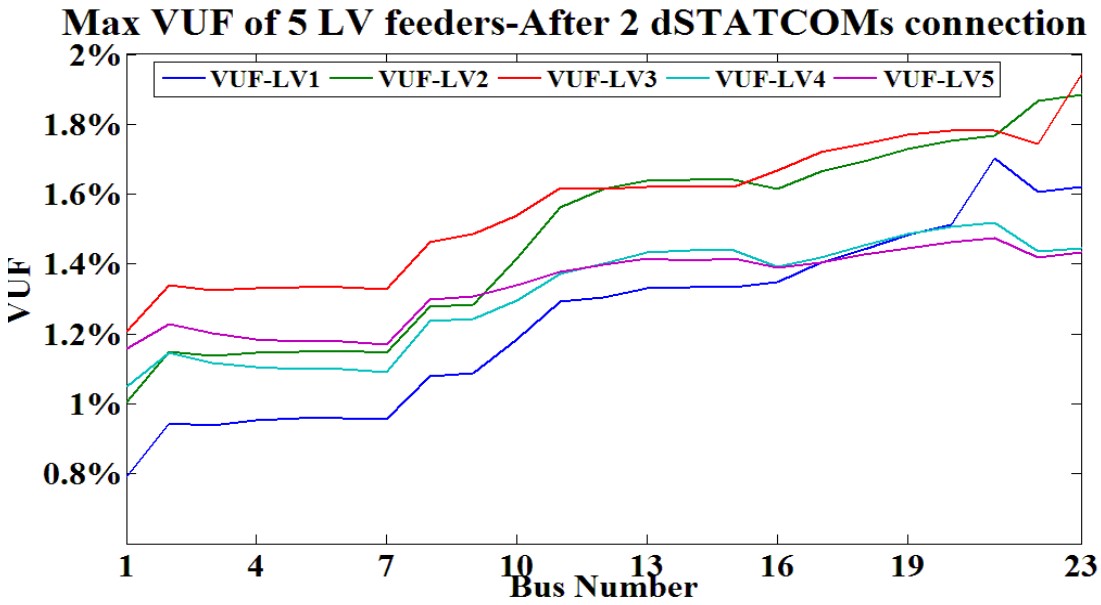

Figure 6-8. VUF mitigation after dSTATCOM in LV4 & LV5

Table 6-7. VUF improvement in all feeders with random loading

Feeder Number	Max VUF Before Compensation	Number of Buses in violation Before	Max VUF After Compensation	DSTATCOM Size Per phase
LV-1	2.18%	4	1.72%	0
LV-2	2.56%	12	1.92%	0
LV-3	2.93%	19	1.96%	0
LV-4	3.30%	23	1.67%	8
LV-5	3.30%	23	1.48%	8

Table 6-8. Rating and placement of dSTATCOMs in LV4 & LV5

	DSTATCOM Location (Bus)	Phase A Power (kW)	Phase B Power (kW)	Phase C Power (kW)	Phase A Reactive-Power (kVar)	Phase B Reactive-Power (kVar)	Phase C Reactive Power (kVar)
LV-4	16	0	6	-6	-8	4	3
LV-5	16	-7	7	0	-8	6	4

6.7 **Summary**

In this chapter, the applications of dSTATCOMs were investigated for voltage unbalance reduction. It was shown that a dSTATCOM is more effective for voltage profile improvement and VU reduction in comparison with manual phase swaps. However, phase swaps cost much less than a dSTATCOM. The analyses prove that for any random load and PV rating and location scenario, the discussed methods are successful in reducing voltage unbalance to the standard limits. It was shown that one dSTATCOM provides an unbalance reduction benefit at every network node albeit with reducing impact as the nodes are more distant from the PCC. Multiple applications of dSTATCOMs are also possible for longer radial LV lines. It has been shown that the interactions between multiple dSTATCOMs are positive and these will act to mutually reduce the unbalance voltages at every network node. Through extensive analysis and simulation carried out using MATLAB, the efficacy of the discussed methods was verified.

Chapter 7 Conclusions and Recommendations

In this chapter, the general conclusions of the thesis and recommendations for future research are presented.

7.1 **Conclusions**

Development of a feasible method for mitigation of voltage unbalance factor in suburban low voltage distribution networks through effective approaches is the main contribution of this thesis. Although these methods are only applied to two specific LV networks in Australia and UK, the methods can be effective on other similar three-phase four-wire LV networks that exhibit voltage unbalance as a result of uneven load allocation and increase presence of roof top PV. In order to reach the goals of this research the steps as below are followed:

- Phase identification is the first step towards solving the larger problem of phase balancing and we have investigated this problem taking into account various costs associated with phase rebalancing. The voltage profile of each consumer is well correlated with the voltage profile on the same phase of the transformer and we have established a new method to determine the phase connection of consumer loads on a LV distribution network from smart meter voltage measurements of the consumer and transformer log data. The field-testing was successful, with 51 single-phase meters and 24 three-phase meters correctly allocated on a residential LV feeder.
- A thermal model was developed to assess the transformer temperatures over a 12-month cycle, allowing a cumulative measure of loss of life to be determined for various scenarios. PV generation will extend the life of oil-immersed

distribution transformers even when the peak demand occurs well after sunset. The presented results correspond to a three phase residential transformer, but the result of this study could also be applied to single-phase distribution transformers (in the US, or SWER in Australia).

- In this thesis, a cost effective method is proposed to reduce energy losses and improve quality of service in strongly unbalanced low-voltage networks. The method is based on phase swapping, that is single-phase load switching between phases, in order to improve voltage unbalance factor of the network. The objective of the methods developed is to minimise the number of swapped phases and power losses. These objectives are conflicting, which makes the simultaneous minimisation a difficult task. Therefore, methods are developed to determine an optimal set; a particle swarm Optimisation algorithm is used.
- This study has shown systematically that the application of the Particle Swarm Optimisation method can solve the problem of optimal placement and sizing of multiple dSTATCOM units in a medium-sized power network. The algorithm is easy to implement and is able to find multiple optimal solutions to this constrained multi-objective problem, giving more flexibility to take the final decision about the locations and sizes of the dSTATCOM units. The settings of the PSO parameters are shown to be optimal for this type of application; the algorithm is able to find the optimal solutions with a relatively small number of iterations and particles, therefore, with a reasonable computational effort. The load profile has been modified in the buses in order to measure the impact on the size and location of each dSTATCOM unit. The results indicate that the location of the dSTATCOM does not change but its size decreases. Additionally, the impact of the multiple dSTATCOM units in the power system, in terms of the

improvement of the voltage profile, becomes more significant as the loading increases. The results are promising for the medium-sized power network used as an example. For large power systems, the PSO algorithm could have a significant advantage compared to exhaustive search and other methods by giving better solutions with less computational effort.

7.2 **Recommendations for Future Research**

The scope for future research is as follows.

7.2.1 Studying More LV Networks

In this research, only a limited number of low voltage distribution cases were investigated for voltage profile and unbalance studies. Although the studies and improvement methods are studied in detail, the behaviour of more LV systems in the presence of unbalance load and PV can be a topic for future research.

7.2.2 Statistical Analysis of Test Cases

In this thesis, a heuristic approach was taken to reduce the number of unbalance test cases in each scenario in chapter 6 for placement and sizing of dSTATCOM. This heuristic approach was based on choosing the combination of load profiles that generates the worst case instances of maximum voltage unbalance caused by each phase (A, B and C) and different times of the day (peak PV time, peak load time, other times). A more thorough and sophisticated statistical clustering method might be able to select a better and more representative load profiles. Statistical clustering analysis could provide a more rigorous test cases. It would be able to identify non obvious clusters and provide insight into particular load types or behaviours. This ensures optimisation would correctly place dSTATCOMs and determines adequate ratings for compensating voltage unbalance caused by different sources (load, PV) at all times of the day.

7.2.3 Single-phase dSTATCOM

In this research, three-phase optimally placed and sized dSTATCOMs were investigated for voltage unbalance mitigation. Future study could include the potential of single phase dSTATCOMs for voltage unbalance mitigation purposes.

7.2.4 Single/Three Phase Inverters

There has been strong research on the usage of excess capacity of installed single/three phase PV inverters as VAR compensators for voltage profile regulation in the LV network. Possible future research could utilise the extra capacity of PV inverters for coordinated voltage balance improvement in the LV network.

References

[1] L. F. Ochoa, A. Padilha-Feltrin, and G. P. Harrison, "Evaluating distributed generation impacts with a multiobjective index," *Power Delivery, IEEE Transactions on*, vol. 21, pp. 1452-1458, 2006.

[2] P. Paranavithana, S. Perera, and R. Koch, "A generalised methodology for evaluating voltage unbalance influence coefficients," in *Electricity Distribution - Part 1, 2009. CIRED 2009. 20th International Conference and Exhibition on*, 2009, pp. 1-4,2009.

[3] D. Menniti, C. Picardi, A. Pinnarelli, and D. Sgro, "Power management by grid-connected inverters using a voltage and current control strategy for Microgrid applications," in *Power Electronics, Electrical Drives, Automation and Motion, 2008. SPEEDAM 2008. International Symposium on*, 2008, pp. 1414-1419,2008.

[4] T. A. Short, *Electric power distribution handbook*: CRC press, 2014.

[5] A. Von Jouanne and B. Banerjee, "Assessment of voltage unbalance," *Power Delivery, IEEE Transactions on*, vol. 16, pp. 782-790, 2001.

[6] P. Trichakis, P. Taylor, L. Cipcigan, P. Lyons, R. Hair, and T. Ma, "An investigation of voltage unbalance in low voltage distribution networks with high levels of SSEG," in *Universities Power Engineering Conference, 2006. UPEC'06. Proceedings of the 41st International*, 2006, pp. 182-186,2006.

[7] P. Paranavithana, "Contributions towards the development of the technical report IEC/TR 61000-3-13 on voltage unbalance emission allocation," 2009.

[8] P. Pillay and M. Manyage, "Definitions of voltage unbalance," *IEEE Power Engineering Review*, vol. 21, pp. 50-51, 2001.

[9] A. K. Singh, G. Singh, and R. Mitra, "Some observations on definitions of voltage unbalance," in *Power Symposium, 2007. NAPS'07. 39th North American*, 2007, pp. 473-479,2007.

[10] M. T. Bina and E. Pasha Javid, "A critical overview on zero sequence component compensation in distorted and unbalanced three-phase four-wire systems," in *Power Engineering Conference, 2007. IPEC 2007. International*, 2007, pp. 1167-1172,2007.

[11] "IEC/TR 61000-3-13: Electromagnetic compatibility (EMC) - Limits - Assessment of Emission Limits for the Connection of Unbalanced Installations to MV, HV and EHV Power Systems, Ed. 1. Technical report, International Electrotechnical Commission," 2008.

[12] Y.-J. Wang, "Analysis of effects of three-phase voltage unbalance on induction motors with emphasis on the angle of the complex voltage unbalance factor," *Energy conversion, IEEE transactions on*, vol. 16, pp. 270-275, 2001.

[13] D. C. Garcia, F. Nascimento, and J. Cormane, "Study of voltage unbalance conditions based on the behavior of the complex voltage unbalance factor (CVUF)," in *Transmission and Distribution Conference and Exposition: Latin America (T&D-LA), 2010 IEEE/PES*, 2010, pp. 184-189,2010.

[14] "Motors and generators . Technical report, National Electricity Manufacturer's Association," 1993.

[15] A. Siddique, G. Yadava, and B. Singh, "Effects of voltage unbalance on induction motors," in *Electrical Insulation, 2004. Conference Record of the 2004 IEEE International Symposium on*, 2004, pp. 26-29,2004.

[16] "IEEE Recommended Practice for Monitoring Electric Power Quality," IEEE Std 1159-1995,," 1995.
[17] "Planning Limits for Voltage Unbalance in the United Kingdom," The Electricity Council, Engineering recommendation P29," 1990.
[18] "Electric Power Systems and Equipment-Voltage ratings (60 Hz)," ANS Standard C84.1-1995," 1995.
[19] "CENELEC EN 50160, Voltage characteristics of electricity supplied by public distribution systems," 1994.
[20] "National Electricity Code Australia, Version 1.0 - Amendment 9.0. Technical

report, National Electricity Code Administrator Limited, Australia," 2004.
[21] E. T. Gross, J. H. Drinnan, and E. Jochum, "Electromagnetic Unbalance of Untransposed Transmission Lines III. Double Circuit Lines," *Power apparatus and systems, part iii. transactions of the american institute of electrical engineers,* vol. 78, pp. 1362-1370, 1959.
[22] Z. Emin and D. S. Crisford, "Negative phase-sequence voltages on E&W transmission system," *Power Delivery, IEEE Transactions on,* vol. 21, pp. 1607-1612, 2006.
[23] D. Smith, H. Braunstein, and J. Borst, "Voltage unbalance in 3-and 4-wire delta secondary systems," *Power Delivery, IEEE Transactions on,* vol. 3, pp. 733-741, 1988.
[24] C.-Y. Lee, "Effects of unbalanced voltage on the operation performance of a three-phase induction motor," *Energy Conversion, IEEE Transactions on,* vol. 14, pp. 202-208, 1999.
[25] B. Gafford, W. Duesterhoeft, and C. Mosher, "Heating of induction motors on unbalanced voltages," *Power apparatus and systems, part iii. transactions of the american institute of electrical engineers,* vol. 78, pp. 282-286, 1959.
[26] J. Williams, "Operation of 3-Phase Induction Motors on Unbalanced Voltages [includes discussion]," *Power apparatus and systems, part iii. transactions of the american institute of electrical engineers,* vol. 73, 1954.
[27] J. Kuang and S. A. Boggs, "Pipe-type cable losses for balanced and unbalanced currents," *Power Delivery, IEEE Transactions on,* vol. 17, pp. 313-317, 2002.
[28] T.-H. Chen, "Evaluation of line loss under load unbalance using the complex unbalance factor," *IEE Proceedings-Generation, Transmission and Distribution,* vol. 142, pp. 173-178, 1995.
[29] A. B. Baggini, *Handbook of power quality*: Wiley Online Library, 2008.
[30] M. Baran, H. Hooshyar, Z. Shen, J. Gajda, and K. Huq, "Impact of high penetration residential PV systems on distribution systems," in *Power and Energy Society General Meeting, 2011 IEEE*, 2011, pp. 1-5,2011.
[31] P. Mitra, G. T. Heydt, and V. Vittal, "The impact of distributed photovoltaic generation on residential distribution systems," in *North American Power Symposium (NAPS), 2012*, 2012, pp. 1-6,2012.
[32] R. Walling, R. Saint, R. C. Dugan, J. Burke, and L. A. Kojovic, "Summary of distributed resources impact on power delivery systems," *Power Delivery, IEEE Transactions on,* vol. 23, pp. 1636-1644, 2008.
[33] R. P. Broadwater, A. H. Khan, H. E. Shaalan, and R. E. Lee, "Time varying load analysis to reduce distribution losses through reconfiguration," *Power Delivery, IEEE Transactions on,* vol. 8, pp. 294-300, 1993.

[34] M. W. Siti, D. V. Nicolae, A. A. Jimoh, and A. Ukil, "Reconfiguration and load balancing in the LV and MV distribution networks for optimal performance," *Power Delivery, IEEE Transactions on,* vol. 22, pp. 2534-2540, 2007.

[35] T.-H. Chen and J.-T. Cherng, "Optimal phase arrangement of distribution transformers connected to a primary feeder for system unbalance improvement and loss reduction using a genetic algorithm," in *Power Industry Computer Applications, 1999. PICA'99. Proceedings of the 21st 1999 IEEE International Conference*, 1999, pp. 145-151,1999.

[36] E. T. Gross, "Unbalances of untransposed overhead lines," *Journal of the Franklin Institute,* vol. 254, pp. 487-497, 1952.

[37] R. Yan and T. K. Saha, "Voltage Variation Sensitivity Analysis for Unbalanced Distribution Networks Due to Photovoltaic Power Fluctuations," *Power Systems, IEEE Transactions on,* vol. 27, pp. 1078-1089, 2012.

[38] A. Campos, G. Joos, P. D. Ziogas, and J. F. Lindsay, "Analysis and design of a series voltage unbalance compensator based on a three-phase VSI operating with unbalanced switching functions," *Power Electronics, IEEE Transactions on,* vol. 9, pp. 269-274, 1994.

[39] J.-H. Chen, W.-J. Lee, and M.-S. Chen, "Using a static var compensator to balance a distribution system," in *Industry Applications Conference, 1996. Thirty-First IAS Annual Meeting, IAS'96., Conference Record of the 1996 IEEE*, 1996, pp. 2321-2326,1996.

[40] D. Graovac, V. Katic, and A. Rufer, "Power quality problems compensation with universal power quality conditioning system," *Power Delivery, IEEE Transactions on,* vol. 22, pp. 968-976, 2007.

[41] A. Ghosh and G. F. Ledwich, *Power quality enhancement using custom power devices*: Kluwer Academic Publishers, 2002.

[42] B. Singh and S. R. Arya, "Design and control of a DSTATCOM for power quality improvement using cross correlation function approach," *International Journal of Engineering, Science and Technology*, vol. 4, pp. 74-86, 2012.

[43] P. Wolfs and A. M. T. Oo, "Improvements to LV distribution system PV penetration limits using a dSTATCOM with reduced DC bus capacitance," in *Power and Energy Society General Meeting (PES), 2013 IEEE*, 2013, pp. 1-5,2013.

[44] J.-H. Teng, "A direct approach for distribution system load flow solutions," *Power Delivery, IEEE Transactions on,* vol. 18, pp. 882-887, 2003.

[45] E. Demirok, S. B. Kjær, D. Sera, and R. Teodorescu, "Three-phase unbalanced load flow tool for distribution networks," in *2nd International Workshop on Integration of Solar Power Systems*.

[46] W. H. Kersting, *Distribution System Modeling and Analysis, CRC Press*, 2007.

[47] G. Kron, "Tensor analysis of networks," *New York*, 1939.

[48] H. Khodr, J. Gomez, L. Barnique, J. Vivas, P. Paiva, J. Yusta, and A. Urdaneta, "A linear programming methodology for the optimization of electric power-generation schemes," *Power Systems, IEEE Transactions on,* vol. 17, pp. 864-869, 2002.

[49] M. Olofsson, G. Andersson, and L. Soder, "Linear programming based optimal power flow using second order sensitivities," *Power Systems, IEEE Transactions on,* vol. 10, pp. 1691-1697, 1995.

[50] N. Alguacil, A. L. Motto, and A. J. Conejo, "Transmission expansion planning: a mixed-integer LP approach," *Power Systems, IEEE Transactions on,* vol. 18, pp. 1070-1077, 2003.
[51] P. Paiva, H. Khodr, J. Domínguez-Navarro, J. Yusta, and A. Urdaneta, "Integral planning of primary-secondary distribution systems using mixed integer linear programming," *Power Systems, IEEE Transactions on,* vol. 20, pp. 1134-1143, 2005.
[52] A. Kumar and W. Gao, "Optimal distributed generation location using mixed integer non-linear programming in hybrid electricity markets," *IET generation, transmission & distribution,* vol. 4, pp. 281-298, 2010.
[53] R. Roy and S. Ghoshal, "A novel crazy swarm optimized economic load dispatch for various types of cost functions," *International Journal of Electrical Power & Energy Systems,* vol. 30, pp. 242-253, 2008.
[54] J. Kennedy, "Particle swarm optimization," in *Encyclopaedia of Machine Learning,* ed: Springer, 2010, pp. 760-766.
[55] Y. Del Valle, G. K. Venayagamoorthy, S. Mohagheghi, J.-C. Hernandez, and R. G. Harley, "Particle swarm optimization: basic concepts, variants and applications in power systems," *Evolutionary Computation, IEEE Transactions on,* vol. 12, pp. 171-195, 2008.
[56] A. A. Eajal and M. El-Hawary, "Optimal capacitor placement and sizing in unbalanced distribution systems with harmonics consideration using particle swarm optimization," *Power Delivery, IEEE Transactions on,* vol. 25, pp. 1734-1741, 2010.
[57] S. Haffner, L. F. A. Pereira, L. A. Pereira, and L. S. Barreto, "Multistage model for distribution expansion planning with distributed generation—Part I: Problem formulation," *Power Delivery, IEEE Transactions on,* vol. 23, pp. 915-923, 2008.
[58] D. Kothari, "Power system optimization," in *Computational Intelligence and Signal Processing (CISP), 2012 2nd National Conference on*, 2012, pp. 18-21,2012.
[59] A. Ipakchi and F. Albuyeh, "Grid of the future," *Power and Energy Magazine, IEEE,* vol. 7, pp. 52-62, 2009.
[60] B. D. Russell and C. L. Benner, "Intelligent systems for improved reliability and failure diagnosis in distribution systems," *Smart Grid, IEEE Transactions on,* vol. 1, pp. 48-56, 2010.
[61] A. Vojdani, "Smart integration," *Power and Energy Magazine, IEEE,* vol. 6, pp. 71-79, 2008.
[62] C. Chen, J. Hwang, M. Cho, and Y. Chen, "Development of simplified loss models for distribution system analysis," *Power Delivery, IEEE Transactions on,* vol. 9, pp. 1545-1551, 1994.
[63] M. Dilek, R. P. Broadwater, J. C. Thompson, and R. Seqiun, "Simultaneous phase balancing at substations and switches with time-varying load patterns," *Power Systems, IEEE Transactions on,* vol. 16, pp. 922-928, 2001.
[64] W. Fu, J. D. McCalley, and V. Vittal, "Risk assessment for transformer loading," *Power Systems, IEEE Transactions on,* vol. 16, pp. 346-353, 2001.
[65] D. Roberts, "Local Power: Tapping Distributed Energy in 21st-Century Cities," *Scientific American, June,* 2010.
[66] R. Brunelli and T. Poggio, "Face recognition: Features versus templates," *Pattern Analysis and Machine Intelligence, IEEE Transactions on,* vol. 15, pp. 1042-1052, 1993.

[67] R. O. Duda, P. E. Hart, and D. G. Stork, "Pattern Classification and Scene Analysis 2nd ed," 1995.
[68] R. C. Gonzalez and R. E. Woods, "Digital image processing," in vol., Ed.^Eds., ed.: Prentice hall Englewood Cliffs, p.^pp., 2002.
[69] M. Beck, "Correlation in instruments: cross correlation flowmeters," *Journal of Physics E: Scientific Instruments*, vol. 14, p. 7, 2000.
[70] J. Briaire and L. Vandamme, "Uncertainty in Gaussian noise generalized for cross-correlation spectra," *Journal of applied physics*, vol. 84, pp. 4370-4374, 1998.
[71] N. Sampietro, G. Accomando, L. G. Fasoli, G. Ferrari, and E. C. Gatti, "High sensitivity noise measurement with a correlation spectrum analyser," *Instrumentation and Measurement, IEEE Transactions on*, vol. 49, pp. 820-822, 2000.
[72] "American National Standards Institute (2010): ANSI C12.20- 2010 - Electricity Meters - 0.2 and 0.5 Accuracy Classes," in vol., Ed.^Eds., ed., p.^pp.
[73] "Electricity metering equipment (AC) Particular requirements, Part 21: Static meters for active energy (classes 1 and 2) As 62053.21—2005."
[74] L. A. Irwin, "A high accuracy standard for electricity meters," in *Transmission and Distribution Conference and Exposition, 2010 IEEE PES*, 2010, pp. 1-3,2010.
[75] P. Transformers—Part, "7: Loading Guide for Oil-Immersed Power Transformers," *IEC standard*, pp. 60076-7, 2005.
[76] G. C. Montanari, "Aging and life models for insulation systems based on PD detection," *Dielectrics and Electrical Insulation, IEEE Transactions on*, vol. 2, pp. 667-675, 1995.
[77] G. C. Montanari and L. Simoni, "Aging phenomenology and modeling," *Electrical Insulation, IEEE Transactions on*, vol. 28, pp. 755-776, 1993.
[78] L. Simoni, "A general phenomenological life model for insulating materials under combined stresses," *Dielectrics and Electrical Insulation, IEEE Transactions on*, vol. 6, pp. 250-258, 1999.
[79] C. Dervos, P. D. Bourkas, E. A. Kayafas, and I. A. Stathopulos, "Enhanced partial discharges due to temperature increase in the combined system of a solid-liquid dielectric," *Electrical Insulation, IEEE Transactions on*, vol. 25, pp. 469-474, 1990.
[80] J. P. Crine, "On the interpretation of some electrical aging and relaxation phenomena in solid dielectrics," *Dielectrics and Electrical Insulation, IEEE Transactions on*, vol. 12, pp. 1089-1107, 2005.
[81] T. K. Saha and P. Purkait, "Investigation of polarization and depolarization current measurements for the assessment of oil-paper insulation of aged transformers," *Dielectrics and Electrical Insulation, IEEE Transactions on*, vol. 11, pp. 144-154, 2004.
[82] T. K. Saha and P. Purkait, "Investigations of Temperature Effects on the Dielectric Response Measurements of Transformer Oil-Paper Insulation System," *Power Delivery, IEEE Transactions on*, vol. 23, pp. 252-260, 2008.
[83] G. Swift, T. S. Molinski, R. Bray, and R. Menzies, "A fundamental approach to transformer thermal modeling. II. Field verification," *Power Delivery, IEEE Transactions on*, vol. 16, pp. 176-180, 2001.

[84] "IEEE Guide for Loading Mineral-Oil-Immersed Transformers and Step-Voltage Regulators," *IEEE Std C57.91-2011 (Revision of IEEE Std C57.91-1995)*, pp. 1-123, 2012.

[85] F. Shahnia, R. Majumder, A. Ghosh, G. Ledwich, and F. Zare, "Voltage imbalance analysis in residential low voltage distribution networks with rooftop PVs," *Electric Power Systems Research*, vol. 81, pp. 1805-1814, 2011.

[86] K. M. Nor and M. Abdel-Akher, "Analysis of three phase distribution networks with distributed generation," in *Power and Energy Conference, 2008. PECon 2008. IEEE 2nd International*, 2008, pp. 1563-1568,2008.

[87] A. Woyte, V. Van Thong, R. Belmans, and J. Nijs, "Voltage fluctuations on distribution level introduced by photovoltaic systems," *Energy Conversion, IEEE Transactions on*, vol. 21, pp. 202-209, 2006.

[88] A. Guinane, G. Shafiullah, A. M. Oo, and B. E. Harvey, "Voltage fluctuations in PV penetration on SWER networks—A case study for regional Australia," in *Power and Energy Society General Meeting, 2012 IEEE*, 2012, pp. 1-6,2012.

[89] L. W. Pierce, "An investigation of the thermal performance of an oil filled transformer winding," *Power Delivery, IEEE Transactions on*, vol. 7, pp. 1347-1358, 1992.

[90] D. Susa and H. Nordman, "A simple model for calculating transformer hot-spot temperature," *IEEE transactions on power delivery*, vol. 24, pp. 1257-1265, 2009.

[91] "IEEE Standard Test Procedure for Thermal Evaluation of Insulation Systems for Liquid-Immersed Distribution and Power Transformers," *IEEE Std C57.100-2011 (Revision of IEEE Std C57.100-1999)*, pp. 1-37, 2012.

[92] "IEC Loading Guide for Oil Immersed Power Transformers, IEC Standard 60076-7, 2005," *IEC Standard 60076-7,*, 2005.

[93] Q. He, J. Si, and D. J. Tylavsky, "Prediction of top-oil temperature for transformers using neural networks," *Power Delivery, IEEE Transactions on*, vol. 15, pp. 1205-1211, 2000.

[94] D. J. Tylavsky, H. Qing, G. A. McCulla, and J. R. Hunt, "Sources of error in substation distribution transformer dynamic thermal modeling," *Power Delivery, IEEE Transactions on*, vol. 15, pp. 178-185, 2000.

[95] H. A. Gil and G. Joos, "Models for Quantifying the Economic Benefits of Distributed Generation," *Power Systems, IEEE Transactions on*, vol. 23, pp. 327-335, 2008.

[96] (2012, November 5, 2012). *Australian bureau of metrology. Recent weather patterns*. Available: http://www.bom.gov.au/wa/?ref=hdr

[97] H. Pezeshki and P. Wolfs, "Consumer Phase Identification in a Three Phase Unbalanced LV Distribution Network," in *Innovative Smart Grid Technologies Conference Europe (ISGT Europe), 2012 IEEE PES*, 2012, pp. 1-7,2012.

[98] M. Y. Huang, C. S. Chen, C. H. Lin, M. S. Kang, H. J. Chuang, and C. W. Huang, "Three-phase balancing of distribution feeders using immune algorithm," *Generation, Transmission & Distribution, IET*, vol. 2, pp. 383-392, 2008.

[99] L. Chia-Hung, C. Chao-Shun, C. Hui-Jen, H. Ming-Yang, and H. Chia-Wen, "An Expert System for Three-Phase Balancing of Distribution Feeders," *Power Systems, IEEE Transactions on*, vol. 23, pp. 1488-1496, 2008.

[100] "Australian Standard AS2374 Overview and Test Procedures " in AS2374 Distribution Transformers vol., Ed.^Eds., ed., p.^pp., 2007.
[101] A. Canova, L. Giaccone, F. Spertino, and M. Tartaglia, "Electrical impact of photovoltaic plant in distributed network," *Industry Applications, IEEE Transactions on,* vol. 45, pp. 341-347, 2009.
[102] "Australian Standard Voltage, 60038-2000."
[103] J. Zhu, M.-Y. Chow, and F. Zhang, "Phase balancing using mixed-integer programming [distribution feeders]," *Power Systems, IEEE Transactions on,* vol. 13, pp. 1487-1492, 1998.
[104] P. Trichakis, "Multi agent systems for the active management of electrical distribution networks," Durham University, 2009.
[105] S. Devi and M. Geethanjali, "Optimal location and sizing determination of Distributed Generation and DSTATCOM using Particle Swarm Optimization algorithm," *International Journal of Electrical Power & Energy Systems,* vol. 62, pp. 562-570, 2014.
[106] L. B. Perera, G. Ledwich, and A. Ghosh, "Distributed DSTATCOMs for distribution line enhancement," in *Universities Power Engineering Conference (AUPEC), 2011 21st Australasian*, 2011, pp. 1-6,2011.
[107] U. Jayatunga, S. Perera, and P. Ciufo, "Voltage Unbalance Emission Assessment in Radial Power Systems," *Power Delivery, IEEE Transactions on,* vol. 27, pp. 1653-1661, 2012.
[108] R. C. Eberhart and Y. Shi, "Particle swarm optimization: developments, applications and resources," in *Evolutionary Computation, 2001. Proceedings of the 2001 Congress on*, 2001, pp. 81-86,2001.
[109] R. D. Zimmerman and H.-D. Chiang, "Fast decoupled power flow for unbalanced radial distribution systems," *Power Systems, IEEE Transactions on,* vol. 10, pp. 2045-2052, 1995.
[110] A. Arefi, M. R. Haghifam, and S. H. Fathi, "Distribution harmonic state estimation based on a modified PSO considering parameters uncertainty," in *PowerTech, 2011 IEEE Trondheim*, 2011, pp. 1-7,2011.
[111] M. Clerc, "The swarm and the queen: towards a deterministic and adaptive particle swarm optimization," in *Evolutionary Computation, 1999. CEC 99. Proceedings of the 1999 Congress on*, 1999,1999.
[112] R. C. Eberhart and Y. Shi, "Comparing inertia weights and constriction factors in particle swarm optimization," in *Evolutionary Computation, 2000. Proceedings of the 2000 Congress on*, 2000, pp. 84-88,2000.
[113] M. Clerc and J. Kennedy, "The particle swarm-explosion, stability, and convergence in a multidimensional complex space," *Evolutionary Computation, IEEE Transactions on,* vol. 6, pp. 58-73, 2002.
[114] A. Ratnaweera, S. Halgamuge, and H. C. Watson, "Self-organizing hierarchical particle swarm optimizer with time-varying acceleration coefficients," *Evolutionary Computation, IEEE Transactions on,* vol. 8, pp. 240-255, 2004.

Appendix A Transformer Characteristic

A1. 200 kVA Transformer Characteristics

Table A-1. Electric characteristics of transformer under study

Property	Value
Apparent power	200 kVA
Cooling mode	ONAN
Primary voltage	22 kV
Secondary voltage	415 V
Primary current	5.25 A
Secondary current	262.5 A
No-load loss	424 W
Load Loss	2963 W
Calculated impedance	4.30 %
Calculated % Io	0.614 %

Table A-2. Geometric characteristics of transformer under study

Approximate Mass	Value
Untanked	700.00 kg
Tank and fittings	270.00 kg
Insulating liquid (Oil)	400/360 L/kg
Transformer (Total)	1330.00 kg

Table A-3. Parameters for the thermal model of the 200 kVA transformer

Symbol	Value	Units	Symbol	Value	Units
Gr	14.5	Ws/K	X	0.8	
H	1.4		Y	1.6	
k_{11}	1		$\Delta\theta_{hr}$	35	Kelvin
K_{21}	1		$\Delta\theta_{or}$	45	Kelvin
K_{22}	2		τ_0	180	minutes
R	6.98		τ_W	6	minutes
D_t	15	minutes			

Appendix B Case Study Networks

B1. Australian LV Network-Overhead

Table B-1. Australian overhead cable parameters

Cable Type	Impedance at 45°C
4x7/3.75 AAC (Mar)	0.452+ 0.304j ohm/km
4x7/4.5 AAC (Moo)	0.316+ 0.292j ohm/km
6 mm^2 (Service line)	3.700+ 0.369j ohm/km

Table B-2. Australian overhead system connectivity

From Bus	To Bus	Cable Type	Length (metre)	From Bus	To Bus	Cable Type	Length (metre)
1	**2**	Mar	46	**12**	**13**	Mar	45
2	**3**	Mar	45	**13**	**14**	Mar	45
3	**4**	Mar	42	**10**	**15**	Moo	30
4	**5**	Mar	42	**15**	**16**	Moo	35
5	**6**	Mar	42	**16**	**20**	Moo	35
6	**7**	Mar	39	**20**	**17**	Moo	45
1	**8**	Mar	44	**17**	**18**	Moo	45
8	**9**	Mar	45	**18**	**19**	Moo	45
8	**10**	Mar	44	**20**	**21**	Moo	43
10	**11**	Mar	46	**21**	**22**	Moo	25
11	**12**	Mar	44	**22**	**23**	Moo	23

B2. UK LV Network-Underground

Table B-3. UK underground cable parameters

Cable Type	Rph ohm/km	Xph ohm/km	Rn ohm/km	Ro ohm/km	X0 ohm/km	Iz (A)
1	0.1	0.073	0.164	0.593	0.042	465
2	0.164	0.074	0.164	0.656	0.05	355
3	0.253	0.071	0.253	1.012	0.046	280
4	0.443	0.076	0.443	1.772	0.052	205

Table B-4. UK underground system connectivity

From Bus	To Bus	Cable Type	Length (metre)	From Bus	To Bus	Cable Type	Length (metre)
1	**2**	1	32	**15**	**17**	1	17
2	**3**	3	73	**17**	**18**	4	40
2	**4**	1	90	**1**	**19**	2	27
4	**5**	4	67	**19**	**20**	2	82
5	**6**	4	24	**20**	**21**	3	40
5	**7**	4	52	**20**	**21**	3	17
4	**8**	1	41	**20**	**23**	3	26
8	**9**	4	93	**23**	**24**	4	90
8	**10**	1	35	**23**	**25**	3	53
10	**11**	3	70	**1**	**26**	2	15
11	**12**	4	53	**26**	**27**	3	80
11	**13**	4	32	**27**	**28**	3	85
11	**14**	4	41	**1**	**29**	1	78
10	**15**	1	33	**29**	**30**	4	36
15	**16**	3	68	**30**	**31**	2	85

Appendix C Annual Consumption data

Table C-1. Annual consumption data of customers connect to Australian LV feeder

House Number	Phase Connection	Annual Energy Consumption (kWhr)	House Number	Phase Connection	Annual Energy Consumption (kWhr)
1	B	6860	**40**	C	1904
2	B	3360	**41**	C	3626
3	A	4007	**42**	B	1247
4	C	4431	**43**	A	2903
5	C	3384	**44**	C	2921
6	B	7598	**45**	A	662
7	A	4078	**46**	B	150
8	A	147	**47**	C	1531
9	B	7085	**48**	A	173
10	C	650	**49**	B	2123
11	A	1008	**50**	C	40
12	B	844	**51**	C	3524
13	C	2904	**52**	A	5899
14	A	1786	**53**	A	8953
15	B	8667	**54**	A	1229
16	B	1876	**55**	A	1721
17	C	3893	**56**	B	55
18	A	2109	**57**	C	339
19	A	1786	**58**	A	1475
20	B	656	**59**	B	1178
21	C	546	**60**	C	365
22	A	4131	**61**	A	6494
23	B	585	**62**	B	2618
24	C	1709	**63**	B	4188
25	B	1855	**64**	B	3939
26	C	3632	**65**	C	2779
27	B	5309	**66**	C	2344
28	C	4096	**67**	B	4122
29	A	4327	**68**	A	191
30	A	6220	**69**	B	1354
31	C	1741	**70**	C	1888
32	A	134	**71**	A	2710
33	B	1378	**72**	B	109
34	C	5969	**73**	C	1246
35	A	1566	**74**	B	4878
36	B	5008	**75**	A	1510
37	C	801	**76**	B	2367
38	A	164	**77**	C	1818
39	B	4820			

Appendix D Particle Swarm Optimization Extended Results

A sample of simulation results produced by the PSO at different iterations for a given scenario (dSTATCOM with battery storage) is shown in this appendix. Figure D.1 shows the reduction in Gbest value after each iteration, while Figure D.2 and Figure D.3 shows the location and size of dSTATCOM at each iteration of the PSO. As shown in figure D.1 there are two distinctive jumps in the PSO algorithm (before iteration 20 and 80), this is due to the particles finding the optimum size and location. The last jump (iteration 80) places the location of the dSTATCOM towards the two third of the longest branch of the feeder (14-19) which is well in line with what shown in literature as well.

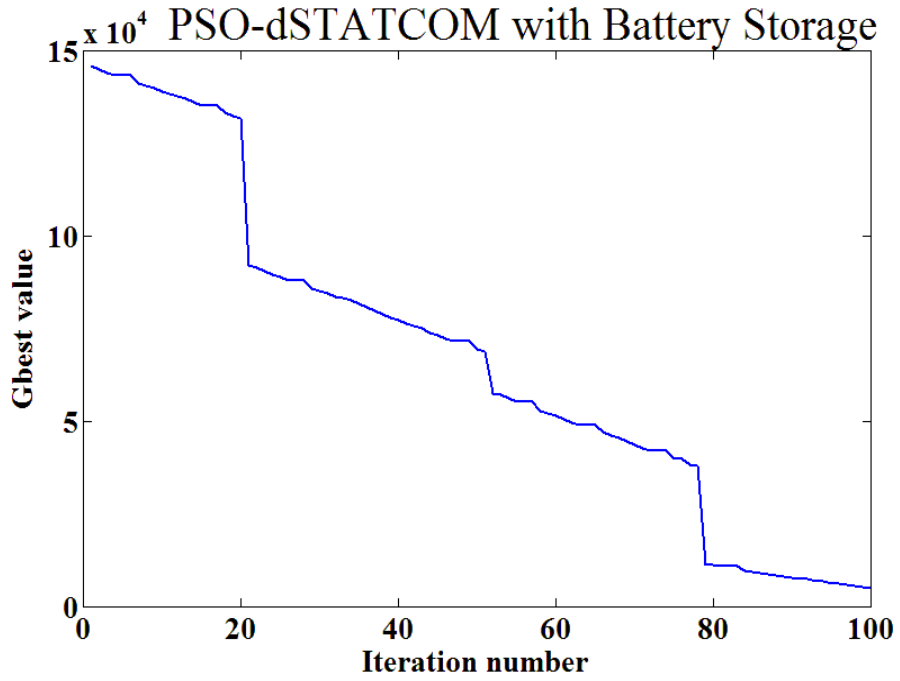

Figure D-1 Simulation results produced by the PSO at different iterations for sample case study

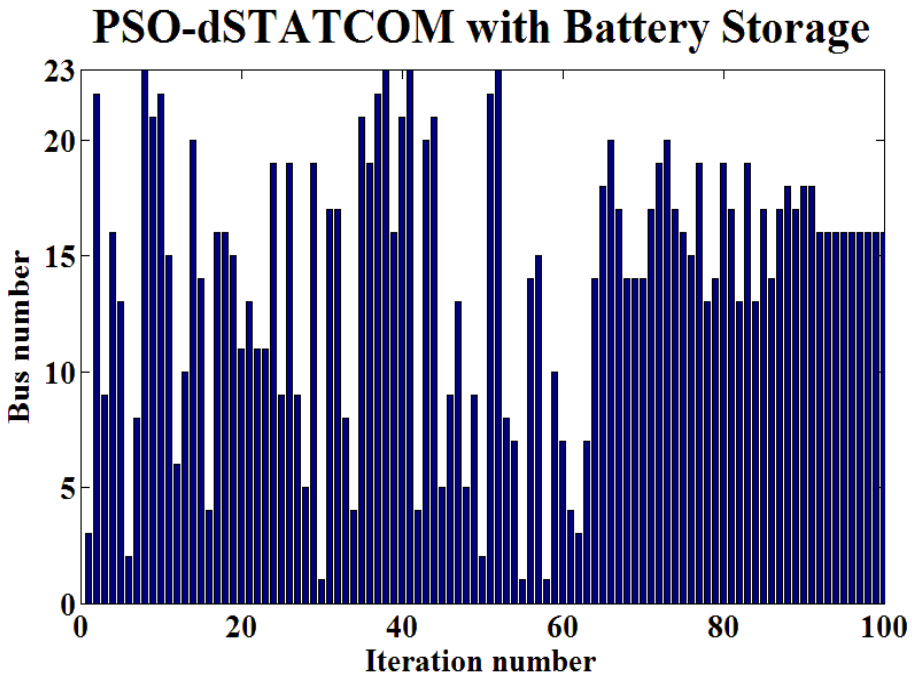

Figure D-2 Location of dSTATCOM at each iteration

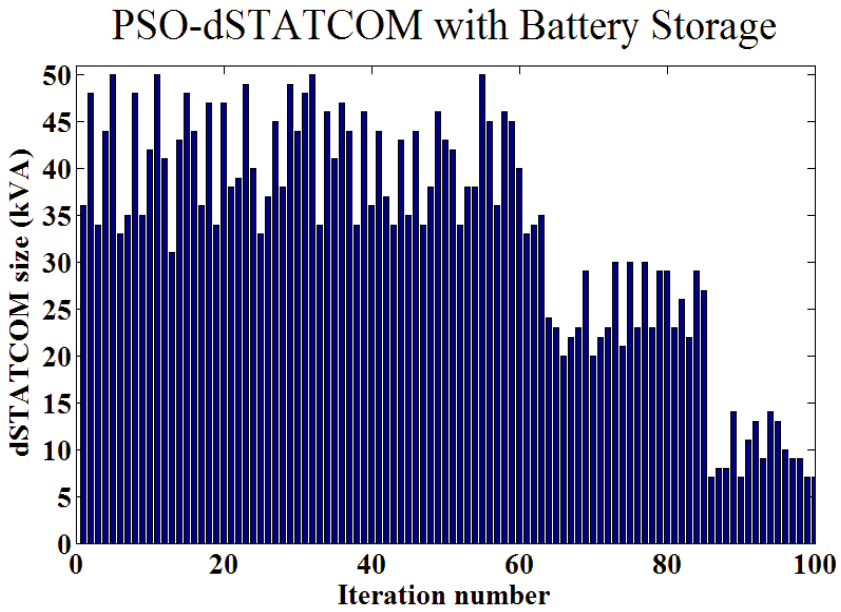

Figure D-3 Size of dSTATCOM at each iteration